

Consequences of redox-active phenazines on the physiology of  
the opportunistic pathogen *Pseudomonas aeruginosa*

by

Suzanne E. Kern  
B.A. Biochemistry  
The Colorado College (2004)

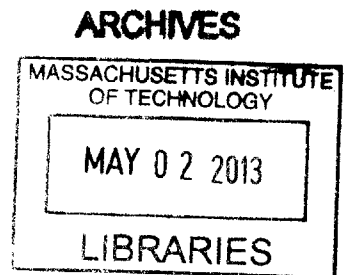
Submitted to the Department of Biology in Partial  
Fulfillment of the Requirements for the Degree of

DOCTOR OF PHILOSOPHY IN BIOLOGY  
AT THE  
MASSACHUSETTS INSTITUTE OF TECHNOLOGY

JUNE 2013

© Suzanne E. Kern. All rights reserved.

The author hereby grants to MIT  
permission to reproduce and to distribute publicly paper  
and electronic copies of this thesis document in whole  
or in part in any medium now known or hereafter created.



Signature of Author .....

A handwritten signature in black ink, appearing to be "Suzanne E. Kern", written over a dotted line.

Department of Biology  
March 29, 2013

Certified by .....

A handwritten signature in black ink, appearing to be "Dianne K. Newman", written over a dotted line.

Dianne K. Newman  
Professor of Biology  
Thesis Supervisor

Accepted by .....

A handwritten signature in black ink, appearing to be "Amy E. Keating", written over a dotted line.

Amy E. Keating  
Professor of Biology  
Chairman, Committee for Graduate Studies



# Consequences of redox-active phenazines on the physiology of the opportunistic pathogen *Pseudomonas aeruginosa*

by  
Suzanne E. Kern

Submitted to the Department of Biology on March 29, 2013  
in Partial Fulfillment of the Requirements  
for the Degree of Doctor of Philosophy in Biology

## ABSTRACT

Phenazines are redox-active small molecules produced by bacteria. Although phenazines have been studied extensively for their roles as toxins, how phenazines benefit producing organisms is still being uncovered. *Pseudomonas aeruginosa* is a phenazine-producing Gram-negative bacterium that inhabits soil and water, and can establish persistent infections in plants, animals, and humans. *P. aeruginosa* produces phenazines upon activation of its quorum-sensing system, which is involved in numerous physiological changes, including biofilm development. Phenazines have been proposed to aid catabolism of *P. aeruginosa* under conditions like those found in biofilms—rich in nutrients but low in suitable respiratory oxidants, *e.g.*, oxygen and nitrate—and phenazines are known to oxidize nicotinamide adenine dinucleotides (NAD(P)H) and thereby affect biofilm structure and development.

The work in this thesis demonstrates that *P. aeruginosa* PA14 can survive under anoxic conditions in the presence of glucose and oxidized endogenous phenazines, including pyocyanin, 1-hydroxyphenazine, and phenazine-1-carboxylic acid. Exogenous oxidants such as methylene blue, paraquat, and 2,6-anthraquinone disulphonate, do not support anaerobic survival, suggesting that phenazine survival is an evolved trait that enhances the fitness of *P. aeruginosa*. Phenazines enable anaerobic survival with glucose but not succinate, and pyruvate fermentation is important for this process. Phenazine redox cycling yields higher levels of ATP, likely by facilitating the oxidation of glucose to pyruvate and acetate by recycling NAD(P)H to NAD(P)<sup>+</sup>. ATP hydrolysis through the F<sub>0</sub>F<sub>1</sub> ATPase sustains a membrane potential, which is necessary for survival. Similar results were observed for both pyruvate and arginine fermentation. Common features across these survival conditions included NADH/NAD<sup>+</sup> ratios less than 3, a polarized membrane, and higher ATP levels than those measured in conditions that do not sustain viability. To perform this work, robust methods for quantifying NADH/NAD<sup>+</sup> and phenazines were developed and are described herein.

The findings of this thesis represent an important step forward in our understanding of how phenazines physiologically benefit the organisms that produce them. Furthermore, they point us to a more general model of survival for the opportunistic pathogen *P. aeruginosa*.

Thesis Supervisor: Dianne K. Newman  
Title: Professor of Biology and Geobiology, California Institute of Technology and  
Investigator, Howard Hughes Medical Institute



## Table of Contents

Title Page	1
Abstract	3
Table of Contents	5
Acknowledgements	7
Chapter 1: Introduction	9
Chapter 2: Background	13
Chapter 3: Endogenous phenazine antibiotics promote anaerobic survival of <i>Pseudomonas aeruginosa</i> via extracellular electron transfer	35
Chapter 4: <i>Pseudomonas aeruginosa</i> has multiple metabolic pathways that enable anaerobic survival and maintenance of the membrane potential	51
Chapter 5: Method for the Extraction and Measurement of NAD(P) <sup>+</sup> and NAD(P)H	85
Chapter 6: Method for Measurement of Phenazines in Bacterial Cultures	103
Chapter 7: Method for assaying anaerobic survival by phenazine redox cycling	117
Chapter 8: Conclusions and Future Directions	139
Appendix A: Effects of varying experimental conditions on <i>P. aeruginosa</i> PA14 anaerobic survival with phenazine redox cycling	147
Appendix B: Applications of an assay to measure pyocyanin reduction rates by mutants of <i>Pseudomonas aeruginosa</i>	163



## Acknowledgements

I would like to thank many people for their assistance and support throughout my time as a PhD student. First and foremost, I am grateful to Dianne for taking me on as a student and fostering in me a sense of fascination about the world of microbial physiology, and for making it possible for me to follow the lab's move to Caltech. Through my experiences and our conversations, I have grown as a scientist and as a person. I want to thank all of the wonderful people I have overlapped with during my time in the group, especially Lars, Alexa, Yun, Nora, Jessie, Maureen, Chia, Lina, Seb, and Nate for engaging in helpful discussions.

At the end of my third year at MIT, I moved with the lab to Caltech, which has turned out to be a great place to conduct research and to call home. Thanks to the many people who have been integral to my sense of community here, in particular the Resident Associates, Becky, Jill, Janet, and the undergrads of Fleming House who keep life interesting and provide balance to my life.

The support of key staff and administrators at both Caltech and MIT has made a world of difference to me. Thank you to Betsey, Taso, Dean Hunt, Tess, Kristy, Olga, Mieke, Portia, Dean Staton, Araceli, and Jill.

I also appreciate all of the encouragement and interest from my family members—Kern, Merdinger, Kempes, and Poling. Chris is at the top of this list for always being there for me, ready to talk about science or anything else.

Finally, a warm thanks to my thesis committee members, Graham Walker, Penny Chisholm, and Ned Ruby, for your guidance and helpful suggestions. And I gratefully acknowledge the funding that has made it possible for me to pursue the interesting story of my research: NSF Graduate Research Fellowship Program, NIH training grant, and HHMI.





# **Chapter 1**

## **Introduction**

## Motivation

Unlike animals, which can move and maintain homeostasis in the face of environmental variation, single-celled organisms such as bacteria must instead acclimate to physical and chemical changes, or die. The formation of multicellular assemblages of bacteria, also known as biofilms, is a common mechanism for enhancing fitness under stressful environmental conditions. In the case of microbial pathogens, we are interested in understanding what underpins their ability to grow or survive within particular conditions so that other scientists might be able to design new and effective antimicrobial treatments.

*Pseudomonas aeruginosa* is an environmental bacterium and opportunistic human pathogen capable of establishing infections that are highly resistant to eradication by antibiotic therapies. *P. aeruginosa* forms biofilms under a variety of conditions, and produces redox-active compounds called phenazines upon reaching high cell densities. Due to elevated levels of respiration by *P. aeruginosa* close to the surface, cells near the center of biofilms often inhabit niches with little to no oxygen. In such a context, when a terminal oxidant is in very limited supply, it has been proposed that soluble redox-active mediators could relieve the buildup of electrons that might exist when cells transition from aerobic to anaerobic conditions (Hernandez & Newman, 2001; Price-Whelan *et al*, 2006).

In this thesis, I present evidence of the physiological benefits of phenazines to *P. aeruginosa*, an organism that produces and secretes these compounds at levels in the micromolar range.

## Overview

**Chapter 2** introduces the topic of phenazines and their physiological impacts on the organisms that produce them, with a particular focus on pseudomonads. While phenazines have long been recognized for their antibiotic properties, more recently they have garnered recognition for their role in the physiological development of biofilms and in survival under conditions of terminal-oxidant limitation. Parts of Chapter 2 will be included in a review chapter regarding the physiological impacts of phenazines in the forthcoming book *Microbial Phenazines: Use in Agriculture, Energy and Health*, published by Springer and compiled by Sudhir Chincholkar and Linda Thomashow.

**Chapter 3** documents the discovery that phenazine redox-cycling can enable the anaerobic survival of *P. aeruginosa*. Using well-mixed planktonic cultures in an oxygen-free atmosphere, we approximated the oxygen-depleted conditions of a typical biofilm, where the redox activity of phenazines has been proposed to alleviate the stress of terminal-oxidant limitation (Hernandez & Newman, 2001; Price-Whelan *et al*, 2006). This work was published in the Journal of Bacteriology: Wang Y, Kern SE & Newman DK (2010) Endogenous phenazine antibiotics promote anaerobic survival of *Pseudomonas aeruginosa* via extracellular electron transfer. J Bacteriol **192**: 365–369.

**Chapter 4** examines the physiological underpinnings of the phenazine-enabled anaerobic survival described in Chapter 3, and reveals common features of anaerobic survival in *P. aeruginosa* PA14. In addition to mutant analyses in the context of the phenazine redox-cycling assay, this chapter reports levels of ATP, NAD(H) and membrane polarization for cells surviving on arginine, pyruvate, or nitrate, in the case of a respiratory nitrate reductase mutant. This chapter underscores the importance of maintaining a membrane potential for bacterial viability and strongly suggests that phenazines enable anaerobic survival by facilitating the catabolism of glucose. Glucose catabolism yields ATP, which in turn facilitates the translocation of protons via the  $F_1F_0$  ATP synthase, resulting in the maintenance of a polarized membrane. This work has been peer-reviewed and is in revision: Glasser N, Kern SE & Newman DK. *Pseudomonas aeruginosa* has multiple metabolic pathways that enable anaerobic survival and maintenance of the membrane potential.

**Chapters 5, 6 and 7** provide detailed methods for performing key physiological measurements and characterizations. **Chapter 5** describes the procedure for measuring NAD(P)(H) in cells, with special provisions for applications involving anaerobic cultures containing phenazines. The redox activity of phenazines can undermine the accuracy of NAD(P)(H) extraction and measurement by oxidizing NAD(P)H, thereby leading to its destabilization and elimination from the sample. However, with the appropriate precautions, it is possible to accurately measure NAD(P)(H) levels. **Chapter 6** describes how to measure the concentration of phenazines in a solution using high-performance liquid chromatography (HPLC). Both chapters will be included in the forthcoming book *Methods in Pseudomonas*, published by Humana Press and compiled by Allain Filloux and Juan Luis Ramos. Finally, **Chapter 7** details the steps and precautions for performing the anaerobic phenazine redox-cycling assay utilized in Chapters 3 and 4.

**Chapter 8** concludes the thesis with a perspective of what lies ahead, and how the methods and findings described in this work have contributed to understanding *P. aeruginosa* physiology, particularly those aspects pertaining to phenazine utilization and anaerobic survival.

The appendices offer notes on the variables impacting the outcomes of anaerobic phenazine redox cycling (**Appendix A**) and on the development and applications of an assay for measuring the rate of pyocyanin reduction by a culture of bacterial cells (**Appendix B**). This assay has the potential to be used as a discovery tool, perhaps as part of the search for determining cellular component(s) of *P. aeruginosa* involved in the reduction of phenazines, a process that remains poorly characterized.

## References

- Hernandez ME & Newman DK (2001) Extracellular electron transfer. *Cell Mol Life Sci* **58**: 1562–1571.
- Price-Whelan A, Dietrich LEP & Newman DK (2006) Rethinking ‘secondary’ metabolism: physiological roles for phenazine antibiotics. *Nature Chem Biol* **2**: 71–78.

## Chapter 2

### Physiological impacts of phenazines on producing organisms

This chapter will be modified and combined with material pertaining to the physiological impacts of phenazines on non-producing organisms for a chapter tentatively entitled “Physiological Consequences of Phenazines,” to be co-written with Nora Grahl, Debora Hogan, and Dianne Newman for publication in the forthcoming book entitled *Microbial Phenazines: Use in Agriculture, Energy and Health*, edited by Sudhir Chincholkar and Linda Thomashow and to be published by Springer.

Contributions:

I wrote this chapter and generated the figures herein.

Many microorganisms produce phenazines, brightly colored, heterocyclic small molecules that reversibly gain and lose electrons (see Figure 1). Pseudomonads are perhaps the best-studied phenazine producers, known as agents of human infection, and for their potential as biological control agents that protect agricultural crops (Mavrodi *et al*, 2012). In both instances, phenazines are key to the success of pseudomonads, serving as toxins and virulence factors due to their redox activity. Still, we are just at the early stages of determining what roles phenazines play in the physiology and fitness of the organisms that produce them.

Given the material and energetic costs associated with both making phenazines and retaining necessary biosynthetic proteins, the benefits to phenazine producers must be substantial. In the sections that follow, a brief review of the redox properties of phenazines leads into a discussion of some common features of phenazine producers and the conditions favoring the production of various phenazines. Collectively, these characteristics suggest various ways in which phenazines may confer fitness benefits to the bacteria that produce them. This chapter concludes with a survey of experiments that have directly tested the physiological consequences of phenazines, and that validate some of the hypotheses put forward in earlier reviews (Hernandez & Newman, 2001; Price-Whelan *et al*, 2006).

### **Redox properties of phenazines**

Phenazines accept and donate two electrons, stepwise, according to the redox properties of nearby compounds, and they are soluble in aqueous solution at micro- to millimolar levels (Price-Whelan *et al*, 2006). Consequently, phenazines can carry electrons from intracellular reductants to extracellular oxidants, thereby undergoing redox-cycling and serving as “electron shuttles.” Suitable oxidants, such as oxygen, may be present intra- or extracellularly, while others, including insoluble ferric iron (Fe(III)) and manganese (Mn(IV)), remain outside of the cell (Hernandez *et al*, 2004). The dynamics of these interactions vary according to the phenazine structure and environmental parameters. For example, pyocyanin reacts quickly with oxygen and slowly with ferric iron, while PCA shows the opposite affinity (Wang & Newman, 2008).

In addition to their precise chemical structure, phenazines and their redox activity are affected by the pH of the milieu, which determines the degree of protonation. In the range of pH 5 to pH 8, phenazines have standard reduction potentials spanning +69 mV to -245 mV relative to the normal hydrogen electrode (Wang & Newman, 2008). Within this range of

redox potentials, as shown in Figure 2, phenazines can accept electrons from reduced nicotinamide cofactors (NAD(P)H,  $E^{\circ} = -320$  mV) and donate electrons to compounds with more positive reduction potentials, such as oxygen ( $E^{\circ} = +816$  mV for conversion to water), nitrate ( $E^{\circ} = +431$  mV for conversion to nitrite), and ferric iron ( $E^{\circ} = +770$  mV for conversion to  $Fe^{2+}$ , although this value varies depending on how iron is complexed with other elements). Redox reactions proceed spontaneously *in vitro* with each of these compounds, with the exception of nitrate. Phenazine oxidation by nitrate has only been observed when *Pseudomonas aeruginosa* cells are present (Alexa Price-Whelan and Suzanne Kern, unpublished data), suggesting that this particular reaction may be cell-mediated. In contrast to earlier reports indicating that phenazines could oxidize glutathione ( $E^{\circ} = -263$  mV) (O'Malley *et al*, 2004), later experiments have shown that no direct redox transformations occur between these compounds (Muller, 2011).

Although carefully designed experiments can probe the kinetics and thermodynamics of the interactions between phenazines and either reductants or oxidants, at present it is only possible to suggest likely redox partners and reactivities for phenazines *in vivo*. Direct tests of possible cellular components involved in reducing phenazines have so far yielded inconclusive results (Price-Whelan, 2009), but this question continues to be an area of active research.

The redox properties and reactivities of phenazines influence the chemistry of producing organisms and the environments in which they live. Clues about the physiological roles of phenazines can come from an understanding of the types of cells that produce them, and the context in which these microorganisms exist.

### **Features of phenazine producers and their habitats**

Phenazine-producing microorganisms inhabit diverse habitats, including water, soil, and animal infection sites. They can be free-living or intimately associated with other microbes, animals or plants and phenazine production increases the fitness of the producers under specific circumstances (*e.g.*, (Price-Whelan *et al*, 2006; Mazzola *et al*, 1992; Turner & Messenger, 1986). Their ecological success has been largely attributed to the antibiotic properties of phenazines, including the generation of reactive-oxygen species (ROS) formed when reduced phenazines react with molecular oxygen (Hassett *et al*, 1992; O'Malley *et al*, 2004), interference with electron flow in cellular respiration (Baron *et al*, 1989) and the

disruption of enzyme function due to the reactivity of phenazines with iron-sulfur clusters (Gu & Imlay, 2011).

Nonetheless, poisoning neighboring organisms is not the only role for these small molecules. Their redox activity is also responsible for reducing ferric iron solids to bioavailable, soluble ferrous iron (Wang & Newman, 2008; Hernandez *et al*, 2004), and shuttling electrons out of oxidant-limited cells (Rabaey *et al*, 2005; Wang *et al*, 2010). Infection sites, soil habitats, and biofilms can become limited for oxygen (Højberg *et al*, 1999; Worlitzsch *et al*, 2002), which suggests that phenazine production might aid microorganisms in these environments, where growth is slow or halted (see Figure 3). Understanding the role of phenazines in such contexts will be important for disabling slowly or non-growing cells, which are well known to be highly resistant to antibiotics (for reviews on this topic, see Høiby *et al*, 2010 and Martínez & Rojo, 2011).

Strains of *P. aeruginosa* and *Pseudomonas chlororaphis* synthesize among the highest (micromolar) levels of phenazines in nature, and typically do so when their populations reach high densities (Mavrodi *et al*, 2006). Environmental conditions accompanying phenazine production can include low levels of oxygen, and may also trigger the formation of biofilms. It is in these contexts that phenazines have been predicted to play key physiological roles, relieving the stress of limited access to terminal oxidants (Hernandez & Newman, 2001; Price-Whelan *et al*, 2006).

*P. aeruginosa* is a phenazine-producing soil microbe and opportunistic human pathogen capable of establishing infections of lungs, eyes, and burn wounds. In the case of lung infections of individuals with cystic fibrosis, the environmental habitat of *P. aeruginosa* is thick, oxygen-depleted mucous that is rich in amino acids and low in free iron (Palmer *et al*, 2007; Worlitzsch *et al*, 2002). Longitudinal studies of patients over time have shown a change in the microbial ecology of the lung environment, with *P. aeruginosa* and anaerobic microorganisms becoming predominant in later stages of infection (Reid *et al*, 2007; Tunney *et al*, 2008); this progression may point to decreasing oxygen availability and a redox-balancing role for phenazines.

The pseudomonads, particularly *P. aeruginosa*, *P. chlororaphis*, and *P. fluorescens*, are well-studied examples of phenazine producers, and they share a common operon (*phzABCDEFG*) encoding the enzymes needed for synthesizing PCA, a precursor of other phenazines (Mentel *et al*, 2009). Recent phylogenetic analyses have shown that this operon has likely



undergone purifying selection in pseudomonads (Mavrodi *et al*, 2010; Parejko *et al*, 2012). Researchers have suggested that preservation of the phenazine operon throughout the evolution of this genus may point to a participation of phenazines in a set of core physiological functions (Mavrodi *et al*, 2010). In comparison, among many non-pseudomonads—such as species of *Burkholderia*, *Pectobacterium*, and of the *Actinomycetales*—the phenazine biosynthesis operon appears to be present due to horizontal gene transfer, encoded on plasmids or transposable elements (Mavrodi *et al*, 2010; Fitzpatrick, 2009). In such instances, phenazines might primarily serve as antimicrobials against competing organisms, maintained only in specific ecological contexts (Mavrodi *et al*, 2010; Fitzpatrick, 2009; Parejko *et al*, 2012).

Phenazines also contribute to increased current output in microbial fuel cells (MFCs). In one experiment, bacterial biofilms on the anode of a microbial fuel cell were used to serially inoculate new MFC cultures, with the goal of enriching for enhanced current output. After numerous transfers, the community was enriched in bacteria producing soluble redox mediators, including phenazines (Rabaey *et al*, 2004)). Exogenously added pyocyanin was later shown to increase power output in mixed-species MFCs (Rabaey *et al*, 2005). Phenazines have increasingly garnered interest for their potential role in biotechnology applications (*e.g.*, (Rabaey *et al*, 2005; Pham *et al*, 2008)); however, the full physiological consequences of phenazines on microbial MFC consortia are not yet known.

The preservation of phenazine biosynthesis genes is one indicator of the potential relevance of phenazines to their producers. In pursuit of determining physiological roles of phenazines, we turn to the regulatory controls over when—and which—phenazines are produced in response to particular environmental cues.

### **Factors modulating phenazine production and modification**

Phenazine production is triggered by high cell density, through activation of the quorum sensing system, which involves a regulatory cascade of activated autoinducer sensors and associated response regulators that lead to altered levels of gene expression (Mavrodi *et al*, 2006). Interestingly, pyocyanin goes on to also serve as a signal, regulating gene expression in *P. aeruginosa*, including genes both in the SoxR regulon, and that encode small-molecule efflux pumps (Dietrich *et al*, 2006).

Phenazine-1-carboxylic acid (PCA) and phenazine-1,6-dicarboxylic acid (PDC), the precursors to all other phenazines, are derived from the condensation of two chorismate molecules (see review by Mentel *et al*, 2009), and their synthesis is mediated by the proteins encoded by *phzABCDEFG*. In laboratory cultures a *P. aeruginosa* PA14 phenazine-null mutant ( $\Delta phzA1-G1 \Delta phzA2-G2$ ) shows no growth defect—in fact, upon entering the end of exponential growth phase, when phenazines are produced, cultures of the mutant consistently reach higher optical densities than the wild-type (Price-Whelan *et al*, 2007). This enhanced growth may be due to the diversion, in wild-type, of metabolites away from the production of compounds derived from chorismate, including aromatic amino acids and quinones, in favor of phenazine biosynthesis. Metabolite flux analyses could shed light on this question; however, no systematic studies have yet been performed in phenazine producers.

For decades, researchers have noted the variability of phenazine production by given *Pseudomonas* strains in response to even slight changes in their culturing environment (Kanner *et al*, 1978). Various chemical, physical, and biological determinants can affect the identity and quantity of phenazines produced. For example, in a strain of *P. chlororaphis* (PCL1391), levels of phenazine carboxamide varied from 0 to 21  $\mu\text{M}$  /  $\text{OD}_{620}$  depending on the particular combinations of carbon and nitrogen sources, levels of oxygen, phosphate, magnesium, and iron, as well as temperature and pH (van Rij *et al*, 2004). Several other studies have also demonstrated the influence of environmental factors on the production of phenazines (Slininger & Shea-Wilbur, 1995; Slininger & Jackson, 1992; Kanner *et al*, 1978; Wurtzel *et al*, 2012; Recinos *et al*, 2012) and, collectively, suggest physiological “reasons” for synthesizing different phenazines under different conditions.

In a recent study, Huang and colleagues noted that *Pseudomonas* spp. strain M18, which exhibits strong biocontrol properties, shares considerable sequence identity with *P. aeruginosa* strain PAO1, a known animal pathogen. While both strains encode two copies of the core phenazine biosynthesis operon (*phzABCDEFG*), as well as *phzM* and *phzS*—the genes encoding the proteins responsible for converting PCA to PYO—they produce dramatically different amounts of the two phenazines. Both strains produce more PYO at 37°C than at 28°C, but the pathogen, PAO1, produced over twice as much as M18. Levels of PCA were highest in cultures of M18 grown at 28°C, over four times higher than at 37°C, or at either temperature in the case of PAO1 (Huang *et al*, 2009). All together, these results point to habitat-specific regulation of phenazine production, with levels of plant-protective

PCA produced in the highest amounts by the rhizosphere isolate at soil temperatures, and the virulence factor PYO more highly produced by the pathogenic strain PAO1 at the temperature of a mammalian host.

Other research has shown that the redundant core phenazine biosynthesis operons, *phzA1-G1* and *phzA2-G2*, are differentially regulated and contribute to PCA production to varying degrees under different environmental conditions (Recinos *et al*, 2012). Both operons appear to be regulated by quinolones, which are components of the *P. aeruginosa* quorum-sensing system. The quinolone responsible for increasing *phz1* expression requires oxygen for its production, while the *phz2*-activating quinolone does not. It seems fitting that *phz2* is the primary contributor to phenazine production in colony biofilms (Recinos *et al*, 2012), where oxygen levels are very low (Dietrich *et al*, 2013). The *phz2* operon is also responsible for the majority of phenazine production, both in planktonic cultures and in a mouse model of infection (Recinos *et al*, 2012). The regulation of *phzM* and *phzS*, which encode the methyltransferase and monooxygenase responsible for converting PCA to PYO, is not fully understood, but both genes are adjacent to *phz1*. It is interesting to note that PhzS requires molecular oxygen to add a hydroxyl group onto PCA, and so it may be that these PYO-producing enzymes are in part co-regulated with *phz1* (Recinos *et al*, 2012).

The parameters influencing phenazine production point to several predictions for the role of phenazines, as previously noted (Hernandez & Newman, 2001; Price-Whelan *et al*, 2006). When cells reach high population density—the main trigger for phenazine production—oxygen levels are generally quite low (Price-Whelan *et al*, 2007). For *P. aeruginosa* infections within mucous-filled lungs of individuals with cystic fibrosis, the environmental parameters are strikingly similar: oxygen tension and available iron can be very low (Worlitzsch *et al*, 2002; Højberg *et al*, 1999). Under such conditions, phenazines are often present in expectorated lung sputum, and their levels correlate with an increase in reduced, soluble iron (Ryan C. Hunter, unpublished data). The production of soluble electron shuttles is likely to be advantageous when oxygen is depleted, whether due to changing environmental conditions, or the formation of biofilms (Worlitzsch *et al*, 2002; Dietrich *et al*, 2013).

### **Interactions of phenazines in bacterial habitats**

In the environment or under laboratory conditions, phenazines in their reduced form can interact with a number of oxidants, including ferric iron, oxygen, and anodes (electrodes at

which oxidation occurs). Mineral reduction by redox cycling can be achieved by other small molecules as well, such as flavins produced by *Shewanella oneidensis* (Marsili *et al*, 2008). *Shewanella* species are known for their metabolic versatility, particularly with respect to cellular redox reactions, and can use minerals for respiration (Gralnick & Newman, 2007). Like many phenazine producers, these bacteria can be found in soil and water environments, where they coexist with a multitude of other microorganisms (Hau & Gralnick, 2007). The physiological consequences of mineral reduction may be as simple as the recycling of oxidized phenazines, but can also result in a host of separate chemical reactions and subsequent ecological consequences.

The reduction of ferric (Fe(III)) iron minerals to ferrous (Fe(II)) iron makes a solid substrate soluble and readily bioavailable, and circumvents the need for Fe(III)-chelators such as siderophores to access iron. Concomitant with endogenous phenazine production during aerobic planktonic growth, the fraction of iron as Fe(II) in cultures of *P. aeruginosa* PA14 increases as the cell density increases (Kreamer *et al*, 2012). In the context of *P. aeruginosa*-infected lungs of patients with cystic fibrosis, there is again a correlation between the presence of phenazines and a higher proportion of Fe(II) (Ryan C. Hunter, unpublished data). This clinical finding underscores the importance of understanding the environmental impacts of phenazine producers; for instance, recent antimicrobial therapies have included Fe(III)-chelation, which may be less effective in later-stage infections or when phenazines and Fe(II) are present.

Iron serves as a nutrient as well as a behavioral signal for *P. aeruginosa*, affecting both twitching motility and biofilm attachment (Harmsen *et al*, 2010). Phenazines are known to influence biofilm development, in part due to their interaction with extracellular iron (Wang *et al*, 2011). PYO and PCA can liberate iron from chelators (Cox, 1986; Wang *et al*, 2011) and are each capable of rescuing certain aspects of biofilm development when levels of bioavailable iron are very low. A *P. aeruginosa* PA14 mutant unable to produce siderophores or phenazines does not form biofilms in a flow-cell apparatus when an iron chelator is included in the growth medium. The addition of PCA or PYO rescues certain aspects of biofilm development, resulting in biofilms with similar cell densities to those formed by the wild-type strain (Wang *et al*, 2011). In separate studies, PCA has been found to decrease swarming motility by cells in colony biofilms, and exogenously supplied PYO restores wild-type-like mushroom-shaped structures in flow-cell biofilms (Ramos *et al*, 2010).

While this chapter—and thesis as a whole—focuses on the consequences of phenazines as redox-active molecules and signals, it is also important to note that phenazines can be metabolized by other organisms once out in the environment. Antibiotics in the soil exist at low levels and commonly end up as food, providing a source of energy and fixed carbon and nitrogen (Davies, 2006). While the level of phenazines in non-dividing, anaerobic laboratory cultures remains approximately constant over at least 8 days at 30°C (Wang *et al*, 2010), the half-life of PCA in the rhizosphere has been reported as 3.4 days, and is likely to be biologically mediated (Mavrodi *et al*, 2012). A strain of *Sphingomonas* that degrades PCA—using this as its sole carbon, nitrogen, and energy source—has been isolated from the soil (Yang *et al*, 2007), and preliminary characterizations have suggested possible degradation products (Chen *et al*, 2008). The recently sequenced genome of *Sphingomonas wittichii* DP58 could lead to an understanding of the enzyme(s) and biochemical pathway(s) responsible for breaking down PCA, and facilitate further characterization of phenazine degradation in the environment (Ma *et al*, 2012).

### **Intracellular consequences of phenazines**

Whether taken up by nearby cells or by the bacteria that produce them, phenazines can alter the redox state of key cellular metabolites. For example, late-exponential and stationary phase planktonic cultures of *P. aeruginosa* grown with glucose as the main carbon source maintain a more oxidized pool of nicotinamide adenine dinucleotide (NAD(H)) when phenazines are present (Price-Whelan *et al*, 2007). The same is true for *P. aeruginosa* colony biofilms grown on agar plates (Dietrich *et al*, 2013). Multiphoton microscopy measurements clearly indicate that the reduction of phenazines over time is accompanied by the oxidation of the NAD(P)H pool in planktonic *P. aeruginosa* (Sullivan *et al*, 2011), however this technique cannot determine whether this redox coupling is direct or indirect—for example, through a mediator such as an enzyme or a cytochrome of the respiratory chain.

Oxidation of the NAD(P)H pool can have profound metabolic effects. Emde and colleagues have demonstrated that anaerobically fermenting cultures of *Propionibacterium freudenreichii* and *Escherichia coli* produce more oxidized end products when redox-active small-molecule mediators and an oxidizing electrode are present (Emde *et al*, 1989; Emde & Schink, 1990). Phenazines, which are another example of redox mediators, have been shown to exert an effect on *P. aeruginosa* metabolism: wild type PA14 grown aerobically

with glucose excretes pyruvate in late-stationary phase, while a phenazine-null mutant does not. Subsequent to pyruvate excretion, pyruvate levels drop back to undetectable levels, suggesting that the wild-type cells consume the pyruvate excreted earlier (Price-Whelan *et al*, 2007). Aerobic glucose metabolism follows the Entner-Doudoroff pathway, depicted in Figure 4, however, in late-stationary phase cultures, cell densities are very high and oxygen levels remain low despite vigorous aeration (Price-Whelan *et al*, 2007). Pyruvate fermentation in *P. aeruginosa* enables anaerobic survival, but not growth, through production of acetate and lactate, and with ATP generation and NAD(H) balance as byproducts (Eschbach *et al*, 2004). Therefore, the consumption of pyruvate in late-stationary phase would seem to provide a useful and timely energy source.

The excretion of pyruvate is somewhat more confusing, and two explanations have been proposed. Price-Whelan and colleagues speculated that the presence of pyocyanin might impair the function of the pyruvate dehydrogenase complex, thereby blocking the downstream catabolism of pyruvate through the TCA cycle, and resulting in its buildup and excretion (Price-Whelan *et al*, 2007). More recent studies from our lab suggest that pyruvate excretion may also result from increased conversion of glucose to pyruvate, promoted by phenazines, which oxidize NAD(P)H that might otherwise build up (Glasser *et al*); see Figure 5 and Chapter 4). Phenazine-null mutants of *P. aeruginosa* PA14 provided with glucose, phenazines, and an oxidizing electrode survived anaerobically (as previously demonstrated by Wang *et al*, 2010). A mutant unable to ferment pyruvate to lactate ( $\Delta$ *ldhA*), and therefore unable to reoxidize NADH, still survived anaerobically under the same conditions. In contrast, a mutant in pyruvate fermentation to acetate,  $\Delta$ *ackA-pta*, which could not generate ATP by this substrate level phosphorylation, lost viability as quickly as cells without phenazines (Glasser *et al*); see Chapter 4). This finding suggests that oxidized phenazines facilitate the oxidation of glucose to acetate in the absence of any respiratory oxidants (*e.g.*, oxygen or nitrate).

Phenazines may contribute to long-term cell viability by numerous mechanisms, including redox balancing under oxidant-limited conditions and altering membrane potential. Additionally, phenazines influence the development of biofilms, which can render cells more tolerant of unfavorable environmental conditions (Høiby *et al*, 2010).

## Influence of phenazines on biofilm physiology

Quorum sensing is primarily responsible for inducing the production of phenazines, and also participates in transitioning cells from planktonic to biofilm growth (De Kievit *et al*, 2001); however, the relative contribution of various phenazines to biofilm development remained unknown until several recent studies. Maddula and colleagues demonstrated that the presence of phenazines is essential for the formation of biofilms by the rhizosphere bacterium *P. chlororaphis* 30-84. The defect in biofilm formation by a mutant unable to produce phenazines was nearly identical to that of mutants deficient in different components of the quorum-sensing system (Maddula *et al*, 2006). The same group later reported that the relative amount of the two phenazines produced by strain 30-84 is a key determinant of biofilm development (Maddula *et al*, 2008). The group compared the development of flow-cell biofilms produced by wild-type 30-84 to that of mutants genetically engineered to overproduce 2-OH-PHZ or PCA. The two phenazines were found to have distinct roles: 2-OH-PHZ enhanced biofilm attachment and growth, as well as diminished dispersal rates, while PCA only impacted growth and dispersal. Biofilms of the PCA-overproducer, like the wild-type, formed mushroom-shaped flow-cell biofilms, while cells overproducing 2-OH-PHZ created a thick, but flat biofilm structure (Maddula *et al*, 2008).

Other recent work has shown that phenazines influence the morphology of *P. aeruginosa* colony biofilms (Dietrich *et al*, 2008; Ramos *et al*, 2010) in ways that maintain intracellular redox balance (Dietrich *et al*, 2013). Colony biofilms produced by the phenazine-null mutant of *P. aeruginosa* PA14 become wrinkled, with a higher surface-to-volume ratio, earlier than the parent strain. Similar morphological consequences in colony biofilms have been reported for the Gram-positive *Streptomyces coelicolor* in relation to the secondary metabolites actinorhodin and undecylprodigiosin (Dietrich *et al*, 2008). Measurements of the NADH/NAD<sup>+</sup> ratio in the *P. aeruginosa* studies indicate similar ratios between the smooth wild-type colonies and the wrinkled mutant colonies. Consistent with the hypothesis that phenazines counteract the buildup of NADH under conditions with limited terminal oxidants, a high NADH/NAD<sup>+</sup> ratio immediately precedes the initiation of wrinkling in the phenazine-null mutant, and the ensuing increase in the ratio of surface area to volume correlates with a return of the NADH/NAD<sup>+</sup> levels to normal (Dietrich *et al*, 2013).

## Conclusion

The studies pursued in the chapters that follow grew out of several key observations about *P. aeruginosa* and phenazines. i.) *P. aeruginosa* is metabolically versatile and can exist in numerous diverse habitats including those with little to no oxygen, yet it has very limited options for anaerobic metabolism; ii.) phenazines are produced in late-exponential phase, stationary phase, and in biofilms, when oxygen levels tend to be very low; iii.) phenazine reduction potentials lie between common cellular reductants (*e.g.* NAD(P)H) and external oxidants (*e.g.* Fe(III) and O<sub>2</sub>); and iv.) phenazines are slightly soluble in aqueous solution and can be present both intra- and extracellularly. I set out to determine whether phenazines contribute to the anaerobic metabolism of *P. aeruginosa* through a series of experiments measuring survival and various physiological parameters. As indicated earlier in this chapter, phenazines that undergo redox cycling in anaerobic planktonic cultures can sustain the viability of *P. aeruginosa* for a week or more when glucose is also present (see Chapter 3) and we have started to uncover the physiological mechanisms responsible for this result (Chapter 4).



## References

- Baron SS, Terranova G & Rowe JJ (1989) Molecular mechanism of the antimicrobial action of pyocyanin. *Curr Microbiol* **18**: 223–230
- Chen K, Hu H, Wang W, Zhang X & Xu Y (2008) Metabolic degradation of phenazine-1-carboxylic acid by the strain *Sphingomonas* sp. DP58: the identification of two metabolites. *Biodegradation* **19**: 659–667
- Cox CD (1986) Role of pyocyanin in the acquisition of iron from transferrin. *Infect Immun* **52**: 263–270
- Davies J (2006) Are antibiotics naturally antibiotics? *J. Ind. Microbiol. Biotechnol.* **33**: 496–499
- De Kievit TR, Gillis R, Marx S, Brown C & Iglewski BH (2001) Quorum-sensing genes in *Pseudomonas aeruginosa* biofilms: their role and expression patterns. *Appl Environ Microbiol* **67**: 1865–1873
- Dietrich LEP, Okegbe C, Price-Whelan A, Sakhtah H, Hunter RC & Newman DK (2013) Bacterial community morphogenesis is intimately linked to the intracellular redox state. *J Bacteriol*
- Dietrich LEP, Price-Whelan A, Petersen A, Whiteley M & Newman DK (2006) The phenazine pyocyanin is a terminal signalling factor in the quorum sensing network of *Pseudomonas aeruginosa*. *Mol Microbiol* **61**: 1308–1321
- Dietrich LEP, Teal TK, Price-Whelan A & Newman DK (2008) Redox-active antibiotics control gene expression and community behavior in divergent bacteria. *Science* **321**: 1203–1206
- Emde R & Schink B (1990) Oxidation of glycerol, lactate, and propionate by *Propionibacterium freudenreichii* in a poised-potential amperometric culture system. *Arch Microbiol* **153**: 506–512
- Emde R, Swain A & Schink B (1989) Anaerobic oxidation of glycerol by *Escherichia coli* in an amperometric poised-potential culture system. *Appl Microbiol Biot* **32**: 170–175
- Eschbach M, Schreiber K, Trunk K, Buer J, Jahn D & Schobert M (2004) Long-term anaerobic survival of the opportunistic pathogen *Pseudomonas aeruginosa* via pyruvate fermentation. *J Bacteriol* **186**: 4596–4604
- Fitzpatrick DA (2009) Lines of evidence for horizontal gene transfer of a phenazine producing operon into multiple bacterial species. *J. Mol. Evol.* **68**: 171–185
- Glasser NR, Kern SE & Newman DK *Pseudomonas aeruginosa* has multiple metabolic pathways that enable anaerobic survival and maintenance of the membrane potential. *submitted to Mol Microbiol*
- Gralnick JA & Newman DK (2007) Extracellular respiration. *Mol Microbiol* **65**: 1–11

- Gu M & Imlay JA (2011) The SoxRS response of *Escherichia coli* is directly activated by redox-cycling drugs rather than by superoxide. *Mol Microbiol* **79**: 1136–1150
- Harmsen M, Yang L, Pamp SJ & Tolker-Nielsen T (2010) An update on *Pseudomonas aeruginosa* biofilm formation, tolerance, and dispersal. *Fems Immunol Med Mic* **59**: 253–268
- Hassett DJ, Charniga L, Bean K, Ohman DE & Cohen MS (1992) Response of *Pseudomonas aeruginosa* to pyocyanin: mechanisms of resistance, antioxidant defenses, and demonstration of a manganese-cofactored superoxide dismutase. *Infect Immun* **60**: 328–336
- Hau HH & Gralnick JA (2007) Ecology and biotechnology of the genus *Shewanella*. *Annu Rev Microbiol* **61**: 237–258
- Hernandez ME & Newman DK (2001) Extracellular electron transfer. *Cell Mol Life Sci* **58**: 1562–1571
- Hernandez ME, Kappler A & Newman DK (2004) Phenazines and other redox-active antibiotics promote microbial mineral reduction. *Appl Environ Microbiol* **70**: 921–928
- Huang J, Xu Y, Zhang H, Li Y, Huang X, Ren B & Zhang X (2009) Temperature-dependent expression of *phzM* and its regulatory genes *lasI* and *ptsP* in rhizosphere isolate *Pseudomonas* sp. strain M18. *Appl Environ Microbiol* **75**: 6568–6580
- Højby N, Bjarnsholt T, Givskov M, Molin S & Ciofu O (2010) Antibiotic resistance of bacterial biofilms. *Int. J. Antimicrob. Agents* **35**: 322–332
- Højberg O, Schnider U, Winteler HV, Sorensen J & Haas D (1999) Oxygen-sensing reporter strain of *Pseudomonas fluorescens* for monitoring the distribution of low-oxygen habitats in soil. *Appl Environ Microbiol* **65**: 4085–4093
- Kanner D, Gerber NN & Bartha R (1978) Pattern of phenazine pigment production by a strain of *Pseudomonas aeruginosa*. *J Bacteriol* **134**: 690–692
- Kreamer NNK, Wilks JC, Marlow JJ, Coleman ML & Newman DK (2012) BqsR/BqsS constitute a two-component system that senses extracellular Fe(II) in *Pseudomonas aeruginosa*. *J Bacteriol* **194**: 1195–1204
- Ma Z, Shen X, Hu H, Wang W, Peng H, Xu P & Zhang X (2012) Genome sequence of *Sphingomonas wittichii* DP58, the first reported phenazine-1-carboxylic acid-degrading strain. *J Bacteriol* **194**: 3535–3536
- Maddula VSRK, Pierson EA & Pierson LS (2008) Altering the ratio of phenazines in *Pseudomonas chlororaphis (aureofaciens)* strain 30-84: effects on biofilm formation and pathogen inhibition. *J Bacteriol* **190**: 2759–2766
- Maddula VSRK, Zhang Z, Pierson EA & Pierson LS (2006) Quorum sensing and phenazines are involved in biofilm formation by *Pseudomonas chlororaphis (aureofaciens)* strain 30-84. *Microb Ecol* **52**: 289–301

- Marsili E, Rollefson JB, Baron DB, Hozalski RM & Bond DR (2008) Microbial biofilm voltammetry: direct electrochemical characterization of catalytic electrode-attached biofilms. *Appl Environ Microbiol* **74**: 7329–7337
- Martínez JL & Rojo F (2011) Metabolic regulation of antibiotic resistance. *FEMS Microbiol Rev* **35**: 768–789
- Mavrodi DV, Blankenfeldt W & Thomashow LS (2006) Phenazine compounds in fluorescent *Pseudomonas* spp. biosynthesis and regulation. *Annu Rev Phytopathol* **44**: 417–445
- Mavrodi DV, Parejko JA, Mavrodi OV, Kwak Y-S, Weller DM, Blankenfeldt W & Thomashow LS (2012) Recent insights into the diversity, frequency and ecological roles of phenazines in fluorescent *Pseudomonas* spp. *Environ Microbiol*
- Mavrodi DV, Peever TL, Mavrodi OV, Parejko JA, Raaijmakers JM, Lemanceau P, Mazurier S, Heide L, Blankenfeldt W, Weller DM & Thomashow LS (2010) Diversity and evolution of the phenazine biosynthesis pathway. *Appl Environ Microbiol* **76**: 866–879
- Mazzola M, Cook RJ, Thomashow LS, Weller DM & Pierson LS (1992) Contribution of phenazine antibiotic biosynthesis to the ecological competence of fluorescent pseudomonads in soil habitats. *Appl Environ Microbiol* **58**: 2616–2624
- Mentel M, Ahuja EG, Mavrodi DV, Breinbauer R, Thomashow LS & Blankenfeldt W (2009) Of two make one: the biosynthesis of phenazines. *Chembiochem* **10**: 2295–2304
- Muller M (2011) Glutathione modulates the toxicity of, but is not a biologically relevant reductant for, the *Pseudomonas aeruginosa* redox toxin pyocyanin. *Free Radic Biol Med* **50**: 971–977
- O'Malley YQ, Reszka KJ, Spitz DR, Denning GM & Britigan BE (2004) *Pseudomonas aeruginosa* pyocyanin directly oxidizes glutathione and decreases its levels in airway epithelial cells. *Am J Physiol-Lung C* **287**: L94–103
- Palmer KL, Aye LM & Whiteley M (2007) Nutritional cues control *Pseudomonas aeruginosa* multicellular behavior in cystic fibrosis sputum. *J Bacteriol* **189**: 8079–8087
- Parejko JA, Mavrodi DV, Mavrodi OV, Weller DM & Thomashow LS (2012) Population structure and diversity of phenazine-1-carboxylic acid producing fluorescent *Pseudomonas* spp. from dryland cereal fields of central Washington State (USA). *Microb Ecol* **64**: 226–241
- Pham TH, Boon N, De Maeyer K, Höfte M, Rabaey K & Verstraete W (2008) Use of *Pseudomonas* species producing phenazine-based metabolites in the anodes of microbial fuel cells to improve electricity generation. *Appl Microbiol Biot* **80**: 985–993
- Price-Whelan A (2009) Physiology and mechanisms of pyocyanin reduction in *Pseudomonas aeruginosa* Ph.D. Thesis. California Institute of Technology, USA
- Price-Whelan A, Dietrich LEP & Newman DK (2006) Rethinking 'secondary' metabolism: physiological roles for phenazine antibiotics. *Nature Chem Biol* **2**: 71–78

- Price-Whelan A, Dietrich LEP & Newman DK (2007) Pyocyanin alters redox homeostasis and carbon flux through central metabolic pathways in *Pseudomonas aeruginosa* PA14. *J Bacteriol* **189**: 6372–6381
- Rabaey K, Boon N, Hofte M & Verstraete W (2005) Microbial phenazine production enhances electron transfer in biofuel cells. *Environ Sci Technol* **39**: 3401–3408
- Rabaey K, Boon N, Siciliano SD, Verhaege M & Verstraete W (2004) Biofuel cells select for microbial consortia that self-mediate electron transfer. *Appl Environ Microbiol* **70**: 5373–5382
- Ramos I, Dietrich LEP, Price-Whelan A & Newman DK (2010) Phenazines affect biofilm formation by *Pseudomonas aeruginosa* in similar ways at various scales. *Res Microbiol* **161**: 187–191
- Recinos DA, Sekedat MD, Hernandez A, Cohen TS, Sakhtah H, Prince AS, Price-Whelan A & Dietrich LEP (2012) Redundant phenazine operons in *Pseudomonas aeruginosa* exhibit environment-dependent expression and differential roles in pathogenicity. *Proc Natl Acad Sci USA* **109**: 19420–19425
- Reid DW, Carroll V, O'May C, Champion A & Kirov SM (2007) Increased airway iron as a potential factor in the persistence of *Pseudomonas aeruginosa* infection in cystic fibrosis. *Eur Respir J* **30**: 286–292
- Slininger PJ & Jackson MA (1992) Nutritional factors regulating growth and accumulation of phenazine 1-carboxylic acid by *Pseudomonas fluorescens* 2-79. *Appl Microbiol Biot* **37**: 388–392
- Slininger PJ & Shea-Wilbur MA (1995) Liquid-culture pH, temperature, and carbon (not nitrogen) source regulate phenazine productivity of the take-all biocontrol agent *Pseudomonas fluorescens* 2-79. *Appl Microbiol Biot* **43**: 794–800
- Sullivan NL, Tzeranis DS, Wang Y, So PTC & Newman DK (2011) Quantifying the dynamics of bacterial secondary metabolites by spectral multiphoton microscopy. *ACS Chem Biol* **6**: 893–899
- Tunney MM, Field TR, Moriarty TF, Patrick S, Doering G, Muhlebach MS, Wolfgang MC, Boucher R, Gilpin DF, McDowell A & Elborn JS (2008) Detection of anaerobic bacteria in high numbers in sputum from patients with cystic fibrosis. *Am J Respir Crit Care Med* **177**: 995–1001
- Turner JM & Messenger AJ (1986) Occurrence, biochemistry and physiology of phenazine pigment production. *Adv Microb Physiol* **27**: 211–275
- van Rij ET, Wesselink M, Chin-A-Woeng TFC, Bloemberg GV & Lugtenberg BJJ (2004) Influence of environmental conditions on the production of phenazine-1-carboxamide by *Pseudomonas chlororaphis* PCL1391. *Mol Microbiol* **17**: 557–566
- Wang Y & Newman DK (2008) Redox reactions of phenazine antibiotics with ferric (hydr)oxides and molecular oxygen. *Environ Sci Technol* **42**: 2380–2386

- Wang Y, Kern SE & Newman DK (2010) Endogenous phenazine antibiotics promote anaerobic survival of *Pseudomonas aeruginosa* via extracellular electron transfer. *J Bacteriol* **192**: 365–369
- Wang Y, Wilks JC, Danhorn T, Ramos I, Croal L & Newman DK (2011) Phenazine-1-carboxylic acid promotes bacterial biofilm development via ferrous iron acquisition. *J Bacteriol* **193**: 3606–3617
- Worlitzsch D, Tarran R, Ulrich M, Schwab U, Cekici A, Meyer KC, Birrer P, Bellon G, Berger J, Weiss T, Botzenhart K, Yankaskas JR, Randell S, Boucher RC & Döring G (2002) Effects of reduced mucus oxygen concentration in airway *Pseudomonas* infections of cystic fibrosis patients. *J. Clin. Invest.* **109**: 317–325
- Wurtzel O, Yoder-Himes DR, Han K, Dandekar AA, Edelheit S, Greenberg EP, Sorek R & Lory S (2012) The single-nucleotide resolution transcriptome of *Pseudomonas aeruginosa* grown in body temperature. *PLoS Pathog* **8**: e1002945
- Yang Z-J, Wang W, Jin Y, Hu H-B, Zhang X-H & Xu Y-Q (2007) Isolation, identification, and degradation characteristics of phenazine-1-carboxylic acid-degrading strain *Sphingomonas* sp. DP58. *Curr Microbiol* **55**: 284–287

## Figures

**Figure 1.** Phenazines are redox-active, heterocyclic small molecules with a core structure as indicated in **a**). Through a two-electron, two-proton transformation, phenazines can reversibly undergo oxidation and reduction at the central nitrogen atoms. **b**) Phenazine-1-carboxylate and pyocyanin are examples of phenazines produced by *P. aeruginosa*. Their oxidized forms are shown.

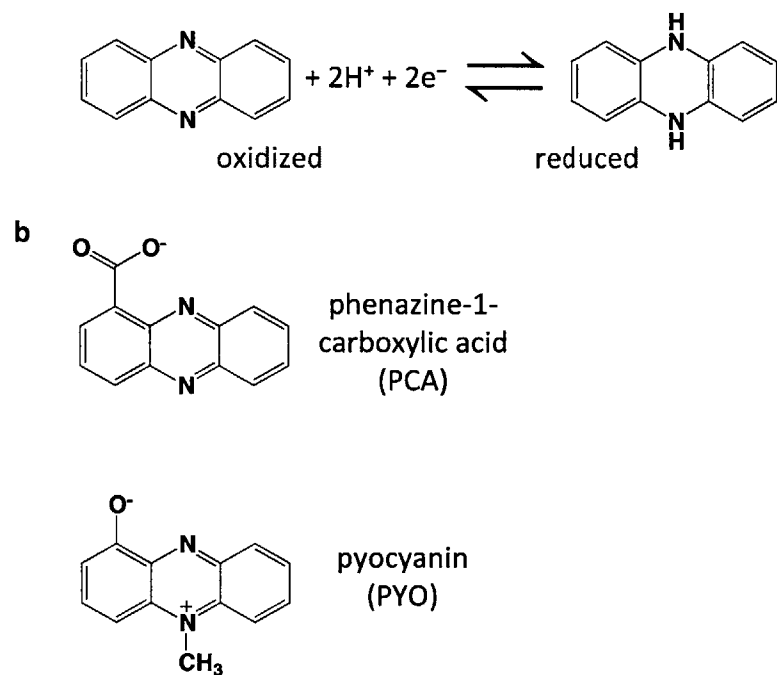


**Figure 2.** Standard reduction potentials of biologically relevant molecules. As indicated by the equation  $\Delta G = -nFE$  — where  $\Delta G$  is the free energy of a system,  $n$  is the number of electrons transferred in a reaction, and  $E$  is the potential (in Volts) for the reduction and oxidation half reactions—electrons spontaneously move from reduced compounds with more negative reduction potentials to oxidized compounds with more positive reduction potentials. For example, aerobic glucose catabolism involves the oxidation of glucose with the transfer of electrons through components of the respiratory chain—listed in green—to the terminal oxidant,  $O_2$ . Phenazines, for example PCA and PYO (highlighted), can take electrons from NADH or iron-sulfur clusters in proteins (blue), and give up electrons to oxygen, superoxide radical, and Fe(III) (red).

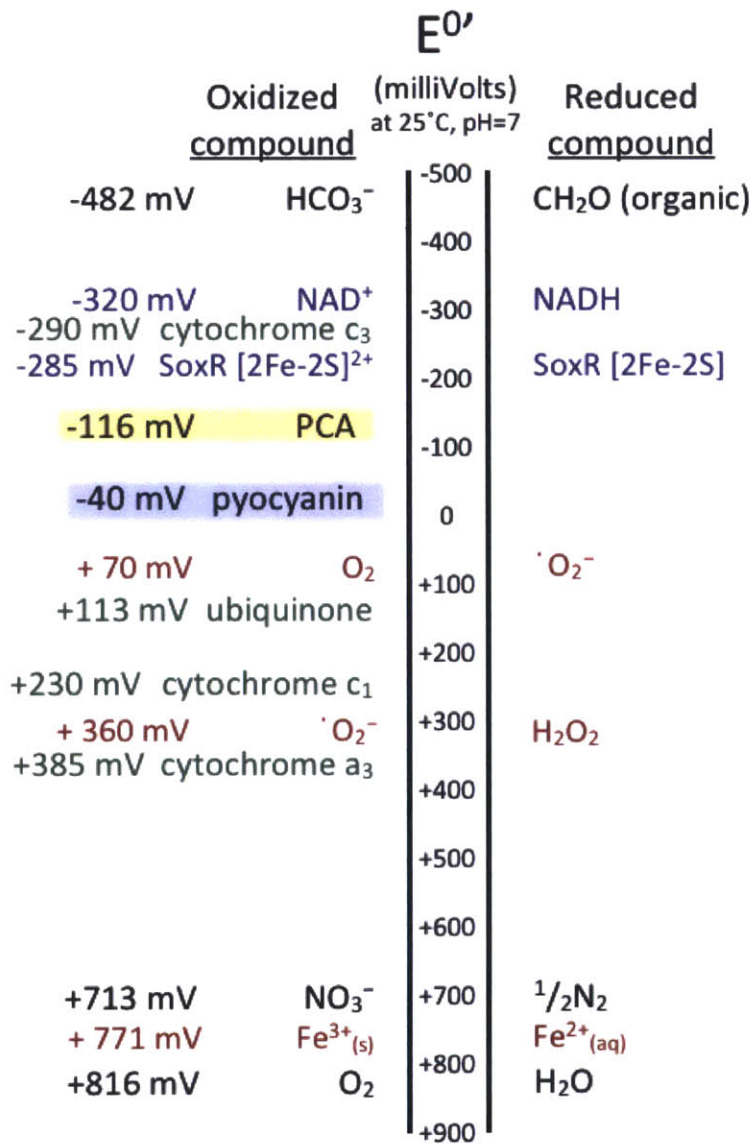


**Figure 3.** Biofilms are clusters of cells enclosed in a polymeric matrix. Chemical, physical, and metabolic heterogeneity characterizes these structures. For example, cells at the liquid interface (blue star) have access to higher levels of oxygen than cells at the biofilm's base due to the depletion of oxygen throughout the biofilm by cellular respiration. Phenazine redox cycling might sustain essential metabolism by offering an alternative electron sink when oxygen is absent (red star). Reduced phenazines can undergo oxidation upon interaction with a number of compounds that might be external to the biofilm ( $X_{ox}$ ), such as oxygen, Fe(III), or a properly poised oxidizing electrode.

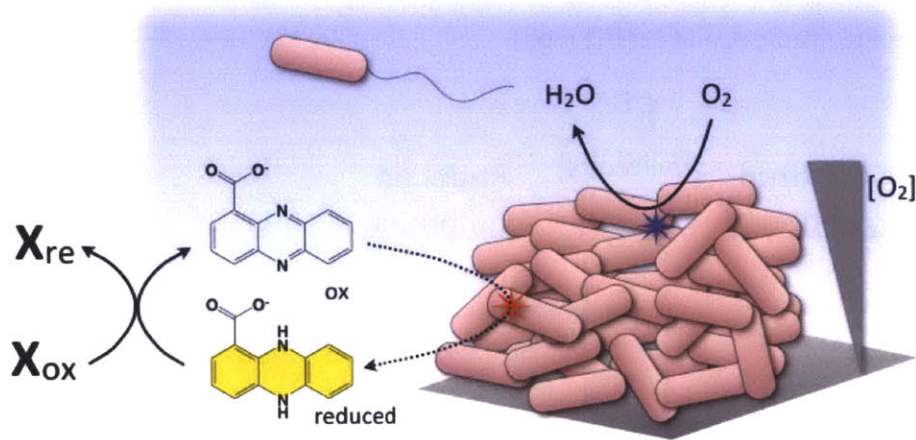
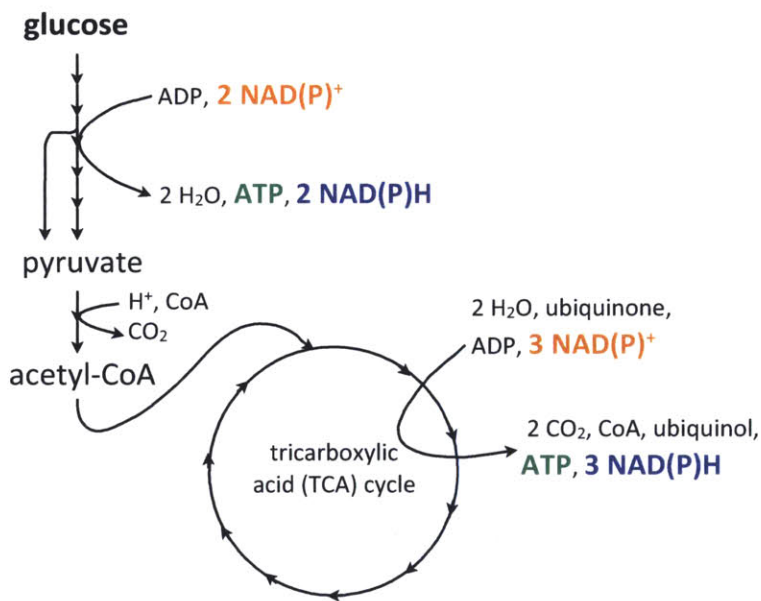




**Figure 4.** a) Aerobic glucose metabolism in *P. aeruginosa* follows the Entner-Doudoroff pathway, which generates two pyruvate molecules, one molecule of ATP and two reduced nicotinamide cofactors. Each pyruvate molecule can yield 3 more reducing equivalents and one ATP through the tricarboxylic acid cycle. b) NADH can contribute electrons to the *P. aeruginosa* respiratory chain, which transfers electrons to quinones, cytochromes and, finally, to oxygen, along the way pumping protons out of the cytoplasm. This proton motive force can be used to phosphorylate ADP by the membrane-bound F<sub>1</sub>F<sub>0</sub> ATP synthase. From a single glucose as many as 35 ATP molecules may be made through aerobic respiration.

**a**



**b**

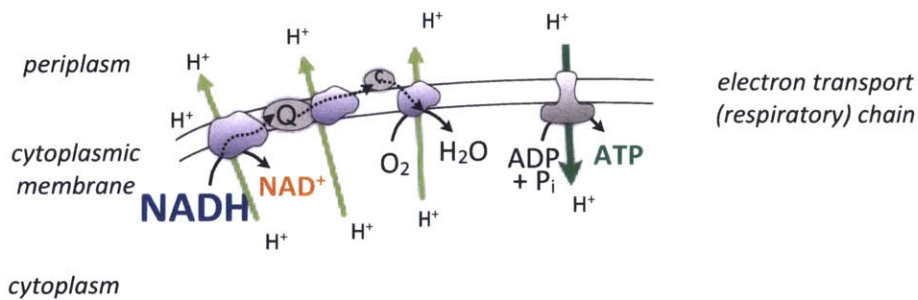
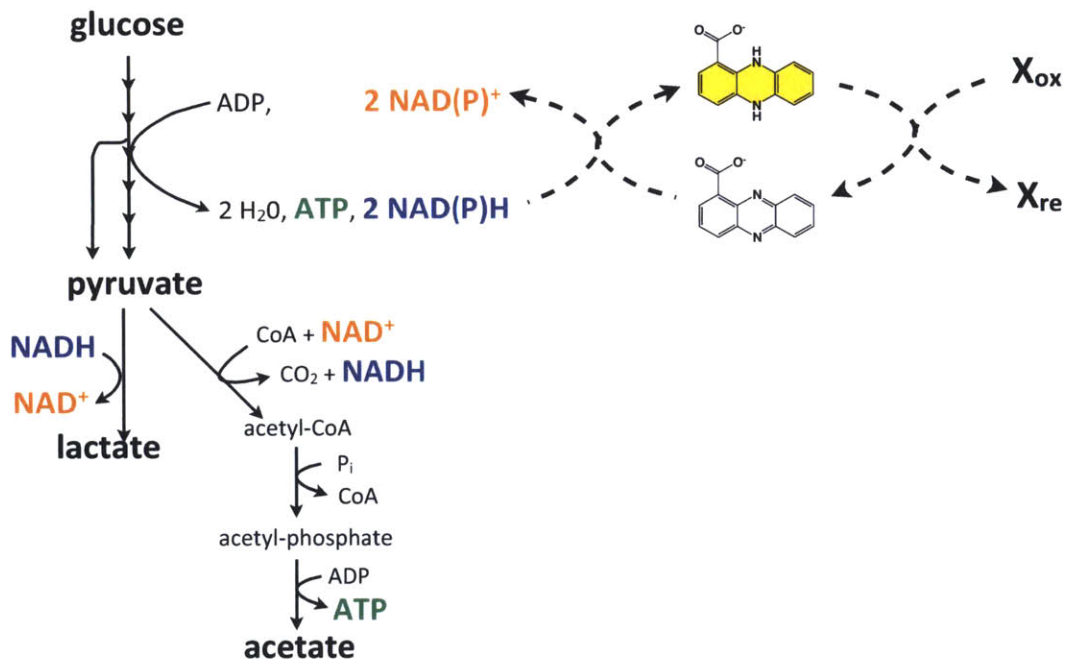


**Figure 5.** *P. aeruginosa* can survive (but not grow) anaerobically with pyruvate as its sole carbon and electron source, however, cells die rapidly when provided with glucose in the absence of a respiratory oxidant. Glucose oxidation can only proceed when NAD(P)H, which is generated by the Entner-Doudoroff pathway, is re-oxidized to NAD(P)<sup>+</sup> (see Figure 4). Phenazine redox cycling oxidizes the NAD(P)H pool and enables anaerobic survival of *P. aeruginosa* when glucose is present, likely by facilitating the conversion of glucose to pyruvate, a fermentable substrate.



## Chapter 3

### **Endogenous phenazine “antibiotics” promote anaerobic survival of *Pseudomonas aeruginosa* via extracellular electron transfer**

Yun Wang, Suzanne E. Kern, Dianne K. Newman

This chapter is reformatted from the published manuscript: Wang Y, Kern SE & Newman DK (2010) Endogenous phenazine antibiotics promote anaerobic survival of *Pseudomonas aeruginosa* via extracellular electron transfer. *Journal of Bacteriology* **192**: 365–369.

#### Contributions:

I performed the initial experiments using this new experimental setup during my rotation in the Newman Lab, however the data and figures presented here are entirely the work of Yun Wang. I contributed to discussions of experimental design and to the writing of this manuscript.

## Abstract

Antibiotics are increasingly recognized as having other, important physiological functions for the cells that produce them. An example of this is the effect phenazines have on signaling and community development for *Pseudomonas aeruginosa* (e.g. Dietrich *et al*, 2008). Here we show that phenazine-facilitated electron transfer to poised-potential electrodes promotes anaerobic survival but not growth of *Pseudomonas aeruginosa* PA14 under conditions of oxidant limitation. Other electron shuttles that are reduced but not made by PA14 do not facilitate survival, suggesting the survival effect is specific to endogenous phenazines.

## Introduction

Phenazines have long been recognized for their redox properties. While most attention concerning their redox activity has focused on their role in generating reactive oxygen species in the context of infection (Hassan & Fridovich, 1980; Hassett *et al*, 1992; Lau *et al*, 2004a; Mahajan-Miklos *et al*, 1999), as early as 1931, Friedheim hypothesized that phenazine reduction might benefit producer cells as an alternative respiratory pigment (Friedheim, 1931). Several years ago, our group suggested that the context in which this might be most important would be in biofilms, where cell densities are high and access to oxidants is limited (Hernandez & Newman, 2001; Price-Whelan *et al*, 2006); consistent with this, we recently showed that mutants unable to produce phenazines are defective in community development (Dietrich *et al*, 2008). While this phenotype is likely due to many factors, including a signaling function for phenazines in later stages of growth (Dietrich *et al*, 2006), given the 1931 hypothesis by Friedheim (Friedheim, 1931) and our related recent work demonstrating that phenazines control redox homeostasis in *P. aeruginosa* (Price-Whelan *et al*, 2007), we reasoned that phenazines might contribute to the survival of cells experiencing oxidant limitation.

As a first step towards testing this, we investigated the effect of redox-active small molecules on anaerobic survival of *P. aeruginosa* PA14 in stationary phase planktonic cultures. We justified beginning with planktonic cultures rather than biofilms based on previous studies which have suggested that cells in stationary phase planktonic culture physiologically resemble cells in established biofilms (Hentzer *et al*, 1999; Spoering & Lewis,

2001; Waite *et al*, 2005). Moreover, by working with cells in planktonic cultures, we could build on voltammetric methods that had previously been used to determine how *E. coli*'s metabolism changes in the presence of the synthetic redox-shuttle ferricyanide (Emde *et al*, 1989). Similar voltammetric approaches have also been used to study how phenazines (Rabaey *et al*, 2005; 2004) and structurally related flavins (Marsili *et al*, 2008) mediate power generation by microbial fuel cells.

## Methods

### Bioreactor setup

We assembled bulk electrolysis-based glass bioreactors housed within an O<sub>2</sub>- and H<sub>2</sub>-free glovebox (MBraun) and controlled by a multichannel potentiostat (Gamry, Series G 300) outside the glovebox. Each bioreactor held a graphite rod working electrode (Alfa Aesar) with an operating surface area of 6 cm<sup>2</sup>, a Ag/AgCl reference electrode (BASi, RE-5B) with a constant potential of +207 mV vs. the normal hydrogen electrode (NHE), and about 100 mL MOPS culture medium [100 mM MOPS at pH 7.2, 93 mM NH<sub>4</sub>Cl, 43 mM NaCl, 2.2 mM KH<sub>2</sub>PO<sub>4</sub>, 1 mM MgSO<sub>4</sub>, 5.0 μM FeCl<sub>3</sub>] (modified from (Palmer *et al*, 2005)). The bioreactor was joined by a fritted glass junction to a small side chamber, in which a Pt counter electrode made from Pt mesh (Alfa Aesar) soldered to a copper wire completed the circuit. In order to selectively examine different redox-active small molecules, we used the phenazine-null mutant of PA14 ( $\Delta phz$ ) which is deleted in its two phenazine biosynthetic operons (Dietrich *et al*, 2006).

### Survival assay

We began by focusing on three endogenous phenazines – pyocyanin (PYO), phenazine-1-carboxylic acid (PCA), and 1-hydroxyphenazine (1-OHPHZ) – that are known to be excreted by PA14 during stationary phase growth cycle in laboratory cultures (Dietrich *et al*, 2006; Ingram & Blackwood, 1970). We harvested cells from cultures grown aerobically on Luria-Bertani (LB, Fisher Scientific) medium at 37 °C, and concentrated and resuspended them in anaerobic MOPS medium at 10<sup>9</sup> CFU/mL. These resuspended cells were incubated in bioreactors over a period of seven days at 30 °C. To perform the survival experiments, we incubated dense suspensions (10<sup>9</sup> cells/mL) in the MOPS medium containing 20 mM D-

glucose to ensure excess electron donor, added ~90  $\mu$ M phenazine (PYO, or PCA, or 1-OHPHZ), and poised the working electrode at +200 mV vs. NHE to make certain it was just high enough to efficiently oxidize bacterially-reduced phenazine but not other medium components (*e.g.*, D-glucose).

## Results

### Phenazine characterization

To confirm the poised potential was appropriate to ensure phenazine was the sole reversible redox-active component, we compared cyclic voltammetry (CV) of  $\Delta phz$  cultures with or without phenazine at the time point immediately prior to the start of the survival test. Using the CV method described in detail previously (Wang & Newman, 2008), we found that  $\Delta phz$  cultures supplemented with phenazine exhibited single anodic (oxidation) and cathodic (reduction) peaks; these peaks were absent when phenazine was not present. This is illustrated in Figure 1 for PYO. For  $\Delta phz$  cultures supplemented with phenazine, we collected supernatants at the beginning and the end of each survival test for HPLC analyses using a previously developed method (Dietrich *et al*, 2006). In both cases, HPLC samples yielded the same single phenazine peak with characteristic peak size, implying degradation did not occur in these experiments.

### Anaerobic survival

Throughout the incubation period, we continuously recorded the anodic (oxidation) current as well as the charge transferred due to the oxidation of electrochemically active component(s) at the working electrode. Periodically, we sampled to measure viability by means of counting colony forming units (CFU) on LB agar (Eschbach *et al*, 2004).

### Survival with phenazines

We observed that the  $\Delta phz$  mutant maintained a constant viable cell number at the original  $10^9$  CFU/mL over seven days, characteristic of survival but not growth (Fig. 2). In contrast, when we incubated the  $\Delta phz$  mutant in the bioreactors without adding phenazine or applying a potential, or both, the cells sustained their viability up to day 3, and then dropped logarithmically down to 0.1-1% of the original  $10^9$  CFU/mL by day 7 (Fig. 2).

Our electrochemical observations were in agreement with the CFU results. Without phenazine supplementation, we observed a constant anodic current in the range of 5-10  $\mu\text{A}$  with the poised potential, most likely reflecting a background current due to slow oxidation of medium components, which was not able to help *Aphz* survive over 7 days. In the presence of phenazine, however, the anodic current increased from the background level to  $80\pm 10 \mu\text{A}$  for PYO and PCA,  $45\pm 10 \mu\text{A}$  for 1-OHPHZ within 2 hours, and stayed at the high current levels with slow decay (less than 20%) throughout the incubation period. The slow current decay was likely due to electrode fouling (Marsili *et al*, 2008) and/or the accumulation of toxic metabolic byproducts in the batch reactors over time. The facile reversibility of redox-active phenazines, which are reduced within the bacterial cell and oxidized outside the cell by the working electrode, led to the high current readings and was key to *Aphz* survival.

We then estimated the average number of redox cycles (defined as “a”) for each phenazine molecule, which is known to undergo two-electron oxidation-reduction (Wang & Newman, 2008), throughout the 7-day incubation based on the equation (Eq. 1) adapted from Faraday’s law for bulk electrolysis (Bard & Faulkner, 2000):

$$Q = 2FN = 2F(acv) \quad [1]$$

with  $c$  as phenazine concentration (M),  $v$  as reaction volume (L), and  $F$  as Faraday’s constant (96,485 coulombs/mole),  $N (= acv)$  as the amount of phenazine (in moles) involved in the electrolysis,  $Q$  (in coulombs) as the net charge quantity associated with the electrochemical oxidation of reduced phenazine during the electrolysis (by subtracting the background charge without phenazine from the total charge passed with phenazine). By recording  $Q$ , and knowing  $c$  and  $v$ , we calculated the number of redox cycles over 7 days for PYO, PCA, and 1-OHPHZ to be 31, 22, and 14, respectively. Moreover, each of the three phenazines showed the color characteristic of its oxidized form during redox cycling rather than its reduced form, which was apparent when cycling was prevented by not applying the poised potential (Wang & Newman, 2008); this indicated that intracellular phenazine reduction was the rate-limiting step of each redox cycle. In addition, we observed a correlation between the reaction kinetics and phenazine thermodynamic properties: both phenazine reduction potential (see Table 1) and the intracellular reduction rate decreased in the order: PYO > PCA > 1-OHPHZ. In summary, despite different electron shuttling

efficiencies, all three phenazines supported *Δphz* survival equally well within the testing period by acting as electron acceptors (Fig. 2).

By comparing the survival of *Δphz* in medium with or without D-glucose in pair wise experiments, we confirmed that D-glucose was the electron donor promoting survival in the presence of phenazines. As shown in Fig. 3, without D-glucose, but with added PYO and a poised potential, *Δphz* maintained a constant viable cell number of  $10^9$  CFU/mL for just 2 days and then dropped by 4 orders of magnitude by day 6. These results also indicate that survival over the first 2-3 days is independent of phenazine electron shuttling and glucose utilization. As has been observed, bacterial cells are able to store internal energy reserves to support their short-term survival, which might explain this effect (Dawes & Ribbons, 1964; Kadouri *et al*, 2005). Phenazine electron shuttling supported survival but not growth even when cells were suspended at much lower initial concentrations ( $10^7$  CFU/mL), indicating that the survival effect was independent of the concentration of cells.

#### **No survival with other redox active compounds**

To determine whether the observed electron shuttling-promoted survival was specific to *P. aeruginosa*'s endogenous phenazines or more general, we performed analogous bioreactor experiments with four other redox-active compounds (listed in Table 1).

Methylene blue (MB) is a synthetic compound that shares the core redox-active structure of natural phenazines. Its cyclic voltammogram at pH 7 exhibited reversible voltammetry peaks centered at 0 mV (vs. NHE) (Table 1), about 40 mV higher than the phenazine PYO, indicating that MB was electrochemically redox active. In the survival control experiments without a poised potential, the color of MB changed from blue (its oxidized form) to colorless (its reduced form), confirming that MB was reduced intracellularly. In contrast, during the survival experiments with the poised potential, MB remained blue, suggesting that reduced MB can be readily oxidized at the electrode surface. Unlike PYO, however, the redox cycling of MB was so inefficient that the current ( $\sim 12$   $\mu$ A) with MB was only marginally higher than the background current (5-10  $\mu$ A), and we estimated that MB oxidation-reduction only cycled 3 times over 7 days. The viable cells dropped 3 orders of magnitude regardless of bioreactor experimental conditions, i.e., with or without MB being added, and/or a potential being applied, revealing that MB redox cycling cannot support *Δphz* survival.



2,6-AQDS, the well-studied anthraquinone-type exogenous electron shuttle used by *Shewanella* and *Geobacter* species among others (Lovley *et al*, 1996; Newman & Kolter, 2000), has a reduction potential similar to the phenazine 1-OHPHZ (Table 1). In contrast to 1-OHPHZ, we did not observe 2,6-AQDS redox cycling between the electrode surface and  $\Delta phz$  cells, due to apparently slow intracellular 2,6-AQDS reduction. After 7 days' incubation, the cell cultures of the control conditions (no potential applied) showed a faint orange color. Considering that oxidized 2,6-AQDS is colorless and the reduced form is bright red-orange in the 100  $\mu$ M concentration range (Newman & Kolter, 2000), this indicated that only a small portion of 2,6-AQDS was reduced. Consistent with this observation, 2,6-AQDS was not able to support  $\Delta phz$  survival as measured by viable cell counts.

Paraquat is a redox-active compound that undergoes reversible single electron transfer between the colorless oxidized form and the blue-colored reduced radical with a reduction potential (-446 mV vs. NHE, pH 7) lower than most cellular reducing equivalents (*e.g.*, NAD(P)H, reduced glutathione) (Michaelis & Hill, 1933a; 1933b). Despite its low reduction potential, paraquat is known for its ability to undergo *in vivo* redox cycling in some eukaryotic and bacterial cells (Bus & Gibson, 1984). The reduced paraquat radical produced during this process can react with intracellular oxygen and catalyze the formation of toxic superoxide radical (Bus & Gibson, 1984) via a mechanism similar to that of PYO-induced toxicity under aerobic conditions (Hassan & Fridovich, 1980; Hassett *et al*, 1992; Lau *et al*, 2004a; Mahajan-Miklos *et al*, 1999). In contrast to PYO, we did not observe paraquat electron shuttling between the electrode surface and  $\Delta phz$  cells because it cannot be reduced by  $\Delta phz$ . We did not observe any reduction-associated color change or current readings higher than the background level. Not surprisingly, paraquat supplementation did not support anaerobic survival of  $\Delta phz$  according to the CFU measurements.

The last putative electron shuttling compound we tested was homogentisic acid (HMA), a phenolic small molecule known as the primary precursor for synthesizing (pyo)melanin (Chatfield & Cianciotto, 2007; Turick *et al*, 2002). For (pyo)melanin-producing organisms, including some *P. aeruginosa* strains, HMA is secreted in its reduced form, auto-oxidized, and polymerized into red-brown humic-like compound, (pyo)melanin (Chatfield & Cianciotto, 2007; Nosanchuk & Casadevall, 2003; Turick *et al*, 2002), which has been reported to function as an electron shuttle for enhanced Fe(III) reduction in *Shewanella* species (Turick *et al*, 2002). By performing cyclic voltammetry (CV) as described previously

(Wang & Newman, 2008), we determined that HMA is subject to reversible oxidation-reduction via single electron transfer, resulting in a reduction potential of +306 mV vs. NHE (pH 7), higher than the potential applied to test for *Δphz* survival. Consequently, oxidation of HMA by the electrode was not thermodynamically feasible. As expected, HMA could not support *Δphz* survival. Together, these results imply that electron shuttling-promoted *P. aeruginosa* survival is likely to be specific to endogenous phenazines, not other type redox-active molecules. This is likely because sophisticated systems are necessary for controlling the reactivity of these molecules within the cell, and that this machinery has evolved in *Pseudomonads* to be specific for the electron shuttles it produces.

## Summary

In conclusion, this work indicates that “enabling survival” can now be added to the list of roles performed by phenazines for their producers, which includes: altering the intracellular redox state (Price-Whelan *et al*, 2007), making iron more bioavailable by reducing ferric (hydr)oxides (Wang & Newman, 2008), serving as a signaling compound (Dietrich *et al*, 2006), facilitating biofilm development (Dietrich *et al*, 2008; Maddula *et al*, 2006; Ramos *et al*, 2010), contributing to virulence (Lau *et al*, 2004b), and killing microbial competitors (Baron & Rowe, 1981; Hassan & Fridovich, 1980). In mixed species communities where pseudomonads live, be they on the surfaces of plant roots (Mazzola *et al*, 1992) or in the mucus-filled lungs of patients with cystic fibrosis (Costerton *et al*, 1999), it seems possible that phenazines might benefit other organisms in the community as well. Indeed, support for this idea comes from work with *Pseudomonas* species in the context of microbial fuel cells, where it was suggested that other organisms in these consortia engage in redox shuttling using the phenazines produced by *P. aeruginosa* (Rabaey *et al*, 2004; 2005). Whether these types of beneficial effects contribute to shaping the ecological structure of the communities phenazine-producing pseudomonads inhabit remains to be determined.

## Acknowledgements

We thank Jordan Katz for his help with making the Pt mesh counter electrodes, and Alexa Price-Whelan and other Newman lab members for discussions. This work was supported

by grants to D. K. N. from Packard Foundation and Howard Hughes Medical Institute, and a NSF graduate research fellowship to S.E.K.. D.K.N. is an Investigator of the Howard Hughes Medical Institute.

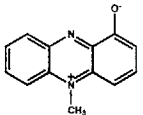
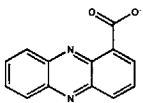
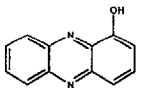
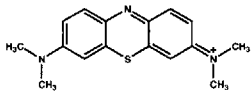
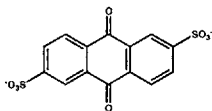
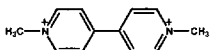
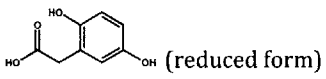
## References

- Bard AJ & Faulkner LR (2000) *Electrochemical Methods: Fundamentals and Applications* New York: Wiley.
- Baron SS & Rowe JJ (1981) Antibiotic action of pyocyanin. *Antimicrob Agents Chemother* **20**: 814–820.
- Bus JS & Gibson JE (1984) Paraquat: model for oxidant-initiated toxicity. *Environ Health Perspect* **55**: 37–46.
- Chatfield CH & Cianciotto NP (2007) The secreted pyomelanin pigment of *Legionella pneumophila* confers ferric reductase activity. *Infect Immun* **75**: 4062–4070.
- Costerton JW, Stewart PS & Greenberg EP (1999) Bacterial biofilms: a common cause of persistent infections. *Science* **284**: 1318–1322.
- Dawes EA & Ribbons DW (1964) Some aspects of the endogenous metabolism of bacteria. *Bacteriol Rev* **28**: 126–149.
- Dietrich LEP, Price-Whelan A, Petersen A, Whiteley M & Newman DK (2006) The phenazine pyocyanin is a terminal signalling factor in the quorum sensing network of *Pseudomonas aeruginosa*. *Mol Microbiol* **61**: 1308–1321.
- Dietrich LEP, Teal TK, Price-Whelan A & Newman DK (2008) Redox-active antibiotics control gene expression and community behavior in divergent bacteria. *Science* **321**: 1203–1206.
- Emde R, Swain A & Schink B (1989) Anaerobic oxidation of glycerol by *Escherichia coli* in an amperometric poised-potential culture system. *Appl Microbiol Biot* **32**: 170–175.
- Eschbach M, Schreiber K, Trunk K, Buer J, Jahn D & Schobert M (2004) Long-term anaerobic survival of the opportunistic pathogen *Pseudomonas aeruginosa* via pyruvate fermentation. *J Bacteriol* **186**: 4596–4604.
- Friedheim EA (1931) Pyocyanine, an accessory respiratory enzyme. *J Exp Med* **54**: 207–221.
- Fultz ML & Durst RA (1982) Mediator compounds for the electrochemical study of biological redox systems: a compilation. *Anal Chim Acta* **140**: 1–18.
- Hassan HM & Fridovich I (1980) Mechanism of the antibiotic action of pyocyanine. *J Bacteriol* **141**: 156–163.
- Hassett DJ, Charniga L, Bean K, Ohman DE & Cohen MS (1992) Response of *Pseudomonas aeruginosa* to pyocyanin: mechanisms of resistance, antioxidant defenses, and demonstration of a manganese-cofactored superoxide dismutase. *Infect Immun* **60**: 328–336.
- Hentzer M, Eberl L & Givskov M (1999) Transcriptome analysis of *Pseudomonas aeruginosa* biofilm development: anaerobic respiration and iron limitation. *Biofilms* **2**: 37–61.

- Hernandez ME & Newman DK (2001) Extracellular electron transfer. *Cell Mol Life Sci* **58**: 1562–1571.
- Ingram J & Blackwood A (1970) Microbial Production of Phenazines. *Adv Appl Microbiol* **13**: 267–282.
- Kadouri D, Jurkevitch E, Okon Y & Castro-Sowinski S (2005) Ecological and agricultural significance of bacterial polyhydroxyalkanoates. *Crit Rev Microbiol* **31**: 55–67.
- Lau GW, Hassett DJ, Ran H & Kong F (2004a) The role of pyocyanin in *Pseudomonas aeruginosa* infection. *Trends Mol Med* **10**: 599–606.
- Lau GW, Ran H, Kong F, Hassett DJ & Mavrodi D (2004b) *Pseudomonas aeruginosa* pyocyanin is critical for lung infection in mice. *Infect Immun* **72**: 4275–4278.
- Lovley DR, Coates JD, Blunt-Harris EL & Phillips E (1996) Humic substances as electron acceptors for microbial respiration. *Nature* **382**: 445–448.
- Maddula VSRK, Zhang Z, Pierson EA & Pierson LS (2006) Quorum sensing and phenazines are involved in biofilm formation by *Pseudomonas chlororaphis* (*aureofaciens*) strain 30-84. *Microb Ecol* **52**: 289–301.
- Mahajan-Miklos S, Tan MW, Rahme LG & Ausubel FM (1999) Molecular mechanisms of bacterial virulence elucidated using a *Pseudomonas aeruginosa*–*Caenorhabditis elegans* pathogenesis model. *Cell* **96**: 47–56.
- Marsili E, Rollefson JB, Baron DB, Hozalski RM & Bond DR (2008) Microbial biofilm voltammetry: direct electrochemical characterization of catalytic electrode-attached biofilms. *Appl Environ Microbiol* **74**: 7329–7337.
- Mazzola M, Cook RJ, Thomashow LS, Weller DM & Pierson LS (1992) Contribution of phenazine antibiotic biosynthesis to the ecological competence of fluorescent pseudomonads in soil habitats. *Appl Environ Microbiol* **58**: 2616–2624.
- Michaelis L & Hill ES (1933a) Potentiometric studies on semiquinones. *J Am Chem Soc* **55**: 1481–1494.
- Michaelis L & Hill ES (1933b) The viologen indicators. *J Gen Physiol* **16**: 859–873.
- Newman DK & Kolter R (2000) A role for excreted quinones in extracellular electron transfer. *Nature* **405**: 94–97.
- Nosanchuk JD & Casadevall A (2003) The contribution of melanin to microbial pathogenesis. *Cell Microbiol* **5**: 203–223.
- Palmer K, Mashburn L & Singh P (2005) Cystic fibrosis sputum supports growth and cues key aspects of *Pseudomonas aeruginosa* physiology. *J Bacteriol* **187**: 5267–5277.
- Price-Whelan A, Dietrich LEP & Newman DK (2006) Rethinking ‘secondary’ metabolism: physiological roles for phenazine antibiotics. *Nature Chem Biol* **2**: 71–78.

- Price-Whelan A, Dietrich LEP & Newman DK (2007) Pyocyanin alters redox homeostasis and carbon flux through central metabolic pathways in *Pseudomonas aeruginosa* PA14. *J Bacteriol* **189**: 6372–6381.
- Rabaey K, Boon N, Hofte M & Verstraete W (2005) Microbial phenazine production enhances electron transfer in biofuel cells. *Environ Health Perspect* **39**: 3401–3408.
- Rabaey K, Boon N, Siciliano SD, Verhaege M & Verstraete W (2004) Biofuel cells select for microbial consortia that self-mediate electron transfer. *Appl Environ Microbiol* **70**: 5373–5382.
- Ramos I, Dietrich LEP, Price-Whelan A & Newman DK (2010) Phenazines affect biofilm formation by *Pseudomonas aeruginosa* in similar ways at various scales. *Res Microbiol* **161**: 187–191.
- Spoering AL & Lewis K (2001) Biofilms and planktonic cells of *Pseudomonas aeruginosa* have similar resistance to killing by antimicrobials. *J Bacteriol* **183**: 6746–6751.
- Turick CE, Tisa LS & Caccavo F (2002) Melanin production and use as a soluble electron shuttle for Fe(III) oxide reduction and as a terminal electron acceptor by *Shewanella algae* BrY. *Appl Environ Microbiol* **68**: 2436–2444.
- Waite RD, Papakonstantinou A, Littler E & Curtis MA (2005) Transcriptome analysis of *Pseudomonas aeruginosa* growth: comparison of gene expression in planktonic cultures and developing and mature biofilms. *J Bacteriol* **187**: 6571–6576.
- Wang Y & Newman DK (2008) Redox reactions of phenazine antibiotics with ferric (hydr)oxides and molecular oxygen. *Environ Health Perspect* **42**: 2380–2386.

**Table 1.** Endogenous phenazines and other type redox-active compounds used in this study: properties and results summarized from experiments for testing their roles in promoting anaerobic survival of *P. aeruginosa*.

Chemical name (Abbreviation)	Structure (Oxidized form unless stated otherwise)	$E_0'$ (vs. NHE) (mV)	# of Redox cycles in 7 days	Support survival?	Reduction by PA14?
Pyocyanin (PYO)		-40 <sup>a</sup>	31	Yes	Yes
Phenazine-1-carboxylate (PCA)		-114 <sup>a</sup>	22	Yes	Yes
1-Hydroxyphenazine (1- OHPHZ)		-174 <sup>a</sup>	14	Yes	Yes
Methylene blue (MB)		0 <sup>b</sup> +11 <sup>c</sup>	3	No	Yes
2,6-AQDS		-184 <sup>d</sup>	No cycle	No	Yes (very slowly)
Paraquat		-446 <sup>e</sup>	No cycle	No	No
Homogentisic acid (HMA)	 (reduced form)	+306 <sup>b</sup>	No cycle	No	-

<sup>a</sup> from Wang & Newman, 2008

<sup>b</sup>  $E_0'$  values were measured in aqueous solution at pH 7 in this study

<sup>c</sup> from Fultz & Durst, 1982

<sup>d</sup> from Hernandez & Newman, 2001

<sup>e</sup> from Michaelis & Hill, 1933a; 1933b

“-” not applicable, present in its reduced form

**Figure 1.** Representative cyclic voltammetry (CV) of *P. aeruginosa* PA14  $\Delta phz$  mutant cultures incubated anaerobically in 100 mL MOPS medium containing 20 mM glucose, supplemented with 90  $\mu\text{M}$  PYO (dark trace) versus no PYO (light trace). PYO is the only electrochemically active component with single anodic (oxidation) and cathodic (reduction) peaks characteristic of itself. CV experiments were performed at 100 mV/s with electrodes consisting of a stationary gold disk working electrode (BASi), a Ag/AgCl reference electrode, and a Pt counter electrode.

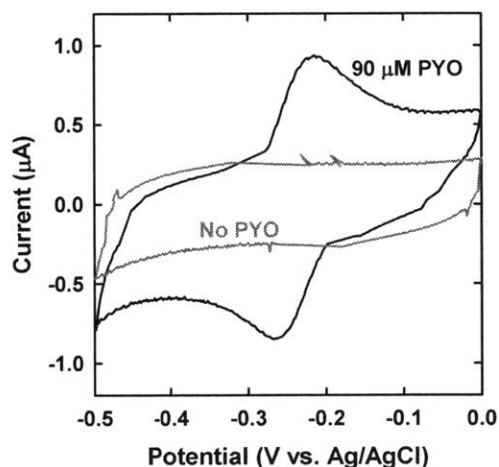




**Figure 2.** a) PYO, b) PCA, and c) 1-OHPHZ function as electron shuttles (■) to promote anaerobic survival of *P. aeruginosa* PA14  $\Delta phz$  mutant when cells are incubated anaerobically in MOPS-buffered medium containing 20 mM D-glucose,  $\sim 90 \mu\text{M}$  phenazine (PYO, or PCA, or 1-OHPHZ), and with the graphite rod working electrode poised at +0.2 V vs. NHE. Survival was determined by measuring colony forming units (CFU) on LB agar plates. CFU of  $\Delta phz$  anaerobic incubations without phenazine (∇), or poised potential (Δ), or both (◇) served as controls. Error bars represent standard deviations from at least triplicate samples in each experimental set. Plots represent results from at least three independent experiments.

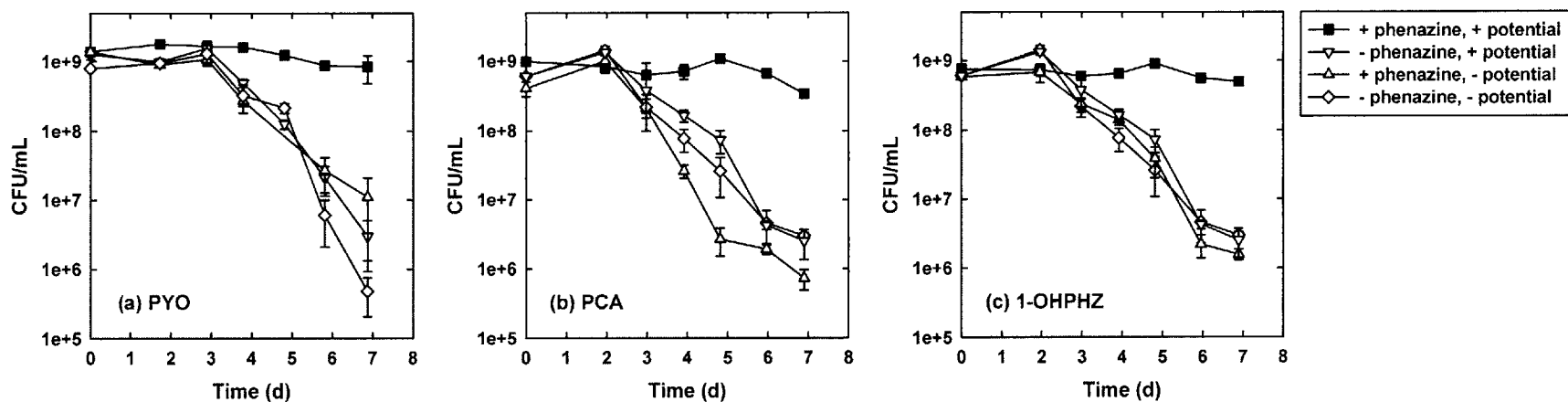
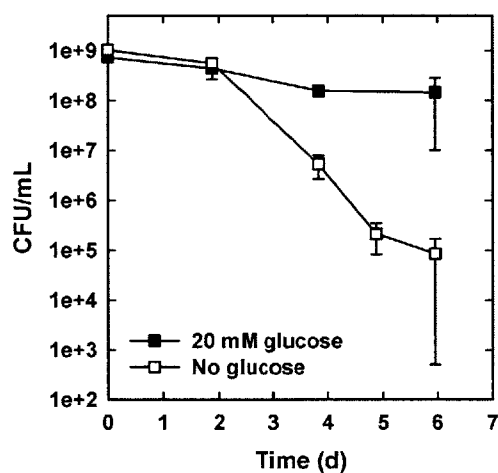


**Figure 3.** Anaerobic survival of *P. aeruginosa* PA14  $\Delta phz$  mutant without D-glucose (□) and in the presence of 20 mM D-glucose (■), for cells incubated in MOPS medium containing ~90  $\mu$ M PYO, and with the graphite rod working electrode poised at +0.2 V vs. NHE. Survival was determined by colony forming units (CFU) on LB agar plates. Error bars represent standard deviations from triplicate samples in each experimental set. Plots represent results from two independent experiments.



## Chapter 4

### ***Pseudomonas aeruginosa* has multiple metabolic pathways that enable anaerobic survival and maintenance of the membrane potential**

Nathaniel R. Glasser, Suzanne E. Kern and Dianne K. Newman

This chapter is a copy of a manuscript in revision following submission and peer review.

#### Contributions:

My contributions include obtaining the data in Figures 1D, 3 and 4, collaboratively planning experiments and assisting with the writing of the manuscript.

## Summary

In search of common mechanisms underpinning the anaerobic survival of *Pseudomonas aeruginosa* strain PA14, we characterized planktonic cultures under different anoxic conditions. In minimal medium, glucose promoted anaerobic survival only in the presence of oxidized phenazine-1-carboxylic acid (PCA) or nitrate, whereas pyruvate or arginine alone promoted anaerobic survival. We characterized ATP levels, NAD(H) concentrations, and the membrane potential for cultures surviving on pyruvate or arginine: viability correlated with elevated ATP levels and maintenance of the membrane potential. Notably, ATP synthesis was coupled to redox homeostasis during pyruvate fermentation, and a mutant deficient in lactate dehydrogenase failed to maintain both redox and ATP homeostasis. PCA redox cycling facilitated survival by promoting glucose oxidation to pyruvate; however, mutants lacking acetate kinase could not be rescued by PCA. During pyruvate fermentation, ATP hydrolysis drove the generation of a proton motive force. Drugs that dissipate the proton motive force or inhibit the F<sub>1</sub>F<sub>0</sub>-ATPase complex reduced the viability of cultures fermenting pyruvate. Because non-replicating cells have been shown to be highly resistant to common antibiotics, our results suggest that targeting multiple physiological states using multiple drugs might lead to improved treatment outcomes for persistent infections.

## Introduction

*Pseudomonas aeruginosa* is a bacterial opportunistic human pathogen that forms persistent infections in the lungs of cystic fibrosis patients. During lung infections, *P. aeruginosa* reportedly forms biofilm-like macrocolonies in the hypoxic intraluminal mucus of the lung (Worlitzsch *et al*, 2009), and microelectrode measurements have shown that oxygen becomes depleted in the interior of biofilms (Xu *et al*, 1998; Werner *et al*, 2004). Given the hypoxic and even anoxic niches in which it thrives, *P. aeruginosa* has surprisingly few annotated anaerobic pathways. In the absence of oxygen, it can grow by respiring nitrate (Carlson & Ingraham, 1983) or by using arginine to generate adenosine triphosphate (ATP) through substrate-level phosphorylation (Vander Wauven *et al*, 1984). *P. aeruginosa* can survive anaerobically by fermenting pyruvate, but this process does not support growth

(Eschbach *et al*, 2004), and *P. aeruginosa* is not known to ferment glucose or other sugars (Barnishan & Ayers, 1979; Eschbach *et al*, 2004).

Microbial stasis is thought to complicate the treatment of many persistent infections. For example, cells at the base of *P. aeruginosa* biofilms enter a dormant state with decreased levels of transcription and translation, and they undergo physiological adaptations to hypoxic conditions (Alvarez-Ortega & Harwood, 2007; Williamson *et al*, 2012). These cells are substantially more resistant to antibiotics than actively growing cells (Williamson *et al*, 2012). Moreover, nutrient deprivation triggers active responses for *P. aeruginosa* that increase antibiotic resistance in growth-arrested cells (Nguyen *et al*, 2011). Even under active growth, many bacterial species maintain a small population of phenotypically resistant cells called persisters (Lewis, 2010). The persister state is thought to be controlled by stochastic changes in cell physiology and metabolism (Keren *et al*, 2004; Lewis, 2010; Allison *et al*, 2011), and metabolic cues can sensitize persister cells to antibiotics (Allison *et al*, 2011). Together, these subpopulations of resistant nonreplicating cells can serve as reservoirs for recurrent infections (Lewis, 2010). Our incomplete understanding of the metabolic changes underpinning microbial dormancy thus limits our ability to effectively treat persistent infections.

Pseudomonads are known for the biosynthesis of a class of low-potential, redox-active pigments collectively termed phenazines (Price-Whelan *et al*, 2006; Mavrodi *et al*, 2006). Phenazines are important virulence factors (Lau *et al*, 2005) that serve as antibiotics towards microbial competitors (Baron & Rowe, 1981) and damage mammalian cells (Britigan *et al*, 1992). Phenazines can benefit *P. aeruginosa* by serving as signaling molecules (Dietrich *et al*, 2006), regulating persister cell formation (Möker *et al*, 2010), influencing colony morphology (Dietrich *et al*, 2008), and promoting iron acquisition and biofilm development (Wang *et al*, 2011). In addition, we previously reported that micromolar levels of phenazines can support anaerobic survival by facilitating electron transfer to an extracellular oxidant in a cyclic manner (Wang *et al*, 2010). Although the physiological mechanism for this phenomenon is unknown, phenazine redox cycling is correlated with a more oxidizing intracellular redox state for planktonic cultures (Price-Whelan *et al*, 2007; Sullivan *et al*, 2011) and colony biofilms (Dietrich *et al*, 2013), suggesting that phenazines alter the metabolism of *P. aeruginosa*. In many cystic fibrosis patients, the sputum of *P. aeruginosa*-infected lungs contains phenazines at concentrations that can support anaerobic survival (Wilson *et al*, 1988; Hunter *et al*, 2012; Wang *et al*,

2010). As infections progress, the concentration of phenazines rises in sputum (Hunter *et al*, 2012), and so phenazines may directly alter the physiology of *P. aeruginosa* infections *in situ*.

In the course of further characterizing phenazine-mediated anaerobic survival, we discovered that oxidized phenazines can facilitate the conversion of glucose to pyruvate, the fermentation of which promotes anaerobic survival (Eschbach *et al*, 2004). To search for common themes in the anaerobic survival of *P. aeruginosa*, we expanded our physiological characterization to include survival on pyruvate, arginine, and nitrate.

## Results

### ***Pseudomonas aeruginosa* has multiple metabolic pathways that enable anaerobic survival**

Pyruvate fermentation promotes the anaerobic survival of *P. aeruginosa* for strain PA01 in minimal medium (Eschbach *et al*, 2004) and strain PA14 in complex medium (Price-Whelan *et al*, 2007). To determine whether pyruvate is sufficient for PA14 survival in the absence of yeast extract, we cultured wildtype *P. aeruginosa* PA14 using pyruvate as the sole carbon source, shifted the cells to an anoxic environment, and resuspended the cells in fresh anoxic medium. Anaerobic cultures with pyruvate survived for at least seven days, while cultures without pyruvate quickly declined in viability as measured by colony forming units (Figure 1a), suggesting that pyruvate alone is sufficient to promote anaerobic survival in strain PA14. In PA14 we observed 50% survival after 7 days of anaerobic incubation with pyruvate.

To confirm that pyruvate utilization promotes survival in *P. aeruginosa* PA14, we tested strains containing clean deletions of genes in the pyruvate fermentation pathway (Figure 2a). A mutant deficient in ATP synthesis from pyruvate,  $\Delta$ *ackA-pta*, displayed a pronounced survival defect after two days of anaerobiosis; in contrast, a mutant deficient in the regeneration of oxidized nicotinamide adenine dinucleotide (NAD<sup>+</sup>) from pyruvate,  $\Delta$ *ldhA*, did not display a survival defect until four days of anaerobiosis (Figure 1a). We also used anion-exchange chromatography to confirm the biosynthesis of acetate, lactate, and succinate from pyruvate as previously reported (Eschbach *et al*, 2004) (Figure 1b). The  $\Delta$ *ackA-pta* and  $\Delta$ *ldhA* mutants produced only trace amounts of acetate, lactate, and succinate, and they did not measurably consume pyruvate (Supplemental Figure 1).

Previous work has reported that arginine metabolism contributes to anaerobic survival in rich medium (Schreiber *et al*, 2006). Arginine is used as a source of ATP during fermentative growth through the arginine deiminase pathway (Vander Wauven *et al*, 1984) (Figure 2b), but to our knowledge there have been no reports of arginine directly enabling survival by serving as the sole energy source. To test if arginine is sufficient for anaerobic survival, we cultured *P. aeruginosa* PA14 using arginine as the sole carbon source, shifted the cells to an anoxic environment, and resuspended the cells in fresh anoxic medium with arginine. As with pyruvate, arginine alone was sufficient as a carbon source to promote anaerobic survival (Figure 1c). Wildtype PA14 dropped to 30% viability after one day of anaerobic incubation and slowly decreased in viability to 15% after seven days. In contrast, cells incubated without arginine declined to 0.1% viability after seven days. A transposon insertion mutant that cannot anaerobically utilize arginine, *arcA::MAR2xT7* (Liberati *et al*, 2006), rapidly declined in viability to 0.01% after seven days despite the presence of arginine (Figure 1c). Similar results were obtained with a second independent transposon insertion mutant, *arcC::MAR2xT7*, encoding another protein in the same pathway (Figure 2b), although the defect was less severe (data not shown). This demonstrates that arginine promotes anaerobic survival through the arginine deiminase pathway.

*P. aeruginosa* can grow anaerobically by respiring nitrate (Carlson & Ingraham, 1983; Van Alst *et al*, 2009). The nitrate reductase Nap is predicted to be a periplasmic protein that supports aerobic denitrification but is dispensable for growth (Williams *et al*, 2007). Nap is thought to support redox homeostasis and influences colony morphology (Dietrich *et al*, 2013). Nar, a second nitrate reductase and the major nitrate respiratory complex, is located at the inner membrane, participates in the electron transport chain, and is required for robust anaerobic growth (Van Alst *et al*, 2009). To test if Nap could contribute to survival in the absence of growth, we incubated a strain (grown aerobically in the presence of nitrate) that was deficient in the Nar complex,  $\Delta narG$ , anaerobically with nitrate in a minimal glucose medium. The  $\Delta narG$  strain demonstrated stronger anaerobic viability than a mutant lacking both nitrate reductases,  $\Delta narG \Delta napA$  (Figure 1d).

### **Phenazine redox cycling promotes survival through pyruvate fermentation**

Phenazines, redox-active small molecules produced by *P. aeruginosa*, oxidize NAD(P)H *in vitro* (Cox, 1986) and *P. aeruginosa* cultures that contain phenazines have a more oxidized intracellular NAD(H) pool than those without (Price-Whelan *et al*, 2007; Sullivan *et al*,

2011). Redox cycling occurs when a phenazine molecule undergoes alternating reduction and oxidation reactions, resulting in the transfer of electrons from the reductant (*e.g.*, NAD(P)H) to the oxidant (*e.g.*, oxygen).

We have previously shown that phenazines can support anaerobic survival by serving as extracellular electron shuttles (Wang *et al*, 2010). We found that a carbon source, specifically glucose, is required for anaerobic survival in the presence of oxidized phenazines (Wang *et al*, 2010). Pyruvate is a downstream product of glucose oxidation through the Entner-Doudoroff pathway (Figure 2c). In the absence of additional electron acceptors, *P. aeruginosa* must reduce pyruvate to lactate in order to regenerate oxidants for glucose catabolism, yielding only a single ATP per glucose (Figure 2c). We therefore hypothesized that phenazines, by serving as an additional electron sink, might allow *P. aeruginosa* to increase the ATP yield from glucose fermentation by enabling the oxidation of glucose to pyruvate and then to acetate.

To address this hypothesis, we tested mutants deficient in pyruvate fermentation in a phenazine cycling survival assay as previously described (Wang *et al*, 2010). In this experiment, early stationary phase cells were resuspended in anoxic, buffered minimal medium containing glucose as the sole energy source. To control the concentration of phenazines, we used strains with deletions in both phenazine biosynthetic operons ( $\Delta phzA1-G1 \Delta phzA2-G2$ , abbreviated  $\Delta phz1/2$ ) (Dietrich *et al*, 2006) and added phenazine-1-carboxylic acid (PCA) to the culture at a physiologically relevant concentration (75  $\mu\text{M}$ ) (Hunter *et al*, 2012). We chose PCA because it is the biosynthetic precursor of all other phenazines in *P. aeruginosa* and other pseudomonads (Mavrodi *et al*, 2001), and also because it is synthesized whether oxygen is present or not (Recinos *et al.*, 2012). While oxygen and ferric iron are likely oxidants of phenazines in infection environments (Hunter *et al*, 2012; Wang *et al*, 2010), we excluded both from the anaerobic culture vessels and instead supplied an electrode poised at a potential sufficient to oxidize phenazines. We detected current through the electrode only when phenazines were present (Wang *et al*, 2010 and data not shown), suggesting that phenazines mediate electron transfer from inside the cells to the electrode. This was consistent with phenazines undergoing redox cycling, since phenazines were present at far lower levels than the reductant, glucose (75  $\mu\text{M}$  vs. 20 mM, respectively).



In this phenazine-cycling survival assay, we found that a strain deficient in NAD<sup>+</sup> regeneration,  $\Delta ldhA$ , was unimpaired in survival relative to wildtype *P. aeruginosa* and maintained 100% viability after six days. A strain deficient in ATP generation from pyruvate,  $\Delta ackA-ptA$ , exhibited a weaker survival phenotype, with about 10% of cells remaining viable after six days (Figure 3a). In comparison, only 1% of wildtype cells remained viable in the absence of phenazine redox cycling (Figure 3a). In addition, the non-fermentable carbon source succinate did not enable survival (Figure 3b). Together these results suggest that phenazine cycling enables survival by increasing the ATP yield from sugar catabolism. In particular, phenazine redox cycling appears to facilitate the conversion of glucose to acetate through the pyruvate fermentation pathway.

### **Survival is correlated with ATP homeostasis, a balanced [NADH]/[NAD<sup>+</sup>] ratio, and a polarized membrane**

From the stoichiometry of pyruvate fermentation, we noted that acetate and lactate synthesis could be coupled through the common cofactor NAD(H) (Figure 2a). Sustained pyruvate oxidation to acetate, and thus ATP synthesis, requires the regeneration of NADH to NAD<sup>+</sup> via pyruvate reduction to lactate. To further explore the relationship between redox and ATP homeostasis, we measured the [NADH]/[NAD<sup>+</sup>] ratios and ATP content of anaerobically surviving *P. aeruginosa* cultures.

Following aerobic growth in a minimal medium amended with 40 mM pyruvate, cultures of PA14 wildtype,  $\Delta ldhA$ , and  $\Delta ackA-ptA$  were washed and resuspended in anoxic medium with fresh pyruvate. Among the cultures incubated with pyruvate, only wildtype PA14 and the  $\Delta ackA-ptA$  mutant maintained an [NADH]/[NAD<sup>+</sup>] ratio of less than one, suggesting that the  $\Delta ackA-ptA$  mutant is capable of NAD<sup>+</sup> regeneration (Figure 4a). The  $\Delta ldhA$  mutant displayed the most reducing ratio, as high as 3, and always greater than wildtype or  $\Delta ackA-ptA$  with pyruvate (Figure 4a). Only wildtype cells with pyruvate maintained a high level of ATP, which was roughly 8-fold higher than the  $\Delta ldhA$  and  $\Delta ackA-ptA$  mutants after 24 hours. Similar to the mutants, wildtype cells incubated without pyruvate rapidly became depleted in ATP levels (Figure 4b). These measurements indicate that LdhA activity can sustain NAD<sup>+</sup> regeneration independently of AckA and Pta, while ATP synthesis through AckA and Pta is dependent on NAD<sup>+</sup> regeneration through LdhA.

A similar experiment was performed using arginine as the sole substrate for anaerobic metabolism, with similar outcomes. The levels of NAD(H) were nearly identical between the wildtype with arginine and the negative controls (Figure 4c). In contrast to the sustained ATP levels of the wildtype with pyruvate, when arginine was provided instead, ATP levels increased sharply, before decreasing after about four hours of anaerobic incubation. The negative controls had very low levels of ATP (Figure 4d), consistent with the results of the pyruvate survival experiment.

Previous work suggests that membrane integrity is well correlated with survival (Ericsson *et al*, 2000). To test whether this is true during energy starvation in *P. aeruginosa*, we simultaneously monitored the membrane integrity and the transmembrane potential of surviving cultures using flow cytometry and the dyes TO-PRO-3 and DiOC<sub>2</sub>(3) (Novo *et al*, 2000). TO-PRO-3 is a red-excitable fluorescent dye that is membrane impermeable and binds DNA (Novo *et al*, 2000). DiOC<sub>2</sub>(3) is a green-excitable permeable dye that accumulates intracellularly in polarized cells, where it undergoes a red fluorescence shift that is indicative of a membrane potential (Novo *et al*, 1999). Since the red:green fluorescence ratio is not quantitative in Gram-negative bacteria (Shapiro & Nebe-von-Caron, 2004), we qualitatively assessed the membrane potential by comparing experimental samples to controls depolarized with carbonyl cyanide 3-chlorophenylhydrazone (CCCP), an ionophore which equilibrates the proton concentration across cell membranes and dissipates the proton motive force and transmembrane potential (Hopfer *et al*, 1968). We express depolarization as the similarity in the red/green ratio to the depolarized control. Events that stained positive for TO-PRO-3 were excluded from this analysis, as permeabilized cells are not expected to have a membrane potential.

We cultured *P. aeruginosa* in minimal medium with 40 mM succinate to an OD<sub>500</sub> of 0.4, added 40 mM pyruvate or 20 mM arginine, and then transferred the cells to an anaerobic environment. After six hours, a culture incubated anaerobically with only succinate reached 70% depolarization, while cultures incubated with added pyruvate or arginine reached only 30% and 10% depolarization, respectively (Figure 4e). Exponentially growing cells maintained approximately 0% depolarization (data not shown). Absolute numbers of TO-PRO-3 fluorescent events were rare in all conditions (data not shown), suggesting that depolarized cells maintained intact membranes. TO-PRO-3-positive events fell almost entirely within the depolarized gate (data not shown), suggesting that permeabilized cells were depolarized. In addition, we observed a time-dependent depolarization in the

phenazine cycling survival experiment, with surviving cells maintaining a lower degree of depolarization (Figure 4f). These results suggest that membrane polarization is a leading indicator of long-term cell viability.

### **A membrane potential is required for anaerobic survival and is maintained by the F<sub>1</sub>F<sub>0</sub>-ATPase complex**

Given the correlation between membrane potential and long-term viability, we hypothesized that maintenance of the membrane potential is required for anaerobic survival in *P. aeruginosa*. To test this hypothesis, we incubated cells anaerobically with the protonophore CCCP. We found that 100  $\mu$ M CCCP reduced the viability of anaerobic cultures to below 0.01% after two days (Figure 5a), suggesting that the membrane potential or proton motive force is required for survival. Ethanol from the addition of CCCP did not noticeably affect survival, as a control culture fermenting pyruvate with 0.2% ethanol maintained  $88 \pm 17\%$  viability (Figure 5a).

During fermentation in many bacteria, the F<sub>1</sub>F<sub>0</sub>-ATPase complex, also known as ATP synthase, hydrolyses ATP to extrude protons from the cytoplasm to the periplasm, thereby generating a proton motive force and a membrane potential (Krulwich *et al*, 2011). To test if the membrane potential in fermentative *P. aeruginosa* is generated by the F<sub>1</sub>F<sub>0</sub>-ATPase complex, we incubated cells with *N,N'*-dicyclohexylcarbodiimide (DCCD), an inhibitor of the proton-translocation channel in the F<sub>0</sub> subunit of ATP synthase (Sebald *et al*, 1980). As with CCCP, 2 mM DCCD was efficient at killing anaerobic *P. aeruginosa* in the presence of pyruvate (Figure 5a), reducing viability to  $0.16\% \pm 0.07\%$  after two days. As expected, this suggests that the activity of ATP synthase is required for survival in fermentative *P. aeruginosa*.

To confirm that DCCD induced depolarization in pyruvate-fermenting cultures, we assessed the membrane potential using flow cytometry with the dyes TO-PRO-3 and DiOC<sub>2</sub>(3). After two hours, a culture treated with ethanolic DCCD reached almost 100% depolarization relative to a CCCP-treated control (Figure 5b). In contrast, an ethanol-treated control remained almost fully polarized relative to the CCCP-treated control (Figure 5b). This indicates that the activity of ATP synthase contributes to the membrane potential in fermentative *P. aeruginosa*.

If a membrane potential is required for survival, then restoring the membrane potential should recover survival even in the presence of DCCD. To recover the membrane potential with DCCD treatment, we incubated cells anaerobically with pyruvate and nitrate. Nitrate serves as an alternate terminal electron acceptor for the electron transport chain in *P. aeruginosa* (Carlson & Ingraham, 1983; Van Alst *et al*, 2009). Cultures incubated with pyruvate, DCCD, and nitrate sustained  $46\% \pm 7\%$  viability after two days (Figure 5a), demonstrating that respiration mitigates the effects of DCCD and also suggesting that DCCD kills by specific interactions. We did not observe significant growth after two days in cultures incubated with pyruvate, 0.2% ethanol, and nitrate (Figure 5a).

Together, these results indicate that the membrane potential is required for anaerobic survival in *P. aeruginosa*, that the membrane potential is maintained by the  $F_1F_0$ -ATPase complex, and that dissipating the membrane potential leads to cell death.

We noted one previous report that arginine anaerobically supports a proton motive force in *P. aeruginosa* strain PAC1 (Armitage & Evans, 1983). The addition of the ATP synthase inhibitor venturicidin abolished this effect, suggesting that the  $F_1F_0$ -ATPase complex generates the proton motive force in this condition. We attempted to replicate this result in *P. aeruginosa* PA14. In cultures fermenting pyruvate, venturicidin had no effect on anaerobic survival at concentrations up to 20  $\mu\text{g}/\text{mL}$ . Venturicidin did not perturb the ATP content or membrane potential of PA14 incubated anaerobically with arginine, and venturicidin did not affect the growth rate or ATP content of PA14 growing aerobically on succinate (data not shown). Similarly, the mitochondrial  $F_1F_0$ -ATPase inhibitor oligomycin had no effect on anaerobic survival at a concentration of 50  $\mu\text{g}/\text{mL}$ . We conclude that venturicidin and oligomycin are not effective inhibitors of the *P. aeruginosa* PA14  $F_1F_0$ -ATPase complex in intact cells.

## Discussion

*P. aeruginosa* is often classified as nonfermentative because it requires respiration for robust growth (Barnishan & Ayers, 1979; Carlson & Ingraham, 1983), although arginine can serve as an energy source for limited fermentative growth in complex media (Vander Wauven *et al*, 1984). *P. aeruginosa* is not known to ferment glucose or other sugars (Barnishan & Ayers, 1979; Eschbach *et al*, 2004); however, when provided with glucose, phenazines, and an oxidizing electrochemical potential, *P. aeruginosa* is able to survive in

the absence of respiration (Wang *et al*, 2010, and this study). This underscores the importance of studying survival physiology independently from growth physiology.

In the case of survival via arginine fermentation, we might not expect a difference in the redox state of the NAD(H) pool compared to cells without arginine, since there is no redox component to this fermentation pathway (Figure 2). In agreement with this prediction, we found no difference in the ratio of NADH to NAD<sup>+</sup> during the time these compounds were sufficiently high to measure (up to 24 hours, Figure 4c). Arginine fermentation yields 1 ATP per conversion to ornithine (Figure 2), and we found that ATP levels initially increased for cells fermenting arginine, before declining after about 8 hours (Figure 4d). Negative controls, either lacking arginine or unable to utilize it, had very low levels of ATP.

Whereas phenazines enable survival on glucose for the wildtype, they do not for the  $\Delta ackA$ -*pta* mutant (Figure 3a), suggesting that phenazine redox cycling facilitates the conversion of glucose to pyruvate, and then to acetate, with concomitant ATP synthesis (Figure 2). Consistent with this finding, wild type *P. aeruginosa* cultures incubated aerobically with glucose secrete and later consume pyruvate in late stationary phase, while phenazine-null mutant cultures do not (Price-Whelan *et al*, 2007). Pyruvate is metabolized by pyruvate dehydrogenase to acetyl-coenzyme A, which can then enter the tricarboxylic acid cycle or be further metabolized to acetate as part of pyruvate fermentation. Earlier results suggested that superoxide or pyocyanin radicals inhibit pyruvate dehydrogenase, thus leading to pyruvate accumulation in the culture supernatant (Price-Whelan *et al*, 2007). In light of the results presented here, pyruvate excretion by oxygen-limited PA14 cells may also be due to increased production of pyruvate facilitated by phenazine-mediated glucose oxidation. Given that glucose oxidation to pyruvate yields two excess reducing equivalents (Figure 2c), we propose that phenazines accelerate glucose oxidation by serving as an additional electron sink to regenerate oxidants for glucose catabolism (Figure 6). After the consumption of glucose, the excreted pyruvate can then be fermented or oxidized in the tricarboxylic acid cycle, depending on the cells' needs as defined by the surrounding environment.

During pyruvate fermentation, the activity of AckA is coupled to the activity of LdhA through the common cofactor NAD(H) (Figure 2a), as demonstrated by the failure of an  $\Delta ldhA$  mutant to maintain ATP levels (Figure 4b). The  $\Delta ldhA$  mutant is unimpaired in survival when oxidized phenazines can complement the redox homeostasis defect (Figure

3a), suggesting that ATP synthesis is an essential component of survival. Homeostasis of the NAD(H) pool by LdhA has been correlated with the ability of *P. aeruginosa* to grow microcolonies (Petrova *et al*, 2012), and a mutant lacking LdhA activity exhibits a significantly higher NADH to NAD<sup>+</sup> ratio than wildtype cells whether surviving planktonically or in a biofilm (Petrova *et al*, 2012), this study). Redox balance is likely a precondition for growth or survival, but we have demonstrated that a  $\Delta$ ldhA mutant is altered in its redox state and, as a consequence, also fails to maintain ATP homeostasis (Figure 4a and b). This serves a reminder that it is the coupling between redox homeostasis and ATP generation that is key to survival.

The limited fermentation capacity of *P. aeruginosa* has been attributed to the absence of pyruvate formate lyase and formate hydrogen lyase (Eschbach *et al*, 2004), which permit the oxidation of pyruvate to acetate while preserving the intracellular redox state (Bagramyan & Trchounian, 2003). In addition, *P. aeruginosa* uses the Entner-Doudoroff pathway for glucose oxidation, which yields only a single ATP per glucose and generates two excess reducing equivalents (Figure 2c). This low energy yield may explain the inability of *P. aeruginosa* to grow by fermenting glucose under laboratory conditions. Our results with phenazine redox cycling, however, suggest that this picture is an oversimplification given that *P. aeruginosa* infections can contain over 100  $\mu$ M phenazines (Hunter *et al*, 2012; Wilson *et al*, 1988) and planktonic cultures grown in the lab may contain as much as 250  $\mu$ M phenazines (Price-Whelan *et al*, 2007). Previous studies have demonstrated that small-molecule electron carriers, like phenazines, can couple metabolism to extracellular oxidants and shift metabolism towards the synthesis of more oxidized fermentation products (Emde *et al*, 1989; Emde & Schink, 1990; Benz *et al*, 1998; Beck & Schink, 1995). Under these conditions, as with fermentative *P. aeruginosa*, extracellular electron shuttles may permit organisms to utilize unexpected energy sources by transcending the written stoichiometry of a pathway. For example, *P. aeruginosa* appears capable of fermenting glucose in the presence of oxidized phenazines. Ultimately this depends upon the availability of a terminal oxidant (*e.g.*, molecular oxygen or ferric iron) to regenerate oxidized phenazines. An understanding of environmental parameters that may interface with metabolism is therefore essential to assess the true metabolic capacity of some organisms.

In addition to fermentation, nitrate supported survival even in the absence of the major nitrate respiratory complex Nar (Figure 1d). The periplasmic nitrate reductase Nap appeared to support this survival, as a mutant lacking both Nar and Nap survived only

poorly with nitrate (Figure 1d). Nap is expressed during aerobic denitrification and repressed under anaerobic conditions (Van Alst *et al*, 2009). Interestingly, we observed survival only when cells were pre-grown aerobically with nitrate, suggesting that expression of Nap under aerobic conditions was required to support survival after a subsequent shift to anaerobiosis. This is in agreement with the finding that Nap can support anaerobic growth in a mutant lacking Nar and also NarXL, a negative regulator of Nap (Van Alst *et al*, 2009). Nap may therefore aid in energy generation or maintenance of the membrane potential during transient oxygen starvation.

Integrating these observations, our results suggest that ATP synthesis is a determining factor of survival in nonreplicating *P. aeruginosa*. This conclusion is supported by the following observations. First, an  $\Delta dhA$  mutant (defective in NAD<sup>+</sup> regeneration) is only partially deficient in survival during pyruvate fermentation, while an  $\Delta ackA\text{-}pta$  mutant (defective in ATP synthesis) is more severely deficient in survival (Figure 1a), and both mutants rapidly become depleted in intracellular ATP (Figure 4b). Second, arginine is sufficient to promote anaerobic survival in minimal medium (Figure 1c), and two mutants unable to synthesize ATP through the arginine deiminase pathway (Figure 2b),  $arcA::MAR2xT7$  and  $arcC::MAR2xT7$ , do not survive in the presence of arginine (Figure 1c) and fail to maintain ATP homeostasis (Figure 4d). Third, phenazine redox cycling restores survival in an  $\Delta dhA$  mutant but not in an  $\Delta ackA\text{-}pta$  mutant (Figure 3a), which is defective in ATP synthesis. Finally, inhibition of ATP utilization with the ATP synthase inhibitor DCCD leads to a collapse of the membrane potential and cell death (Figure 5). Redox homeostasis is essential when ATP-generating pathways yield excess reducing equivalents (as in glucose and pyruvate oxidation (Figure 2)), as demonstrated by the ability of phenazine redox cycling to promote survival and complement the  $\Delta dhA$  survival defect (Figure 3a).

It is perhaps unsurprising that anaerobic survival requires ATP synthesis, as previous studies have shown that survival requires transcription (Hu & Coates, 1999), translation (Reeve *et al*, 1984), and proteolysis (Weichart *et al*, 2003), all of which consume ATP. However, our results demonstrate that nonreplicating *P. aeruginosa* retains limited energy stores and must sustain a basal metabolism for survival. We have further shown that maintenance of the membrane potential is required for survival, and collapsing the membrane potential leads to cell death. In Figure 6, we present a model of the known survival pathways and processes in *P. aeruginosa*.

The establishment of *P. aeruginosa* within the lungs of cystic fibrosis patients is associated with high rates of morbidity and mortality (Lyczak *et al*, 2002), yet current treatments are ineffective at clearing *P. aeruginosa* from the lung (Hassett *et al*, 2002). This pattern mirrors the difficulty of treating *M. tuberculosis* infections, which can remain persistent despite years of therapy (Gomez & McKinney, 2004). Interestingly, nonreplicating *M. tuberculosis* uses the electron transport chain to generate a proton motive force, and it requires *de novo* ATP synthesis via the F<sub>1</sub>F<sub>0</sub>-ATPase complex for long-term survival (Rao *et al*, 2008). In contrast, we observed the opposite pattern in nonreplicating *P. aeruginosa*. Instead of maintaining ATP synthesis with energy provided by a proton motive force, nonreplicating *P. aeruginosa* generates a proton motive force using energy from ATP hydrolysis. Unlike *M. tuberculosis*, *P. aeruginosa* does not require the electron transport chain for survival, as both pyruvate and arginine are sufficient to promote survival in the absence of respiration (Eschbach *et al*, 2004, and this study). Nonetheless, the membrane potential and the F<sub>1</sub>F<sub>0</sub>-ATPase complex appear to be essential components of survival in both species, suggesting that the core metabolism of nonreplicating cells may be a common target for novel antibiotic therapies against diverse pathogens.

Together, these findings stress the importance of understanding how bacterial physiology is shaped by the context of infection. Numerous studies have demonstrated the metabolic versatility of *P. aeruginosa* (for example, Behrends *et al*, 2009; Stover *et al*, 2000), and here we have shown that several anaerobic pathways might enable survival under clinically relevant conditions. Characterizations of cystic fibrosis sputum indicate the presence of up to 100  $\mu$ M phenazines (Hunter *et al*, 2012) and significant quantities of nitrate, arginine, and glucose (Palmer *et al*, 2007). Nitrate concentrations may be as high as 350  $\mu$ M (Palmer *et al*, 2005) and oxygen levels vary widely (Worlitzsch *et al*, 2002), potentially resulting in extended periods of slow growth or dormancy. Given the metabolic heterogeneity of biofilms (Williamson *et al*, 2012) and the likely heterogeneity of the cystic fibrosis lung environment, *P. aeruginosa* throughout the lung might exhibit a range of growth rates, including survival without replication. As a result, single antibiotic therapies are unlikely to affect every member of the population, and an optimal treatment will likely comprise compounds that target both dividing and non-dividing cells.



## Materials and Methods

### Bacterial strains and growth conditions

The strains and plasmids used in this study are shown in Supplemental Table 1. For routine growth, *P. aeruginosa* and *E. coli* were cultured at 37 °C in lysogeny broth (LB) containing 10 g/L tryptone, 5 g/L yeast extract, 10 g/L NaCl, and optionally 15 g/L agar for solid medium. *S. cerevisiae* was cultured at 30 °C in YPD medium containing 10 g/L yeast extract, 20 g/L peptone, 20 g/L D-glucose, and optionally 20 g/L agar for solid medium. Specific experimental growth conditions are described where appropriate. For aerobic growth, liquid cultures were shaken at 250 rpm.

### Construction and verification of *P. aeruginosa* mutants

Unmarked deletions of *ldhA* and *ackA-pta* in *P. aeruginosa* PA14 were constructed using a modification of previously described methods (Shanks *et al*, 2006). Briefly, PCR was used to amplify approximately 1-kilobase fragments flanking the target gene. Homologous recombination in yeast was used to assemble these fragments into the *sacB*-counterselectable suicide shuttle vector pMQ30. The knockout vector was transformed into *E. coli* DH5 $\alpha$ , and triparental mating with DH5 $\alpha$  and *E. coli* HB101/pRK2013 was used to conjugate the constructed knockout vector into PA14; merodiploids containing the chromosomally integrated vector were selected on cetrimide agar (HiMedia) containing 100  $\mu\text{g mL}^{-1}$  gentamicin sulfate. Merodiploids were cultured overnight in nonselective LB, and resolved merodiploids were then selected on LB agar plates with 10% sucrose. Potential deletion mutants were screened using colony PCR with primers flanking the target gene, and clean deletions were confirmed by DNA sequencing of the PCR product (Retrogen). Transposon insertions were verified using colony PCR with primers flanking the annotated transposon position. Primer sequences for constructing and confirming the genetic mutants used in this study can be found in Supplemental Table 2.

### Pyruvate, arginine, and nitrate survival and viable cell counting

For measuring anaerobic survival using pyruvate or arginine as a sole carbon source, cultures were grown overnight at 37 °C in a minimal medium containing 14.15 mM  $\text{KH}_2\text{PO}_4$ , 35.85 mM  $\text{K}_2\text{HPO}_4$ , 42.8 mM NaCl, 9.3 mM  $\text{NH}_4\text{Cl}$ , 1 mM  $\text{MgSO}_4$ , 7.2  $\mu\text{M}$   $\text{FeCl}_2$  and trace

elements (Widdel *et al*, 1983), and 40 mM sodium pyruvate or 40 mM arginine (pH adjusted to 7.2 with NaOH or HCl). In the case of survival in the presence of nitrate, cultures were grown aerobically overnight in the same minimal medium with 20 mM succinate and 40 mM nitrate. Overnight cultures were diluted at least 100-fold with fresh medium to an OD<sub>500</sub> of 0.01 and incubated at 37 °C in shaking flasks to an OD<sub>500</sub> of 0.4. After centrifuging the culture for 15 min at 5000×g, the supernatant was removed and the pellet was transferred to a glove chamber (Coy) containing an atmosphere of 15% CO<sub>2</sub>, 80% N<sub>2</sub>, and 5% H<sub>2</sub>. The pellet was washed twice with fresh anoxic medium and then resuspended to a final OD<sub>500</sub> of approximately 0.4 in rubber-stoppered tubes. The sealed tubes were incubated at 37 °C in the anaerobic chamber without shaking. For measurements of colony forming units, 20 µL of each culture was sampled anaerobically and then serially diluted in aerobic 1x phosphate-buffered saline. We pipetted 10 µL drips of the relevant dilution on LB agar plates. After 24 hours of aerobic incubation at 37 °C we averaged the counts of at least 6 pipetting replicates.

### **Phenazine cycling survival**

The assay for anaerobic survival enabled by phenazine redox cycling was performed as previously described (Wang *et al*, 2010). Briefly, strains of PA14 deleted in the core phenazine biosynthesis operons ( $\Delta phz1/2$ ) (Dietrich *et al*, 2006) were grown overnight from fresh colonies in LB. At 12 hours, the cultures were used to inoculate 250 mL LB in 1-L flasks to an OD<sub>500</sub> near 0.06. At early stationary phase (OD<sub>500</sub> between 2.75 and 2.85) cells were pelleted, washed twice aerobically in MOPS-buffered medium (100 mM 3-(N-morpholino)propanesulfonic acid (MOPS), 3.5 µM FeSO<sub>4</sub>, 43 mM NaCl, 3.7 mM KH<sub>2</sub>PO<sub>4</sub>, 93 mM NH<sub>4</sub>Cl at pH 7.2), and resuspended to a concentrated OD<sub>500</sub> of 70 before being transferred to a nitrogen-only atmosphere (MBraun Unilab glove box). There, 1 mL of concentrated cells was added to sealed glass vessels containing 100 mL of anoxic MOPS-buffered medium amended with 20 mM D-glucose or 40 mM sodium succinate, and approximately 75 µM phenazine-1-carboxylic acid, as indicated. To oxidize PCA, a graphite rod (Alfa Aesar #14738) working electrode was poised at a potential of +207 mV vs. NHE against a homemade platinum mesh counter electrode, which was placed in buffer within an attached small chamber separated from the bulk solution by a glass frit. Electrochemical parameters were maintained by a potentiostat (Gamry). An Ag/AgCl electrode (BaSi #RE5B) was used as the reference electrode. Anaerobic cultures of cells were stirred

vigorously and maintained at 31°C for up to 8 days, with daily sampling for colony forming units (CFU) on LB agar plates incubated aerobically as described above. Phenazine turnover was confirmed by the accumulated charge over the duration of the experiment, as previously described (Wang *et al*, 2010).

### **Measurement of NAD<sup>+</sup>, NADH, and ATP**

The method for measuring NAD<sup>+</sup> and NADH in this study was based on established protocols (San *et al*, 2002; Price-Whelan *et al*, 2007). Due to the reactivity of oxidized phenazines with NADH, all steps leading up to the colorimetric assay in a plate reader were performed in completely anoxic conditions inside a glove box (MBraun or Coy). For each condition, two 1.6-mL samples in 1.7 ml plastic tubes were centrifuged for 1 min at maximum speed (16,000×g). The supernatant was removed and 200 µL of either 0.2 M HCl (for NAD<sup>+</sup> extraction) or 0.2 M NaOH (for NADH extraction) was added and mixed by vortexing. After 10 minutes at 55 °C the samples were cooled on ice before 200 µL of 0.1 M NaOH (for NAD<sup>+</sup>) or 0.1 M HCl (for NADH) was added drop-wise while vortexing. After pelleting cell debris (5 minutes at maximum speed), 150 µL of the supernatant was transferred to a fresh tube for storage. Levels of NADH and NAD<sup>+</sup> were found to be stable at room temperature inside an oxygen-free glove box for 24 hours. To assay the amount of NAD<sup>+</sup> or NADH in each sample, 15 µL of sample or a standard of known NAD<sup>+</sup> concentration was added to 80 µL of the reagent mix in a 96-well microtiter plate. The reagent mix contained 250 mM bicine buffer, pH 8.0, 5 mM EDTA, 12.5% ethanol (v/v), 0.525 mM thiazolyl blue, 4.2 mM phenazine ethosulfate. The 96-well plate was then moved out of the anoxic environment and heated to 30 °C inside a BioTek Synergy 4 plate reader. To initiate the colorimetric assay, 5 µL of a 1 mg mL<sup>-1</sup> solution of alcohol dehydrogenase II (Sigma A3263) in 0.1 M bicine pH 8.0 was added to each well. With intermittent shaking, the plate reader then recorded the appearance of reduced thiazolyl blue (with an absorbance peak at 570 nm) every minute for 30 minutes. Concentrations of NADH and NAD<sup>+</sup> were calculated using the slope and intercept derived from A570/time of the standard curve. Amounts of NADH and NAD<sup>+</sup> were reported as a ratio for each sample. The same extracts were assayed for NADP(H) levels by exchanging ethanol for 3.13 mM glucose-6-phosphate, and adding 5 µL of a 0.1 mg/mL glucose-6-phosphate dehydrogenase enzyme solution. Levels of NADP(H) were below the detection limit of 0.025 µM in the cell pellet.

For ATP measurement, 20  $\mu\text{L}$  of culture was added to 180  $\mu\text{L}$  of dimethyl sulfoxide (DMSO) to quench and dissolve the cells. The sample was then diluted with 800  $\mu\text{L}$  of 0.1 M HEPES (pH 7.5) and stored at  $-80\text{ }^{\circ}\text{C}$  for up to 7 days. ATP was quantified by mixing 25  $\mu\text{L}$  of sample with 25  $\mu\text{L}$  of Promega BacTiter-Glo reagent in a 96-well opaque white microtiter plate. The BacTiter-Glo reagent uses luciferase to produce luminescence in an ATP-dependent manner. Total luminescence was measured at  $30\text{ }^{\circ}\text{C}$  in a BioTek Synergy 4 plate reader. In control experiments using pure ATP, DMSO had no effect on luminescence at a final concentration of 9% (data not shown).

### **Assessment of membrane potential**

The membrane potential was measured qualitatively using the dyes 3,3'-diethyloxacarbocyanine iodide ( $\text{DiOC}_2(3)$ ) and TO-PRO-3. Cultures were diluted at least 100-fold into a permeabilization buffer containing 100 mM Tris, 1 mM EDTA, and 80 mM NaCl (pH adjusted to 7.4 using HCl).  $\text{DiOC}_2(3)$  and TO-PRO-3 were then added to a final concentration of 30  $\mu\text{M}$  and 100 nM, respectively. For depolarized controls, CCCP was added to a final concentration of 15  $\mu\text{M}$ . The samples were incubated for 2-5 minutes at room temperature and then analyzed on an Accuri C6 flow cytometer.  $\text{DiOC}_2(3)$  fluorescence was measured using excitation at 488 nm and emission at  $530 \pm 15\text{ nm}$  (FL1) and  $610 \pm 10\text{ nm}$  (FL3). TO-PRO-3 fluorescence was measured using excitation at 640 nm and emission at  $675 \pm 12.5\text{ nm}$  (FL4). Intact cells were gated on a log-scale scatter plot of FL4 vs. FL2 ( $585 \pm 20\text{ nm}$ ) for further analysis. Cells with a membrane potential were distinguished by an increased red/green (FL3/FL1) fluorescence ratio relative to depolarized controls.

### **Ion chromatography and metabolite quantification**

Metabolite samples were collected by centrifuging 550  $\mu\text{L}$  of culture and passing the supernatant through a 0.2- $\mu\text{m}$  nylon centrifugal filter. Samples were stored at  $-80\text{ }^{\circ}\text{C}$  until analysis. Pyruvate, acetate, lactate, and succinate were quantified using anion-exchange chromatography. Metabolite standards ranging from 0 to 40 mM were used to calibrate peak area against metabolite concentration.

A continuous flow of ultrapure water (18.2 megohm, produced from a milliQ Gradient system, Millipore) at 1.00 mL/min was maintained with a Dionex GP40 pump, passed through an anion trap column to remove remaining anionic impurities, then through a potassium hydroxide eluent generator cartridge controlled by an EG40 module and

subsequently through a six-port valve configured for sample loop injection. A 10-microliter sample loop was loaded from a Dionex (Sunnyvale, CA) AS40 autosampler. Separation was effected on Dionex AG-19 (4x50 mm) and AS-19 (4x250mm) columns in series, the eluent was returned to neutral pH with a SRS-300 suppressor operating at 50 mA, and finally analytes were detected with a conductivity cell monitored by an ED-40 detector in conductivity mode. The suppressor was operated in eluent recycle mode. The hydroxide gradient began at 0.01 mM KOH 11 minutes before injection and was held at that concentration until injection. The concentration was increased linearly to 6.0 mM at 15 minutes, then to 15.0 mM at 25 minutes, and finally to 38 mM at 35 minutes where it was held for 3 minutes. Retention times for analytes were validated with single species standards. Data were analyzed with Chromeleon 6.8 (Dionex).

## **Acknowledgements**

This work was supported by the Howard Hughes Medical Institute (HHMI). DKN is an HHMI Investigator, and NRG and SEK were both supported by NSF graduate research fellowships. This work was supported in part by the National Research Service Award (T32GM07676) from the National Institute of General Medical Sciences. We thank Nathan Dalleska and the Environmental Analysis Center (Caltech) for help with metabolite analyses. The authors declare no conflicts of interest.

## References

- Allison KR, Brynildsen MP & Collins JJ (2011) Metabolite-enabled eradication of bacterial persisters by aminoglycosides. *Nature* **473**: 216–220
- Alvarez-Ortega C & Harwood CS (2007) Responses of *Pseudomonas aeruginosa* to low oxygen indicate that growth in the cystic fibrosis lung is by aerobic respiration. *Mol Microbiol* **65**: 153–165
- Armitage JP & Evans MC (1983) The motile and tactic behaviour of *Pseudomonas aeruginosa* in anaerobic environments. *FEBS Lett.* **156**: 113–118
- Bagramyan K & Trchounian A (2003) Structural and functional features of formate hydrogen lyase, an enzyme of mixed-acid fermentation from *Escherichia coli*. *Biochem Mosc* **68**: 1159–1170
- Barnishan J & Ayers LW (1979) Rapid identification of nonfermentative gram-negative rods by the Corning N/F system. *J Clin Microbiol* **9**: 239–243
- Baron SS & Rowe JJ (1981) Antibiotic action of pyocyanin. *Antimicrob Agents Chemother* **20**: 814–820
- Beck S & Schink B (1995) Acetate oxidation through a modified citric acid cycle in *Propionibacterium freudenreichii*. *Arch Microbiol* **163**: 182–187
- Behrends V, Ebbels TMD, Williams HD & Bundy JG (2009) Time-resolved metabolic footprinting for nonlinear modeling of bacterial substrate utilization. *Appl Environ Microbiol* **75**: 2453–2463
- Benz M, Schink B & Brune A (1998) Humic acid reduction by *Propionibacterium freudenreichii* and other fermenting bacteria. *Appl Environ Microbiol* **64**: 4507–4512
- Britigan BE, Roeder TL & Rasmussen GT (1992) Interaction of the *Pseudomonas aeruginosa* secretory products pyocyanin and pyochelin generates hydroxyl radical and causes synergistic damage to endothelial cells. *J. Clin. Invest.* **90**: 2187–2196
- Carlson CA & Ingraham JL (1983) Comparison of denitrification by *Pseudomonas stutzeri*, *Pseudomonas aeruginosa*, and *Paracoccus denitrificans*. *Appl Environ Microbiol* **45**: 1247–1253
- Choi KH, DeShazer D & Schweizer HP (2006) mini-Tn 7 insertion in bacteria with multiple glmS-linked attTn7 sites: example *Burkholderia mallei* ATCC 23344. *Nat Protoc* **1**: 162–169
- Cox CD (1986) Role of pyocyanin in the acquisition of iron from transferrin. *Infect Immun* **52**: 263–270
- Dietrich LEP, Okegbe C, Price-Whelan A, Sakhtah H, Hunter RC & Newman DK (2013) Bacterial community morphogenesis is intimately linked to the intracellular redox state. *J Bacteriol*

- Dietrich LEP, Price-Whelan A, Petersen A, Whiteley M & Newman DK (2006) The phenazine pyocyanin is a terminal signalling factor in the quorum sensing network of *Pseudomonas aeruginosa*. *Mol Microbiol* **61**: 1308–1321
- Dietrich LEP, Teal TK, Price-Whelan A & Newman DK (2008) Redox-active antibiotics control gene expression and community behavior in divergent bacteria. *Science* **321**: 1203–1206
- Emde R & Schink B (1990) Oxidation of glycerol, lactate, and propionate by *Propionibacterium freudenreichii* in a poised-potential amperometric culture system. *Arch Microbiol* **153**: 506–512
- Emde R, Swain A & Schink B (1989) Anaerobic oxidation of glycerol by *Escherichia coli* in an amperometric poised-potential culture system. *Appl Microbiol Biot* **32**: 170–175
- Ericsson M, Hanstorp D, Hagberg P, Enger J & Nystrom T (2000) Sorting out bacterial viability with optical tweezers. *J Bacteriol* **182**: 5551–5555
- Eschbach M, Schreiber K, Trunk K, Buer J, Jahn D & Schobert M (2004) Long-term anaerobic survival of the opportunistic pathogen *Pseudomonas aeruginosa* via pyruvate fermentation. *J Bacteriol* **186**: 4596–4604
- Gomez JE & McKinney JD (2004) *M. tuberculosis* persistence, latency, and drug tolerance. *Tuberculosis (Edinb)* **84**: 29–44
- Grant SG, Jessee J, Bloom FR & Hanahan D (1990) Differential plasmid rescue from transgenic mouse DNAs into *Escherichia coli* methylation-restriction mutants. *Proc Natl Acad Sci USA* **87**: 4645–4649
- Hassett DJ, Cuppoletti J, Trapnell B, Lyman SV, Rowe JJ, Yoon SS, Hilliard GM, Parvatiyar K, Kamani MC, Wozniak DJ, Hwang SH, McDermott TR & Ochsner UA (2002) Anaerobic metabolism and quorum sensing by *Pseudomonas aeruginosa* biofilms in chronically infected cystic fibrosis airways: rethinking antibiotic treatment strategies and drug targets. *Adv Drug Deliv Rev* **54**: 1425–1443
- Hopfer U, Lehninger AL & Thompson TE (1968) Protonic conductance across phospholipid bilayer membranes induced by uncoupling agents for oxidative phosphorylation. *Proc Natl Acad Sci USA* **59**: 484–490
- Hu Y & Coates AR (1999) Transcription of the stationary-phase-associated hspX gene of *Mycobacterium tuberculosis* is inversely related to synthesis of the 16-kilodalton protein. *J Bacteriol* **181**: 1380–1387
- Hunter RC, Klepac-Ceraj V, Lorenzi MM, Grotzinger H, Martin TR & Newman DK (2012) Phenazine content in the cystic fibrosis respiratory tract negatively correlates with lung function and microbial complexity. *Am. J. Respir. Cell Mol. Biol.*
- Keren I, Shah D, Spoering A, Kaldalu N & Lewis K (2004) Specialized persister cells and the mechanism of multidrug tolerance in *Escherichia coli*. *J Bacteriol* **186**: 8172–8180
- Krulwich TA, Sachs G & Padan E (2011) Molecular aspects of bacterial pH sensing and

homeostasis. *Nature Rev Microbiol* **9**: 330–343

Lau GW, Hassett DJ & Britigan BE (2005) Modulation of lung epithelial functions by *Pseudomonas aeruginosa*. *Trends Microbiol* **13**: 389–397

Lewis K (2010) Persister cells. *Annu Rev Microbiol* **64**: 357–372

Liberati NT, Urbach JM, Miyata S, Lee DG, Drenkard E, Wu G, Villanueva J, Wei T & Ausubel FM (2006) An ordered, nonredundant library of *Pseudomonas aeruginosa* strain PA14 transposon insertion mutants. *Proc Natl Acad Sci USA* **103**: 2833–2838

Lyczak JB, Cannon CL & Pier GB (2002) Lung infections associated with cystic fibrosis. *Clin Microbiol Rev* **15**: 194–222

Mavrodi DV, Blankenfeldt W & Thomashow LS (2006) Phenazine compounds in fluorescent *Pseudomonas* spp. biosynthesis and regulation. *Annu Rev Phytopathol* **44**: 417–445

Mavrodi DV, Bonsall RF, Delaney SM, Soule MJ, Phillips G & Thomashow LS (2001) Functional analysis of genes for biosynthesis of pyocyanin and phenazine-1-carboxamide from *Pseudomonas aeruginosa* PAO1. *J Bacteriol* **183**: 6454–6465

Möker N, Dean CR & Tao J (2010) *Pseudomonas aeruginosa* increases formation of multidrug-tolerant persister cells in response to quorum-sensing signaling molecules. *J Bacteriol* **192**: 1946–1955

Nguyen D, Joshi-Datar A, Lepine F, Bauerle E, Olakanmi O, Beer K, McKay G, Siehnel R, Schafhauser J, Wang Y, Britigan BE & Singh PK (2011) Active starvation responses mediate antibiotic tolerance in biofilms and nutrient-limited bacteria. *Science* **334**: 982–986

Novo D, Perlmutter NG, Hunt RH & Shapiro HM (1999) Accurate flow cytometric membrane potential measurement in bacteria using diethyloxycarbocyanine and a ratiometric technique. *Cytometry* **35**: 55–63

Novo DJ, Perlmutter NG, Hunt RH & Shapiro HM (2000) Multiparameter flow cytometric analysis of antibiotic effects on membrane potential, membrane permeability, and bacterial counts of *Staphylococcus aureus* and *Micrococcus luteus*. *Antimicrob Agents Chemother* **44**: 827–834

Palmer K, Mashburn L & Singh P (2005) Cystic fibrosis sputum supports growth and cues key aspects of *Pseudomonas aeruginosa* physiology. *J Bacteriol* **187**: 5267–5277

Palmer KL, Aye LM & Whiteley M (2007) Nutritional cues control *Pseudomonas aeruginosa* multicellular behavior in cystic fibrosis sputum. *J Bacteriol* **189**: 8079–8087

Petrova OE, Schurr JR, Schurr MJ & Sauer K (2012) Microcolony formation by the opportunistic pathogen *Pseudomonas aeruginosa* requires pyruvate and pyruvate fermentation. *Mol Microbiol* **86**: 819–835

Price-Whelan A, Dietrich LEP & Newman DK (2006) Rethinking ‘secondary’ metabolism: physiological roles for phenazine antibiotics. *Nature Chem Biol* **2**: 71–78



- Price-Whelan A, Dietrich LEP & Newman DK (2007) Pyocyanin alters redox homeostasis and carbon flux through central metabolic pathways in *Pseudomonas aeruginosa* PA14. *J Bacteriol* **189**: 6372–6381
- Rahme LG, Stevens EJ, Wolfort SF, Shao J, Tompkins RG & Ausubel FM (1995) Common virulence factors for bacterial pathogenicity in plants and animals. *Science* **268**: 1899–1902
- Rao SPS, Alonso S, Rand L, Dick T & Pethe K (2008) The protonmotive force is required for maintaining ATP homeostasis and viability of hypoxic, nonreplicating *Mycobacterium tuberculosis*. *Proc Natl Acad Sci USA* **105**: 11945–11950
- Reeve CA, Amy PS & Matin A (1984) Role of protein synthesis in the survival of carbon-starved *Escherichia coli* K-12. *J Bacteriol* **160**: 1041–1046
- San K-Y, Bennett GN, Berríos-Rivera SJ, Vadali RV, Yang Y-T, Horton E, Rudolph FB, Sariyar B & Blackwood K (2002) Metabolic engineering through cofactor manipulation and its effects on metabolic flux redistribution in *Escherichia coli*. *Metab Eng* **4**: 182–192
- Schreiber K, Boes N, Eschbach M, Jaensch L, Wehland J, Bjarnsholt T, Givskov M, Hentzer M & Schobert M (2006) Anaerobic survival of *Pseudomonas aeruginosa* by pyruvate fermentation requires an Usp-type stress protein. *J Bacteriol* **188**: 659–668
- Sebald W, Machleidt W & Wachter E (1980) N,N'-dicyclohexylcarbodiimide binds specifically to a single glutamyl residue of the proteolipid subunit of the mitochondrial adenosinetriphosphatases from *Neurospora crassa* and *Saccharomyces cerevisiae*. *Proc Natl Acad Sci USA* **77**: 785–789
- Shanks RMQ, Caiazza NC, Hinsa SM, Toutain CM & O'Toole GA (2006) *Saccharomyces cerevisiae*-based molecular tool kit for manipulation of genes from gram-negative bacteria. *Appl Environ Microbiol* **72**: 5027–5036
- Shapiro HM & Nebe-von-Caron G (2004) Multiparameter flow cytometry of bacteria. *Methods Mol. Biol.* **263**: 33–44
- Stover CK, Pham XQ, Erwin AL, Mizoguchi SD, Warrenner P, Hickey MJ, Brinkman FS, Hufnagle WO, Kowalik DJ, Lagrou M, Garber RL, Goltry L, Tolentino E, Westbrook-Wadman S, Yuan Y, Brody LL, Coulter SN, Folger KR, Kas A, Larbig K, et al (2000) Complete genome sequence of *Pseudomonas aeruginosa* PAO1, an opportunistic pathogen. *Nature* **406**: 959–964
- Sullivan NL, Tzeranis DS, Wang Y, So PTC & Newman DK (2011) Quantifying the dynamics of bacterial secondary metabolites by spectral multiphoton microscopy. *ACS Chem Biol* **6**: 893–899
- Van Alst NE, Sherrill LA, Iglewski BH & Haidaris CG (2009) Compensatory periplasmic nitrate reductase activity supports anaerobic growth of *Pseudomonas aeruginosa* PAO1 in the absence of membrane nitrate reductase. *Can. J. Microbiol.* **55**: 1133–1144
- Vander Wauven C, Piérard A, Kley-Raymann M & Haas D (1984) *Pseudomonas aeruginosa* mutants affected in anaerobic growth on arginine: evidence for a four-gene cluster

encoding the arginine deiminase pathway. *J Bacteriol* **160**: 928–934

- Wang Y, Kern SE & Newman DK (2010) Endogenous phenazine antibiotics promote anaerobic survival of *Pseudomonas aeruginosa* via extracellular electron transfer. *J Bacteriol* **192**: 365–369
- Wang Y, Wilks JC, Danhorn T, Ramos I, Croal L & Newman DK (2011) Phenazine-1-carboxylic acid promotes bacterial biofilm development via ferrous iron acquisition. *J Bacteriol* **193**: 3606–3617
- Weichert D, Querfurth N, Dreger M & Hengge-Aronis R (2003) Global role for ClpP-containing proteases in stationary-phase adaptation of *Escherichia coli*. *J Bacteriol* **185**: 115–125
- Werner E, Roe F, Bugnicourt A, Franklin MJ, Heydorn A, Molin S, Pitts B & Stewart PS (2004) Stratified growth in *Pseudomonas aeruginosa* biofilms. *Appl Environ Microbiol* **70**: 6188–6196
- Widdel F, Kohring G-W & Mayer F (1983) Studies on dissimilatory sulfate-reducing bacteria that decompose fatty acids. *Arch Microbiol* **134**: 286–294
- Williams HD, Zlosnik JEA & Ryall B (2007) Oxygen, cyanide and energy generation in the cystic fibrosis pathogen *Pseudomonas aeruginosa*. *Adv Microb Physiol* **52**: 1–71
- Williamson KS, Richards LA, Perez-Osorio AC, Pitts B, McInnerney K, Stewart PS & Franklin MJ (2012) Heterogeneity in *Pseudomonas aeruginosa* biofilms includes expression of ribosome hibernation factors in the antibiotic-tolerant subpopulation and hypoxia-induced stress response in the metabolically active population. *J Bacteriol* **194**: 2062–2073
- Wilson R, Sykes DA, Watson D, Rutman A, Taylor GW & Cole PJ (1988) Measurement of *Pseudomonas aeruginosa* phenazine pigments in sputum and assessment of their contribution to sputum sol toxicity for respiratory epithelium. *Infect Immun* **56**: 2515–2517
- Worlitzsch D, Rintelen C, Boehm K, Wollschlaeger B, Merkel N, Borneff-Lipp M & Doering G (2009) Antibiotic-resistant obligate anaerobes during exacerbations of cystic fibrosis patients. *Clin Microbiol Infec* **15**: 454–460
- Worlitzsch D, Tarran R, Ulrich M, Schwab U, Cekici A, Meyer KC, Birrer P, Bellon G, Berger J, Weiss T, Botzenhart K, Yankaskas JR, Randell S, Boucher RC & Döring G (2002) Effects of reduced mucus oxygen concentration in airway *Pseudomonas* infections of cystic fibrosis patients. *J. Clin. Invest.* **109**: 317–325
- Xu KD, Stewart PS, Xia F, Huang CT & McFeters GA (1998) Spatial physiological heterogeneity in *Pseudomonas aeruginosa* biofilm is determined by oxygen availability. *Appl Environ Microbiol* **64**: 4035–4039

## Figures

**Figure 1.** Anaerobic survival of *P. aeruginosa* over time. While at least three independent cultures were followed, representative data for a single culture is shown. **(A)** Anaerobic survival of *P. aeruginosa* for wildtype PA14 (WT), PA14  $\Delta ldhA$  ( $\Delta ldhA$ ), and PA14  $\Delta ackA-ptb$  ( $\Delta ackA-ptb$ ) in the presence of 40 mM pyruvate (+pyruvate, closed points). Wildtype PA14 without pyruvate is shown for comparison (-pyruvate, open points). **(B)** Metabolite analysis of wildtype PA14 surviving in the presence of 40 mM pyruvate. Metabolite data for  $\Delta ldhA$  and  $\Delta ackA-ptb$  are shown in Supplemental Figure 1. **(C)** Anaerobic survival of *P. aeruginosa* for wildtype PA14 (WT) and PA14  $arcA::MAR2xT7$  ( $arcA::$ ), a transposon insertion mutant in the arginine deiminase pathway, in the presence of 40 mM arginine (+arginine, closed points). Wildtype PA14 without arginine is shown for comparison (-arginine, open points). **(D)** Anaerobic survival of *P. aeruginosa* in 20 mM D-glucose with 40 mM nitrate (+nitrate, closed points) for wildtype PA14 (WT), PA14  $\Delta narG$  ( $\Delta narG$ ), and PA14  $\Delta narG \Delta napA$  ( $\Delta narG \Delta napA$ ). Wildtype PA14 without nitrate is shown for comparison (-nitrate, open points).

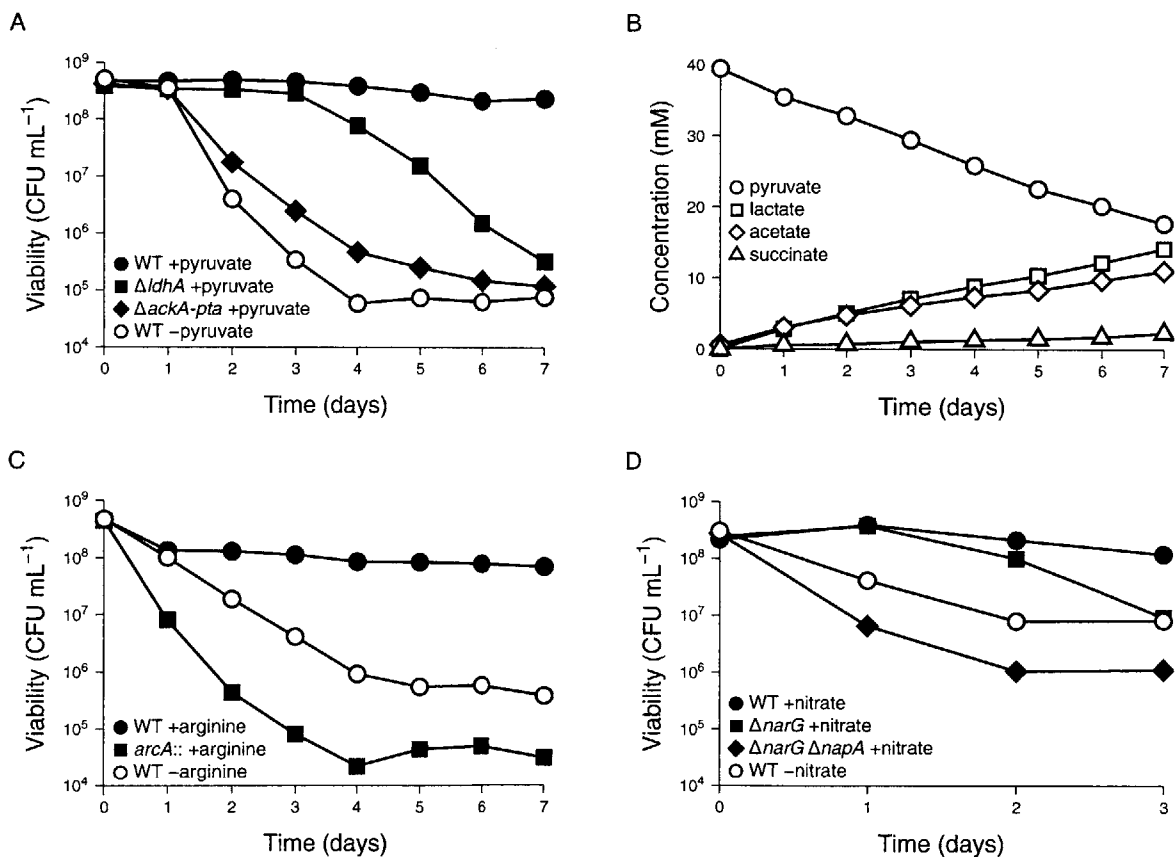


**Figure 2.** Anaerobic metabolic pathways in *P. aeruginosa*. **(A)** Pyruvate fermentation (Eschbach *et al*, 2004). LdhA, lactate dehydrogenase; Pdh, pyruvate dehydrogenase; Pta, phosphate acetyltransferase; AckA, acetate kinase. For clarity, the minor pathway from pyruvate to succinate is omitted. **(B)** The arginine deiminase pathway (Vander Wauven *et al*, 1984). ArcA, arginine deiminase; ArcB, ornithine carbamoyltransferase; ArcC, carbamate kinase. **(C)** The phosphorylative pathway for glucose oxidation via the Entner-Doudoroff pathway (Hunt and Phibbs, 1983). The oxidative pathway, which converts glucose to 6-phosphogluconate using a quinone as an electron acceptor, is not shown because it is expressed primarily under aerobic conditions (Hunt and Phibbs, 1983).

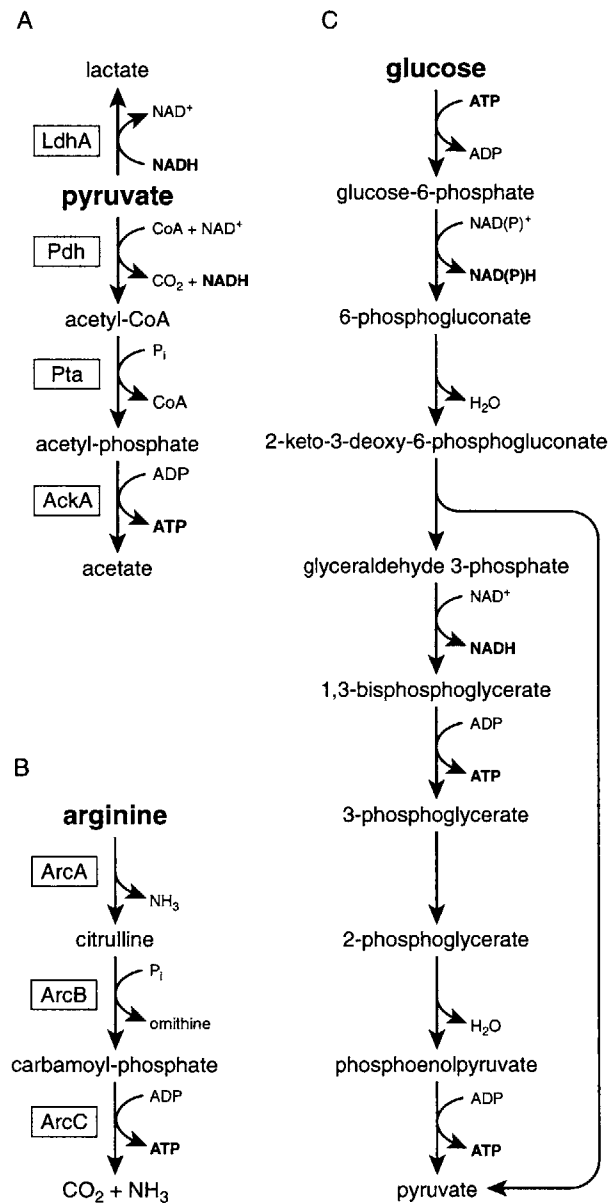


**Figure 3.** Anaerobic survival of *P. aeruginosa* PA14 strains deficient in phenazine biosynthesis ( $\Delta phz1/2$ ). The averages of at least five plating replicates of CFU counts from a single representative experiment are shown. Cells were grown aerobically to an  $OD_{500}$  of 2.8 in LB before being pelleted, washed, and resuspended in anoxic MOPS-buffered minimal medium. **(A)** Strains were incubated with 20 mM glucose. Where noted in the ‘potential’ column, cultures also included 75  $\mu$ M PCA and an electrode poised at a potential to oxidize any reduced PCA. **(B)** PA14  $\Delta phz1/2$  incubated with 20 mM glucose, 40 mM sodium succinate, or no carbon source as indicated. Where noted in the ‘potential’ column, cultures also included 75  $\mu$ M PCA and an electrode poised at a potential to oxidize any reduced PCA.

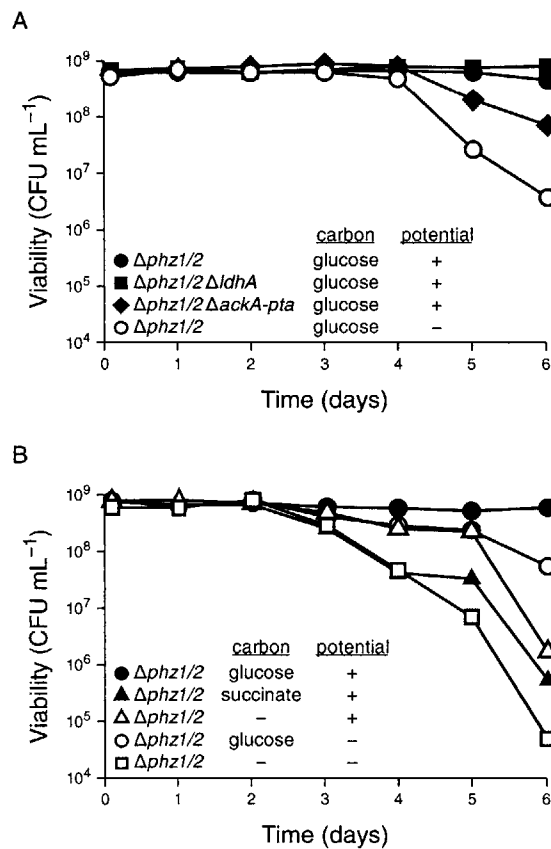


**Figure 4.** Ratios of [NADH] and [NAD<sup>+</sup>], ATP levels, and membrane depolarization measurements from different survival conditions. (A) Ratios of [NADH] and [NAD<sup>+</sup>] during anaerobic incubation of *P. aeruginosa* PA14 WT,  $\Delta dhA$ , and  $\Delta ackA-ptA$  with and without 40 mM pyruvate. While triplicate independent cultures were followed, the results of a single representative experiment are shown (also in B, C and D). (B) ATP levels from the same experiment shown in A. (C) Ratios of [NADH] and [NAD<sup>+</sup>] during anaerobic incubation of *P. aeruginosa* PA14 WT and *arcA::MAR2xT7* with and without 40 mM arginine. (D) ATP levels from the same experiment shown in C. (E) Membrane depolarization for cells incubated anaerobically for 6 h with only succinate, succinate and pyruvate, and succinate and arginine. (F) Membrane depolarization for PA14  $\Delta phz1/2$  and PA14  $\Delta phz1/2 \Delta ackA-ptA$  cells incubated in the anaerobic phenazine redox cycling conditions with 20 mM glucose, as in Figure 3A. Where indicated in the ‘potential’ column, cultures also included 75  $\mu$ M PCA and an electrode poised at a potential to oxidize any reduced PCA.

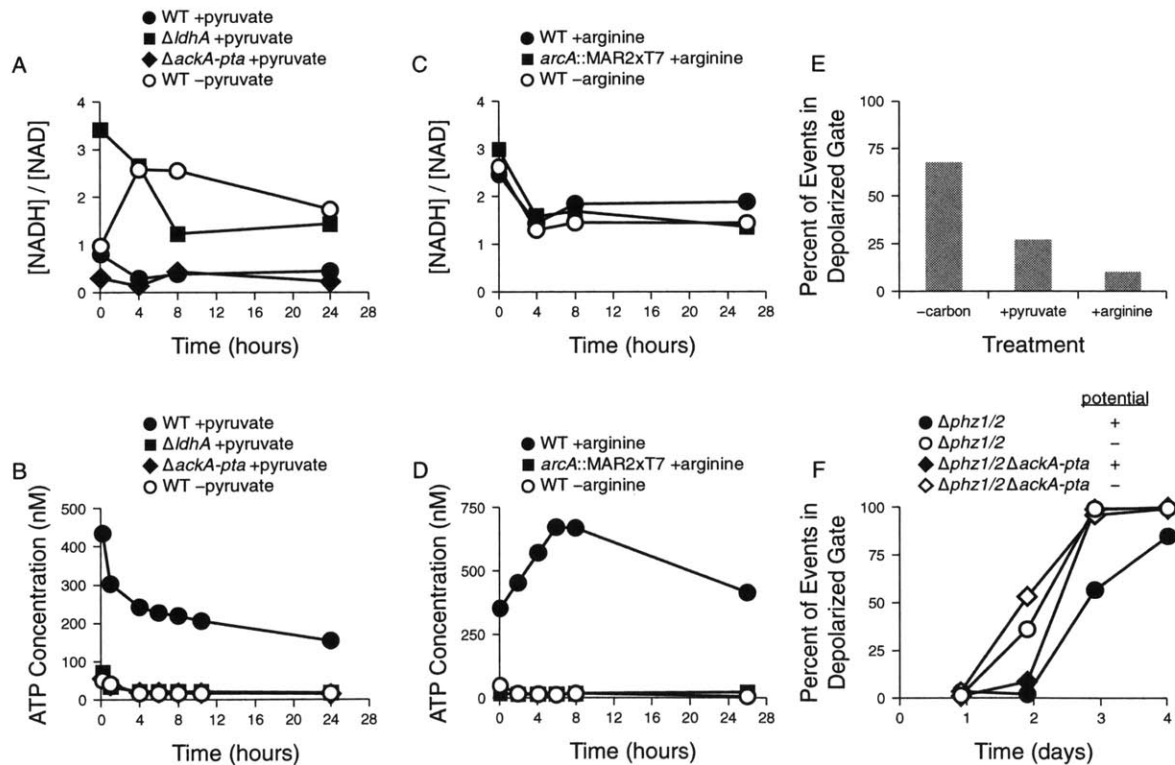


**Figure 5.** Response of fermentative *P. aeruginosa* to drugs that perturb the proton motive force. Cultures were grown aerobically to an OD<sub>500</sub> of 0.4 in minimal medium containing 40 mM pyruvate and 40 mM KNO<sub>3</sub>. Cells were centrifuged and the pellets were then washed and resuspended anaerobically in stoppered glass tubes with fresh anoxic medium containing 40 mM pyruvate. (A) Anaerobic survival of wildtype *P. aeruginosa* PA14 after two days of incubation. At the start of anaerobiosis, potassium nitrate (50 mM), ethanolic DCCD (2 mM), and/or ethanolic CCCP (100 μM) were added as indicated. As a control, ethanol was added to a final concentration of 0.2% where indicated. A culture resuspended without pyruvate added is shown for comparison (-pyruvate). Error bars represent the standard error of four independent experiments. (B) Effect of DCCD on membrane depolarization. After 24 h of anaerobiosis, 2 mM DCCD was added to a culture surviving anaerobically on 40 mM pyruvate (+DCCD). Membrane depolarization was monitored over time as described in Methods. Ethanol was added to a control sample at a final concentration of 0.2% (+ethanol). Time 0 indicates the addition of DCCD and ethanol to the cultures.

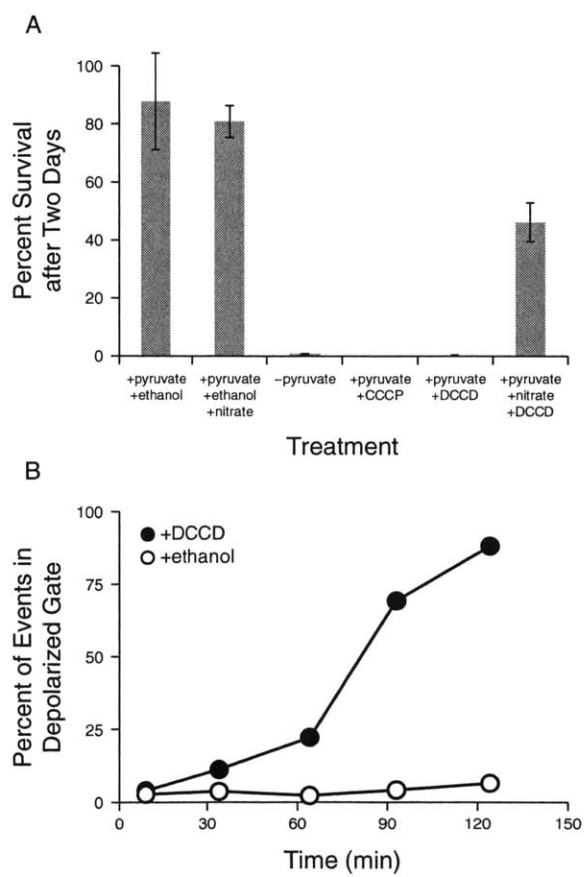
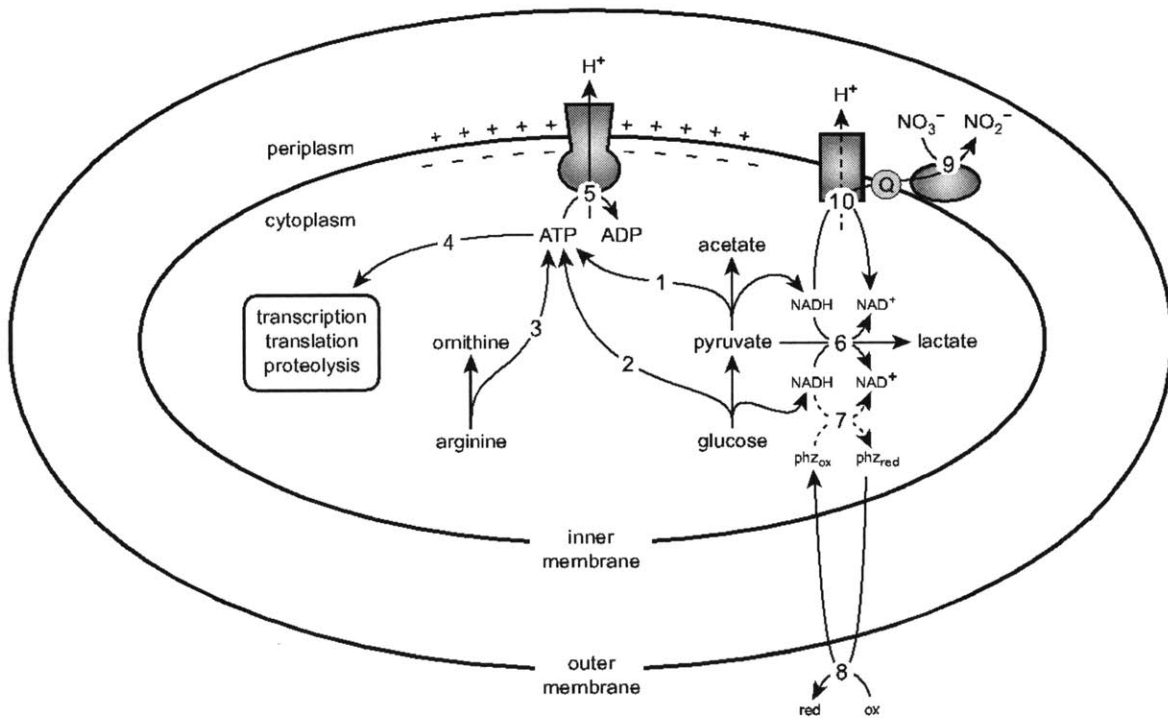


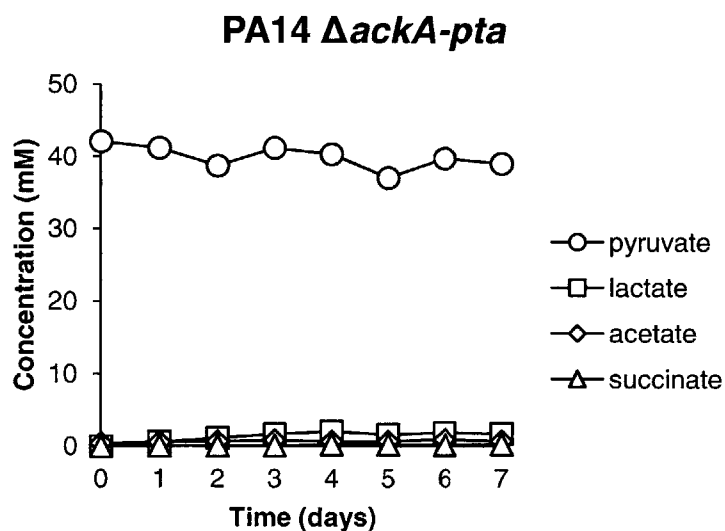
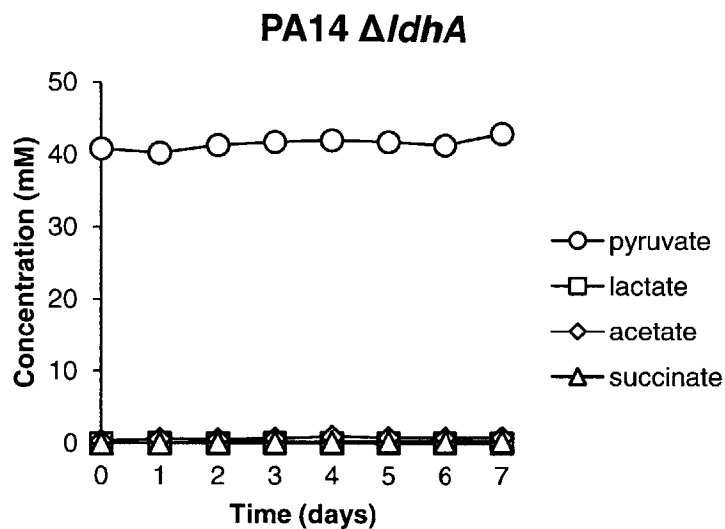
**Figure 6.** A metabolic model of survival in *P. aeruginosa*. The ATP synthesized from pyruvate fermentation (1), glucose oxidation (2), and anaerobic arginine utilization (3) is used for essential processes including transcription, translation, and proteolysis (4). The  $F_1F_0$ -ATPase complex hydrolyses ATP to translocate protons across the inner membrane (5), thereby generating a proton motive force and a membrane potential. Excess reducing equivalents from glucose and pyruvate oxidation can be dispensed by converting pyruvate to lactate (6). In addition, phenazines can regenerate oxidants for metabolism (7); although NAD(P)H is a likely electron donor for phenazines *in vivo* (Price-Whelan *et al*, 2007), the dashed lines indicate that the nature of this interaction has not been elucidated. Phenazines are then oxidized extracellularly (8) and can be reused. Nap, the periplasmic nitrate reductase, can reduce nitrate to nitrite using electrons from the quinone pool (9), permitting oxidation of NADH via NADH dehydrogenase (10), which may or may not result in proton translocation depending on which dehydrogenase complex is used.





## Supplemental Information

**Supplemental Figure 1.** Metabolite analysis of PA14  $\Delta ldhA$  and PA14  $\Delta ackA-ptb$  in the presence of 40 mM pyruvate. Data for wildtype PA14 is presented in Figure 1b of the main text.



**Supplemental Table 1.** Strains and plasmids used in this study.

Strain	Description	Reference
<i>P. aeruginosa</i>		
PA14	Clinical isolate UCBPP-PA14, wild type	Rahme <i>et al</i> , 1995
PA14 $\Delta ldhA$	PA14 with a deletion in <i>ldhA</i> , coding for D-lactate dehydrogenase	This study
PA14 $\Delta ackA-ptA$	PA14 with a deletion in <i>ackA</i> and <i>pta</i> , coding for acetate kinase and phosphate acetyltransferase, respectively	This study
PA14 $\Delta phz1/2$	PA14 with clean deletions of the phenazine biosynthesis operons <i>phzA1-G1</i> and <i>phzA2-G2</i>	Dietrich <i>et al</i> , 2006
PA14 $\Delta phz1/2 \Delta ldhA$	Phenazine-null PA14 with a deletion in <i>ldhA</i>	This study
PA14 $\Delta phz1/2 \Delta ackA-ptA$	Phenazine-null PA14 with a deletion in <i>ackA-ptA</i>	This study
PA14 <i>arcA::MAR2xT7</i>	PA14 with a transposon insertion in <i>arcA</i> , coding for arginine deiminase	Liberati <i>et al</i> , 2006
PA14 <i>arcC::MAR2xT7</i>	PA14 with a transposon insertion in <i>arcC</i> , coding for carbamate kinase	Liberati <i>et al</i> , 2006
PA14 $\Delta narG$	Phenazine-null PA14 with a deletion in <i>narG</i>	Dietrich <i>et al</i> , 2013
PA14 $\Delta narG \Delta napA$	Phenazine-null PA14 with a deletion in <i>narG</i> and <i>napA</i>	Dietrich <i>et al</i> , 2013
<i>E. coli</i>		
DH5 $\alpha$	Host for cloning; F <sup>-</sup> <i>endA1 hsdR17 supE44 thi-1 <math>\lambda</math>-recA1 gryA96 relA1 deoR <math>\Delta(argF-lac)</math>U169 <math>\phi</math>80dlacZ<math>\Delta</math>M15</i>	Grant <i>et al</i> , 1990
HB101/pRK2013	Helper strain for triparental mating	Choi <i>et al</i> , 2006
<i>S. cerevisiae</i>		
INVSc1	Fast growing strain for homologous recombination; <i>MATa his3<math>\Delta</math>1 leu2 trp1-289 ura3-52</i>	Invitrogen
Plasmids		
pMQ30	Conjugal suicide vector for creating clean gene deletions	Shanks <i>et al</i> , 2006
p $\Delta ldhA$	2 kb fragment containing $\Delta ldhA$ cloned into pMQ30	This study
p $\Delta ackA-ptA$	2 kb fragment containing $\Delta ackA-ptA$ cloned into pMQ30	This study

**Supplemental Table 2.** Primer sequences used in the construction and verification of mutants in this study.

Name	Sequence (5'-3')	Comments
ldhA-del-primer1	AGGCAAATTCGTGTTTATCAGACCGCTTCTGCGTTCTGATTTCTGG GAATTCGAACGGCT	For amplification of the ~1 kb region upstream of <i>ldhA</i> . Used to construct p $\Delta$ <i>ldhA</i> .
ldhA-del-primer2	GCGCATGCTACCACGCCAGGTCAGAGTTCGCTGGAGTCGA	
ldhA-del-primer3	TCGACTCCAGCGAACTCTGACCTGGCGTGGTAGCATGCGC	For amplification of the ~1 kb region downstream of <i>ldhA</i> . Used to construct p $\Delta$ <i>ldhA</i> .
ldhA-del-primer4	GGAATTGTGAGCGGATAACAATTTACACAGGAAACAGCTGTGGTC AAGCGGGAATGAAA	
ldhA-C1	TTCGGCCTGGAAGTGAGCGAAT	Bind upstream and downstream of <i>ldhA</i> . Used to sequence the chromosomal <i>ldhA</i> deletion.
ldhA-C4	AAAGAAGCGGTTGAGTGTCTCGGT	
ackA-del-primer1	TTGTGAGCGGATAACAATTTACACAGGAAACAGCTTTCAGGCTGC AGAAGGACTGGATA	For amplification of the ~1 kb region upstream of <i>ackA-pta</i> . Used to construct p $\Delta$ <i>ackA-pta</i> .
ackA-del-primer2	CCACTGGGCGGCTTCCCTCACTGCTCCTTGGTCTGCTCTTC	
ackA-del-primer3	GAAGAGCAGACCAAGGAGCAGTGAGGAACGCCGCCAGTGG	For amplification of the ~1 kb region downstream of <i>ackA-pta</i> . Used to construct p $\Delta$ <i>ackA-pta</i> .
ackA-del-primer4	CAAATTCGTGTTTATCAGACCGCTTCTGCGTTCTGATTACTGATCG CGGCTGGAAGAAA	
ackA-C1	TGCCGTTGACCTCGACCTT	Bind upstream and downstream of <i>ackA-pta</i> . Used to sequence the chromosomal <i>ackA-pta</i> deletion.
ackA-C4	CCGATCGCGAGCAACTCCA	
pMQ-f	ACGGCGTTTCACTTCTGAGT	Bind upstream and downstream of the recombination site in pMQ30. Used to screen inserts from homologous recombination in the construction of p $\Delta$ <i>ldhA</i> and p $\Delta$ <i>ackA-pta</i> .
pMQ-r	ATTAGGCACCCAGGCTTTA	
arcA-tn-vf	TGAAGTGGATCCTCGATCGCAA	Bind upstream and downstream of the annotated transposon insert site in <i>arcA</i> . Used to verify the transposon insertion.
arcA-tn-vr	TGGAACTTGTAGATGGCGGT	
arcC-tn-vf	TACGACCAGGTCTCGCCCTAC	Bind upstream and downstream of the annotated transposon insert site in <i>arcC</i> . Used to verify the transposon insertion.
arcC-tn-vr	AGATGACGATGGTGCCTTTCTC	



## Chapter 5

### Extraction and Measurement of NAD(P)<sup>+</sup> and NAD(P)H

Suzanne E Kern, Alexa Price-Whelan, Dianne K Newman

This document is a reproduction of the chapter in press by the same name in a forthcoming book entitled *Pseudomonas* Methods, edited by Allain Filloux and Juan Luis for Humana Press.

**Contributions:**

I wrote this chapter with assistance from Alexa Price-Whelan and generated the data and figures herein.

## Summary/Abstract

Nicotinamide adenine dinucleotides are critical redox-active substrates for countless catabolic and anabolic reactions. Ratios of NAD<sup>+</sup> to NADH and NADP<sup>+</sup> to NADPH are therefore considered key indicators of the overall intracellular redox potential and metabolic state. These ratios can be measured in bulk conditions using a highly sensitive enzyme-cycling-based colorimetric assay (detection limit at or below 0.05 μM, or 1 picomole) following a simple extraction procedure involving solutions of acid and base. Special considerations are necessary to avoid measurement artifacts caused by the presence of endogenous redox-active metabolites, such as phenazines made by diverse *Pseudomonas* species (see Chapter 6, “Measurement of Phenazines in Bacterial Cultures”).

### 1. Introduction

Oxidized nicotinamide adenine dinucleotide (NAD<sup>+</sup>) is an enzyme cofactor that participates in redox transformations involved in the oxidative conversion of substrates to metabolic end products, such as CO<sub>2</sub> and H<sub>2</sub>O in the case of sugar metabolism. In the process, NAD<sup>+</sup> accepts two electrons and a proton. In its reduced form (NADH) the cofactor can donate electrons to the respiratory chain through NADH dehydrogenase, regenerating NAD<sup>+</sup>. The related nicotinamide adenine dinucleotide phosphate (NADP(H)) is commonly involved in anabolic reactions, such as the synthesis of fatty acids, which require the input of reducing equivalents. The membrane-bound transhydrogenase enzyme interconverts NAD(H) and NADP(H) by coupling NADP<sup>+</sup> reduction to NADH oxidation at the expense of moving one proton from the periplasm to the cytoplasm (de Graef *et al*, 1999; Hoek & Rydström, 1988). This reaction is reversible under physiological conditions and permits the maintenance of appropriate cellular NAD(H) and NADP(H) redox levels. Overall, the relative levels of reduced and oxidized nicotinamide cofactors within living cells affects which metabolic reactions can occur (Harrison & Chance, 1970; de Graef *et al*, 1999; Chen *et al*, 2003).

These compounds can be detected by several methods:

- 1.) direct measurement of NADH fluorescence of cells in culture (London & Knight, 1966; Harrison & Chance, 1970; Chen *et al*, 2003) or of cell extracts (Hung *et al*, 2011; London & Knight, 1966),
- 2.) measurement of NAD(H)-binding GFP fluorescence (Hung *et al*, 2011),

- 3.) *in vitro* colorimetric enzyme-mediated assays of cell extracts (Hoek & Rydström, 1988; Bernofsky & Swan, 1973; Price-Whelan *et al*, 2007), and
- 4.) time-resolved fluorescence profiling of cells *in situ* using multiphoton microscopy (Hoek & Rydström, 1988; Sullivan *et al*, 2011).

It is important to be aware that directly measuring levels of NAD(P)(H) in cell cultures using only spectral properties may be compromised by other endogenous compounds with similar spectral properties, *e.g.* 1-hydroxyphenazine and the iron chelator pyoverdine (de Graef *et al*, 1999; Sullivan *et al*, 2011). Because of its simplicity, sensitivity and specificity, a time-resolved enzymatic colorimetric assay based on the procedures developed by San, *et al* (Harrison & Chance, 1970; San *et al*, 2002; Chen *et al*, 2003) and Bernofsky and Swan (London & Knight, 1966; Bernofsky & Swan, 1973) is our preferred approach (Hung *et al*, 2011; Price-Whelan *et al*, 2007) and the focus of this chapter. With an exchange of the enzyme and substrate, this assay is specific to either NAD(H) or NADP(H) and a single set of cell extracts can be used for both (Fig. 1). NAD(P)(H) levels as low as 0.05  $\mu\text{M}$  (less than 1 picomole in the assay mixture, equivalent to  $\sim 5 \text{ nmol}/10^9$  cells) can be measured by this method. One drawback to the extraction procedure is the length of time that passes before quenching metabolism, which occurs upon the addition of acid or base to the cell pellet following a one-minute centrifugation step to concentrate the sample and exclude any extracellular NAD(P)(H) (Bernofsky & Swan, 1973; Wos & Pollard, 2006; Price-Whelan *et al*, 2007). For time-sensitive measurements, this is an important caveat (Chen *et al*, 2003).

This method has been applied widely to samples grown in well-mixed bacterial cultures (Watanabe *et al*, 2011; San *et al*, 2002; Price-Whelan *et al*, 2007), and has been adapted for use in measuring the NADH/NAD<sup>+</sup> of bacterial colony biofilms (Dietrich *et al*, 2013). Extractions from phenazine-producing organisms, such as pseudomonads, require special consideration: phenazines, another class of redox-active molecules, can oxidize NAD(P)H and participate in cycling reactions to reduce extracellular oxidants, such as oxygen and ferric iron (Denning *et al*, 2003; Kito *et al*, 1974; Wang & Newman, 2008). Because the nature of this extraction procedure is to destabilize the reduced or oxidized nicotinamide cofactor (Burton & Kaplan, 1963a; 1963b) in paired samples, subsequent reactions with phenazines in the cell-free extract can result in the degradation of NAD(P)H, which can artificially skew the measured ratio. In this method, we include notes and precautions for successfully circumventing this problem.

## 2. Materials

Prepare all reagents using distilled, deionized (18.2 megaohm resistivity) water. Diligently follow all waste disposal regulations when disposing waste materials.

### 2.1 Extraction Reagents

1. Sodium hydroxide: 0.2 M and 0.1 M.
2. Hydrochloric acid: 0.2 and 0.1 M.

### 2.2 Extraction Equipment and Supplies

Some extractions may need to be performed in the absence of oxygen (*see Notes 1 and 2*)

1. Water or sand bath at 50°C.
2. Ice.
3. Vortex.
4. Pipettes and tips.
5. Micro-centrifuge tubes.
6. Micro-centrifuge.

### 2.3 NAD(H) Measurement Reagents

1. Bicine buffer solution: 1 M at pH 8.0. Can be prepared in advance and stored at room temperature.
2. Ethylenediaminetetraacetic acid (EDTA) solution: 40 mM at pH 8.0. Can be prepared in advance and stored at room temperature.
3. **Methylthiazolyldiphenyl-tetrazolium bromide** (MTT, also known as thiazolyl blue tetrazolium bromide) solution: 4.2 mM. Can be prepared in advance and stored at room temperature, or frozen at -20°C in aliquots.
4. Phenazine ethosulphate (PES) solution: 16.6 mM. Can be prepared in advance and must be protected from light. Aliquots can be stored in the dark and frozen at -20°C for at least 6 months (*see Note 3*).
5. Ethanol: 100%.



6. Alcohol dehydrogenase II (ADH II) enzyme solution: 1 mg/mL in 0.1 M bicine buffer, pH 8.0. Use Sigma A-3263, which has very low background levels of NAD bound. Make this just before use, in Measurement Step 7.
7.  $\beta$ -nicotinamide adenine dinucleotide (NAD<sup>+</sup>) and/or reduced  $\beta$ -nicotinamide adenine dinucleotide (NADH) solution(s): 0.01 to 100  $\mu$ M, according to concentrations needed for a standard curve (*see Note 4*). If preparing in advance, dissolve NADH in slightly basic solution (0.01 M NaOH) and dissolve NAD<sup>+</sup> in slightly acidic solution (0.01 M HCl). Single-use aliquots of NAD<sup>+</sup> and NADH can be stored at -80°C for at least 6 months.

## 2.4 NADP(H) Measurement Reagents

Materials are identical to those for NAD(H) Measurement (Section 2.3), with only the following changes:

5. Glucose-6-phosphate solution: 25 mM. Prepare aliquots and freeze at -20°C for up to two weeks.
6. Glucose-6-phosphate dehydrogenase (G6PD) enzyme solution: 0.1 mg/mL in 0.1 M bicine buffer, pH 8.0. This can be prepared in advance and frozen in single-use aliquots at -80 °C.
7.  $\beta$ -nicotinamide adenine dinucleotide phosphate (NADP<sup>+</sup>) and/or reduced  $\beta$ -nicotinamide adenine dinucleotide phosphate (NADPH) solution(s): 0.05 to 50  $\mu$ M, according to concentrations needed for a standard curve (*see Note 4*). If preparing in advance, mix NADPH with anoxic water under an oxygen-free atmosphere. Aliquots of NADP<sup>+</sup> and NADPH can be stored at -80°C for at least 6 months.

## 2.5 NAD(P)(H) Measurement Equipment and Supplies

1. Plate reader capable of maintaining a constant internal temperature (at about 30°C) and recording absorbance at 570 nm at regular time intervals (for example, Biotek Synergy 4).
2. Optically-clear flat-bottom styrene 96-well microtiter plate (for example, Thermo Scientific #9205).
3. Single and multichannel pipettes (for 90  $\mu$ L and for 5  $\mu$ L volumes) and tips.
4. Reagent reservoir for multichannel pipetting (for < 25 mL volumes).

## 3. Methods

### 3.1 Extraction

Unless otherwise specified, perform all steps at room temperature.

1. Remove a sample of the culture for measuring viable cell counts, cell mass, or optical density, in order to calculate NAD(P)(H) concentrations relative to the amount of cells, if desired.
2. Per sample, pipette 1 mL of culture into each of two labeled microfuge tubes, one for NAD(P)H extraction, one for NAD(P)<sup>+</sup> extraction (*see Notes 5 and 6*; if cell density is low, *see Notes 7 and 8*).
3. Pellet cells: 1 minute at maximum speed (16,000 rcf).
4. Remove supernatant (*see Note 6*).
5. Resuspend pellet in 0.2 M acid or base, as follows (*see Note 5*):
  - 300  $\mu$ L 0.2 M sodium hydroxide (for NAD(P)H extraction)
  - 300  $\mu$ L 0.2 M hydrochloric acid (for NAD(P)<sup>+</sup> extraction)
6. Incubate tubes at 50°C (using heat block or water bath) for 10 minutes. Then cool on ice, about 5 minutes.
7. With the cap open, add 0.1 M acid or base drop-wise to each tube while vortexing at low speed (*see Note 9*), as follows:
  - 300  $\mu$ L 0.1 M hydrochloric acid (for NAD(P)H extraction)
  - 300  $\mu$ L 0.1 M sodium hydroxide (for NAD(P)<sup>+</sup> extraction)
8. Pellet debris: 5 minutes at maximum speed (16,000 rcf).
9. Transfer 150 - 300  $\mu$ L of supernatant to a clean, labeled microfuge tube (*see Note 10*).
10. Either store extracts at -80°C for up to a week or proceed right away to Measurement Step 1 (*see Note 1*).

### 3.2 NAD(H) Measurement

1. Turn on the plate reader and set it to preheat to 30°C.
2. Prepare a mix of the assay reagents according to the number of samples and expected concentrations of NAD(H) and keep the mix protected from light (*see Notes 3, 7, and 8*).

- 1 vol 1 M bicine buffer, pH 8.0
- 1 vol 100% ethanol
- 1 vol 40 mM EDTA
- 1 vol 4.2 mM MTT
- 2 vol 16.6 mM PES
- 3 vol water

For a full 96-well plate, one volume = 1 mL.

3. Prepare a range of concentrations of NAD<sup>+</sup> and/or NADH in water for a standard curve (*see Note 4*).
4. Pipette 5  $\mu$ L of the standards, water blanks, and sample supernatants into separate wells of the 96-well microtiter plate (*see Note 11*; for higher sensitivity *see Note 8*).
5. In dim light, use a multichannel pipette to add 90  $\mu$ L of the reagent mix to each well. (For higher sensitivity *see Note 8*.)
6. Keeping the plate protected from light, incubate the plate for approximately 10 minutes at 30°C (*see Note 12*).
7. Prepare a fresh solution of alcohol dehydrogenase enzyme:
  - Weigh out 0.7 - 2.0 mg of ADH II
  - Gently dissolve the enzyme powder to 1 mg/mL in 0.1 M bicine buffer, pH 8.0
  - Pipette the enzyme solution into a reagent reservoir for multichannel pipetting
8. In dim light, using a multichannel pipette, add 5  $\mu$ L of the enzyme solution to each well containing the reagent mix with sample or standard.
9. Return the plate to the plate reader and begin recording absorbance at 570 nm according to the following program:
  - Hold temperature at 30°C
  - Start kinetic read, repeating each of the steps below for at least 20 minutes. For maximum resolution, use the software to calculate the minimum interval required between each round. (For higher sensitivity, *see Note 8*.)
    - Shake the plate for 3 seconds at medium speed
    - Read the absorbance at 570 nm ( $A_{570}$ ) for each well

### 3.3 NADP(H) Measurement

Follow the procedure outlined for NAD(H) Measurement (Section 3.2), with the following changes:

2. Prepare a mix of the assay reagents according to the number of samples and expected concentrations of NADP(H) and keep the mix protected from light (*see Notes 3, 7, and 8*).
  - 1 vol 1 M bicine buffer, pH 8.0
  - 1 vol 25 mM glucose-6-phosphate
  - 1 vol 40 mM EDTA
  - 1 vol 4.2 mM MTT
  - 2 vol 16.6 mM PES
  - 3 vol water

For a full 96-well plate, one volume = 1 mL.

3. Prepare a range of concentrations of NADP<sup>+</sup> and/or NADPH in water for a standard curve (*see Note 4*).
7. Thaw a frozen aliquot or prepare a fresh solution of glucose-6-phosphate dehydrogenase:
  - Weigh out 0.07 - 1.0 mg of G6PDH
  - Gently dissolve the enzyme powder to 0.1 mg/mL in 0.1 M bicine buffer, pH 8.0
  - Pipette the enzyme solution into a reagent reservoir for multichannel pipetting

### 3.4 Data Workup

1. Obtain a data table of absorbance at 570 nm ( $A_{570}$ ) for each well over time.
2. To determine absolute concentrations of NAD(P)(H) from samples, start by creating a standard curve (*see Fig. 2a*):
  - a. Make a plot of  $A_{570}$  versus time for the standards and water blanks.
  - b. Define a time frame for which all standards show a linear increase in  $A_{570}$ /time.
  - c. Calculate the slope for each standard during the same time frame (ex. from 1 - 8 minutes).

- d. Plot or use a linear regression to obtain a standard curve and an equation relating the known concentrations of the standards versus  $A_{570}/\text{time}$  (see **Note 13**).
3. Use the standard curve to calculate the concentration of each sample based on its slope ( $A_{570}/\text{time}$ , see **Fig. 2b**)
4. Calculate the ratio of NAD(P)<sup>+</sup> to NAD(P)H for each sample and/or report absolute concentrations of each relative to the amount of cells in the original sample (see **Note 14**).

## 4. Notes

1. The reduced form of pyocyanin tends to associate with the cell pellet and this can lead to carry-over of redox-active compounds that can interfere with the stability of NAD(P)H extracts. For samples with phenazines present, particularly under low-aeration conditions, it is advisable to perform Extraction Step 2 (for anaerobic growth) or Extraction Step 5 (for aerobic growth) through Measurement Step 5 in an oxygen-free glove box, using reagents and supplies that have equilibrated to the anoxic atmosphere. To determine if this precaution is necessary, pellet a sample of cells and remove the supernatant. If, upon resuspending the pellet in base, the extract turns faintly blue (evidence of oxidized pyocyanin in *P. aeruginosa* cultures), then anaerobic extraction is essential. With oxidized phenazines present, NADP(H) reacts to form NAD(P)<sup>+</sup>, which then degrades in the basic extraction solution and leads to artificially low NAD(P)H readings. Anaerobically prepared extracts can be stored for up to 24 hours in an oxygen-free chamber, in the dark at room temperature. To be absolutely sure that no oxygen interferes, switch the order of Measurement Steps 4 and 5, first filling wells of the assay plate with the reagent mix, then adding each sample individually, all in an oxygen-free environment. Residual oxygen associated with tubes and microtiter plates can be sufficient to oxidize phenazines, and therefore, destroy NAD(P)H. For strains that produce little or no pyocyanin, it is worthwhile to perform parallel NAD(P)H extractions under ambient atmospheric conditions and in an oxygen-free context, and compare the measured levels.

2. Equipment and supplies for anaerobic extractions: oxygen-free glove box with all equipment inside--heat block at 50°C, ice or -20°C freezer block for microfuge tubes, vortex, pipettes and tips, microfuge tubes (equilibrated under oxygen-free conditions for at least 24 hours), micro-centrifuge.
3. PES is very sensitive to light and degrades to form a compound that is dark in color, which interferes with the  $A_{570}$  readings of reduced MTT. When pipetting PES or the reagent mix, turn off bright lights and perform these steps in dim lighting, away from windows. Cover tubes of PES aliquots (may be stored at -20°C) and the reagent mix in foil. Protect the final mix of samples and reagents from light by covering the 96-well plate with foil until it is moved inside of the plate reader.
4. Make standard solutions based on concentrations calculated using the following extinction coefficients. NAD(P)H:  $\epsilon_{340} = 6.22 \text{ mM}^{-1}\cdot\text{cm}^{-1}$ , NAD(P)<sup>+</sup>:  $\epsilon_{260} = 18.0 \text{ mM}^{-1}\cdot\text{cm}^{-1}$  (Sigma product information sheets). Because the measurement depends on a cycling reaction, both the reduced and oxidized substrate should result in the same calibration curve.
5. There are many ways to conserve pipette tips during this procedure: For Extraction Step 2, pipette up and down once in the culture to wet the pipette tip before removing the paired 1-mL samples to get equal volumes. In Extraction Step 5 the 0.2 M acid or base can be added using the same tip and the pellet resuspended by vortexing. In Measurement Steps 4 and 5, the reagent mix can be added by multichannel pipette first, followed by the individual standards and samples.
6. Work quickly through Extraction Step 5, to rapidly quench cellular metabolism. Because the cell pellet starts to resuspend back into the supernatant, it may be best to process only two or three paired extraction samples at a time. To remove the supernatant (Extraction Step 4) determine what works best: pouring and tapping out (faster, may leave varying amounts of residual medium) or pipetting (slower, more accurate unless a long time elapses before later samples get processed). For aerobically-cultured cells, it is particularly important to sample as quickly as possible upon removing the culture from its incubation conditions, and to proceed rapidly through Extraction Step 5.
7. Determine whether the higher-sensitivity adaptations are necessary for a given sample:

- a. Is the cell density below OD<sub>500</sub> 0.2 (for actively growing cells) or 0.8 (for dying/late-stationary phase cells)?
- b. Will the redox state be strongly skewed, such that the abundance of either NAD(P)<sup>+</sup> or NAD(P)H is comparatively low?

In either case, it may help to increase the sensitivity by following the adaptations outlined in **Note 8**, below.

8. For very low levels of NAD(P)(H), use the following adaptations. Use 2-mL microcentrifuge tubes and pellet 1.8 mL of culture. Add only 200  $\mu$ L acid and base for Extraction Steps 5 and 7 (instead of 300  $\mu$ L). Use these proportions for a higher-sensitivity reagent mix (keep mix protected from light):
  - 2 vol 1 M bicine buffer, pH 8.0
  - 1 vol 100% ethanol or 25 mM glucose-6-phosphate
  - 1 vol 40 mM EDTA
  - 1 vol 4.2 mM MTT
  - 2 vol 16.6 mM PES
  - 1 vol water

For a full 96-well plate, one volume = 1 mL.

For each reaction, combine 80  $\mu$ L reagent mix, 15  $\mu$ L sample extract or standard, and 5  $\mu$ L enzyme solution (total volume remains at 100  $\mu$ L per well). The larger volume of sample requires stronger pH buffering. The kinetic read in Measurement Step 9 can be extended for up to 40 minutes in order to discern very slight increases in A<sub>570</sub>/time. Include several water blanks so that very low levels can be accurately distinguished from zero. Levels as low as 10 nM NAD(H) and 50 nM NADP(H) can be detected by following these procedural changes.

9. Use a vortex speed that swirls the total volume (600  $\mu$ L) to somewhere below the cap. A high speed will spin the liquid into the cap, but with the proper setting, the cap can be left open and the acid or base can be safely added drop-wise while the solution is mixed.
10. The final pellet in the NAD(P)H extract is very fluffy and viscous. To avoid disturbing the pellet, carefully pipette from the top portion of the liquid and consider taking the supernatants from all NAD(P)H extracts as soon as centrifugation finishes, followed by the NAD(P)<sup>+</sup> extracts.

11. In order to minimize measurement error due to pipetting, include technical replicates of the samples and standards in the 96-well plate and average the resulting  $A_{570}/\text{time}$  values calculated in Data Workup Steps 2 and 3. Since it may be difficult to see the wells in dim lighting (applicable when the reagent mix is added to the 96-well plate before the samples), consider using a guide, for instance a piece of label tape with numbers 1 through 12 placed directly below the row of wells into which you add samples or standards. After pipetting the last sample of a row, move the tape down to just below the next row.
12. Use aluminum foil to completely cover the microtiter plate and protect the reagent mix from light. Foil is not necessary if the plate reader, which is dark inside, is used to incubate the plate at 30°C.
13. If using Excel to process the plate reader data, make use of pre-defined functions. Use the SLOPE function: select the  $A_{570}$  values (known  $y$ 's) and time stamps (known  $x$ 's) over the linear time range to obtain  $A_{570}/\text{time}$ . To generate a standard curve, use INTERCEPT and SLOPE, inputting the known standard concentrations for the  $y$  values and the corresponding  $A_{570}/\text{time}$  for the  $x$  values (*see Fig 2a*). Then the concentration of the samples can then be easily determined by multiplying the  $A_{570}/\text{time}$  of each sample by the calculated slope and adding the intercept as provided by the standard curve.
14. Representing NAD(P)H/NAD(P)<sup>+</sup> (or the inverse) on a log scale conveys the biologically-relevant ratio, yet allows for straight-forward interpretation of ratios both greater and less than one. By comparison, a linear scale makes fractional ratios difficult to discriminate, while reporting percentages of the total pool does not directly indicate the ratio, which is what ultimately defines the equilibrium state of reactions in the cell.

## 5. Acknowledgments

S.E.K. was supported by the National Science Foundation Graduate Research Fellowship Program, and D.K.N. is a Howard Hughes Medical Institute (HHMI) Investigator. We thank the HHMI for supporting our work. N. Glasser provided constructive criticism of earlier drafts of this chapter.



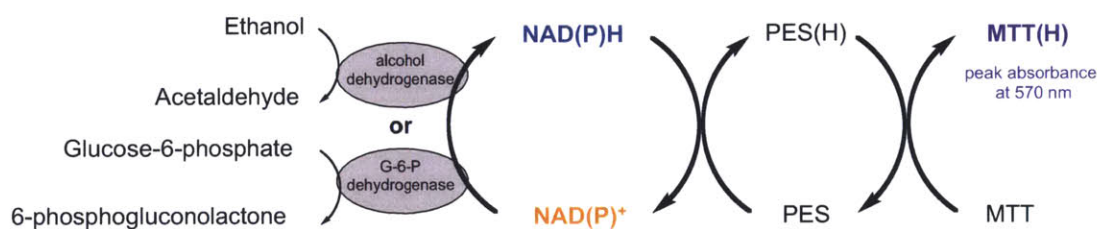
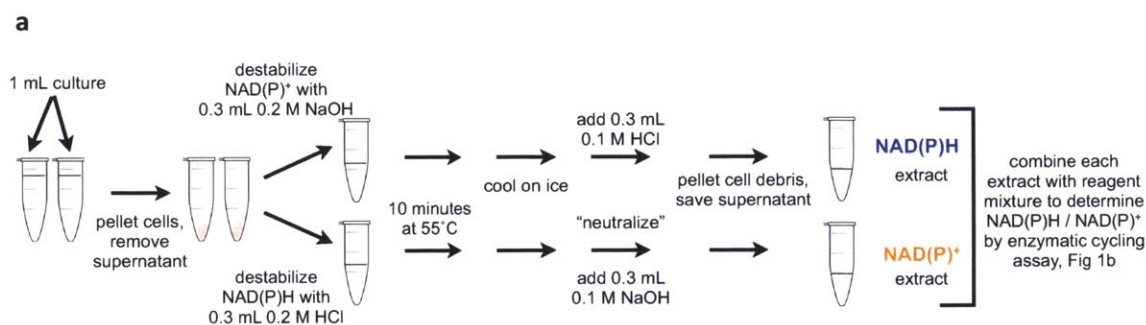
## 6. References

- Bernofsky C & Swan M (1973) An improved cycling assay for nicotinamide adenine dinucleotide. *Anal Biochem* **53**: 452–458.
- Burton RM & Kaplan NO (1963a) The reaction of reduced pyridine nucleotides with acid. *Arch Biochem Biophys* **101**: 150–159.
- Burton RM & Kaplan NO (1963b) The reaction of diphosphopyridine nucleotide and related pyridinium salts with alkali. *Arch Biochem Biophys* **101**: 139–149.
- Chen F, Xia Q & Ju L-K (2003) Aerobic denitrification of *Pseudomonas aeruginosa* monitored by online NAD(P)H fluorescence. *Appl Environ Microbiol* **69**: 6715–6722.
- de Graef MR, Alexeeva S, Snoep JL & Teixeira de Mattos MJ (1999) The steady-state internal redox state (NADH/NAD) reflects the external redox state and is correlated with catabolic adaptation in *Escherichia coli*. *J Bacteriol* **181**: 2351–2357.
- Denning GM, Iyer SS, Reszka KJ, O'Malley Y, Rasmussen GT & Britigan BE (2003) Phenazine-1-carboxylic acid, a secondary metabolite of *Pseudomonas aeruginosa*, alters expression of immunomodulatory proteins by human airway epithelial cells. *Am J Physiol Lung Cell Mol Physiol* **285**: L584–92.
- Dietrich LEP, Okegbe C, Price-Whelan A, Sakhtah H, Hunter RC & Newman DK (2013) Bacterial community morphogenesis is intimately linked to the intracellular redox state. *J Bacteriol*.
- Harrison D & Chance B (1970) Fluorimetric technique for monitoring changes in the level of reduced nicotinamide nucleotides in continuous cultures of microorganisms. *Appl Microbiol* **19**: 446–450.
- Hoek JB & Rydström J (1988) Physiological roles of nicotinamide nucleotide transhydrogenase. *Biochem J* **254**: 1–10.
- Hung YP, Albeck JG, Tantama M & Yellen G (2011) Imaging cytosolic NADH-NAD(+) redox state with a genetically encoded fluorescent biosensor. *Cell Metab* **14**: 545–554.
- Kito N, Ohnishi Y, Kagami M & Ohno A (1974) Reduction by a model of NAD(P)H. Construction of electron bridges. *Chem Lett* 353–356.
- London J & Knight M (1966) Concentrations of nicotinamide nucleotide coenzymes in micro-organisms. *J Gen Microbiol* **44**: 241–254.
- Price-Whelan A, Dietrich LEP & Newman DK (2007) Pyocyanin alters redox homeostasis and carbon flux through central metabolic pathways in *Pseudomonas aeruginosa* PA14. *J Bacteriol* **189**: 6372–6381.
- San K-Y, Bennett GN, Berríos-Rivera SJ, Vadali RV, Yang Y-T, Horton E, Rudolph FB, Sariyar B & Blackwood K (2002) Metabolic engineering through cofactor manipulation and its effects on metabolic flux redistribution in *Escherichia coli*. *Metab Eng* **4**: 182–192.

- Sullivan NL, Tzeranis DS, Wang Y, So PTC & Newman DK (2011) Quantifying the dynamics of bacterial secondary metabolites by spectral multiphoton microscopy. *ACS Chem Biol* **6**: 893–899.
- Wang Y & Newman DK (2008) Redox reactions of phenazine antibiotics with ferric (hydr)oxides and molecular oxygen. *Environ Sci Technol* **42**: 2380–2386.
- Watanabe S, Zimmermann M, Goodwin MB, Sauer U, Barry CE & Boshoff HI (2011) Fumarate reductase activity maintains an energized membrane in anaerobic *Mycobacterium tuberculosis*. *PLoS Pathog* **7**: e1002287.
- Wos M & Pollard P (2006) Sensitive and meaningful measures of bacterial metabolic activity using NADH fluorescence. *Water Res* **40**: 2084–2092.

## 7. Figures

**Figure 1. a)** Schematic overview of the extraction of NAD(P)(H) from cell pellets by destabilization of the reduced cofactor in acid and the oxidized cofactor in base. **b)** Representation of the enzyme-cycling assay used to detect the level of NAD(H) or NADP(H) in a sample. MTT: **methylthiazolyldiphenyl-tetrazolium bromide**, PES: **phenazine ethosulfate**. **c)** When phenazines are present in the sample extract, interactions with oxygen can result in the destabilization of NAD(P)<sup>+</sup>. For example, reduced pyocyanin can give up electrons to oxygen, and then pick up electrons from NAD(P)H. When NAD(P)H gets oxidized, the resulting NAD(P)<sup>+</sup> immediately gets destabilized in the basic extraction solution.



*Rate of MTT(H) appearance is proportional to the concentration of NAD(P)(H) present in assay mixture*

**c**

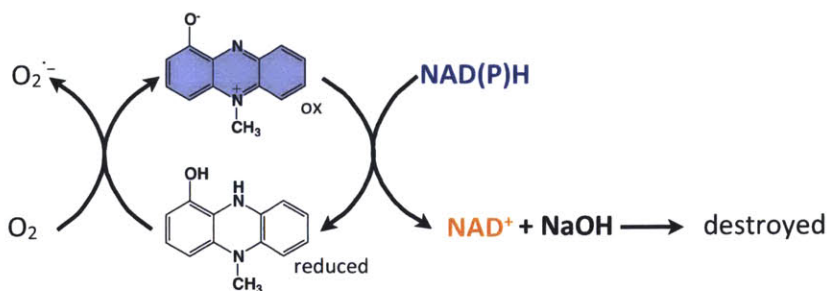
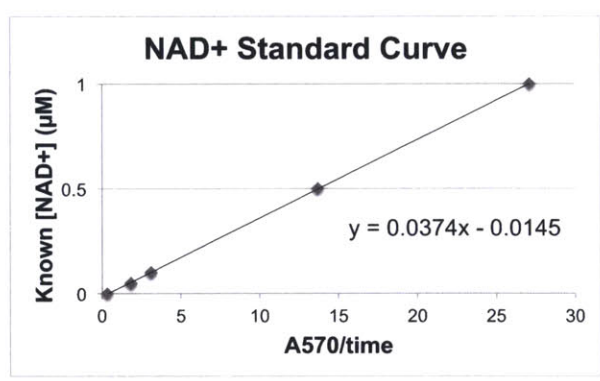
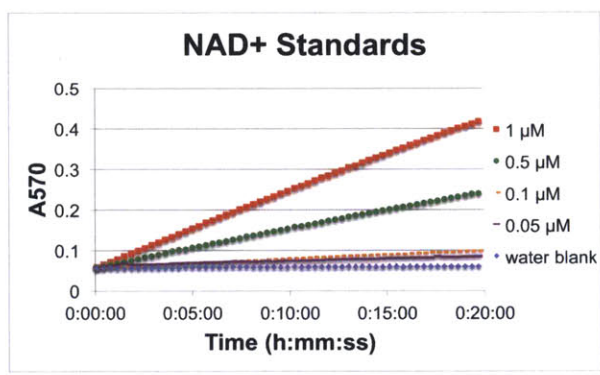


**Figure 2. a)** Example of a standard curve calculated from  $A_{570}$ /time of solutions of known NAD(P)(H) concentration using the “High Sensitivity” reagent mixture and sampling procedure (see **Note 8**). The range of data points used for  $A_{570}$ /time calculation is highlighted in white and bracketed. Using Microsoft Excel, the SLOPE and INTERCEPT functions give the same equation components as shown by the linear regression overlaid on the data plot. **b)** Example of extraction sample data workup:  $A_{570}$ /time and concentrations were calculated using the equation determined by the standard curve. The final ratio of NADH/NAD<sup>+</sup> is represented on both a linear and log-scale plot.

**a**

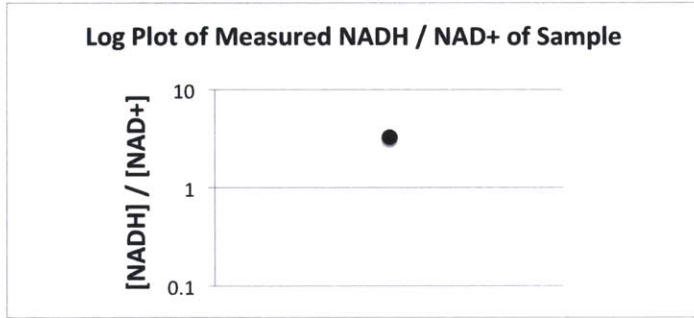
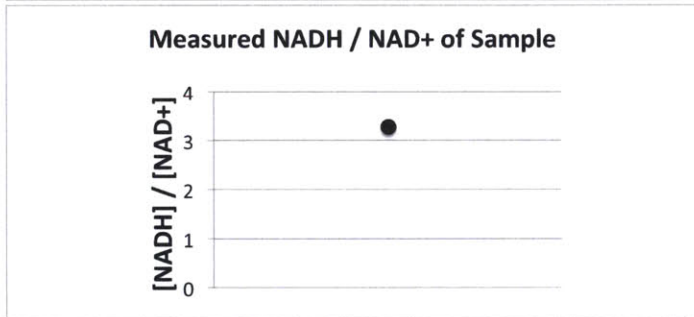
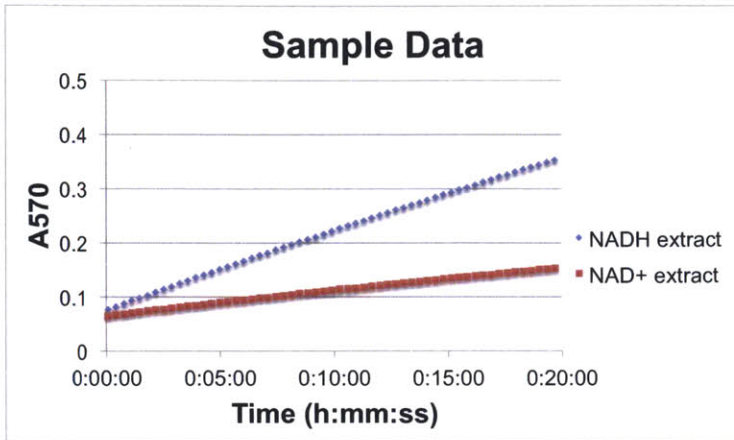
	A570	A570	A570	A570	A570
Kinetic read	1 $\mu$ M	0.5 $\mu$ M	0.1 $\mu$ M	0.05 $\mu$ M	0 $\mu$ M
0:00:05	0.059	0.058	0.059	0.06	0.055
0:00:26	0.065	0.061	0.059	0.061	0.055
0:00:47	0.072	0.065	0.06	0.062	0.056
0:01:08	0.078	0.068	0.061	0.063	0.056
0:01:29	0.086	0.072	0.062	0.068	0.056
0:01:50	0.092	0.075	0.062	0.064	0.056
0:02:11	0.099	0.079	0.063	0.064	0.056
0:02:32	0.106	0.083	0.064	0.065	0.057
0:02:53	0.113	0.086	0.065	0.065	0.057
0:03:14	0.12	0.09	0.065	0.066	0.057
0:03:35	0.127	0.094	0.066	0.066	0.057
0:03:56	0.133	0.098	0.067	0.067	0.057
0:04:17	0.14	0.101	0.068	0.068	0.057
0:04:38	0.147	0.103	0.069	0.068	0.059
0:04:59	0.154	0.107	0.069	0.069	0.058
0:05:20	0.16	0.11	0.07	0.069	0.058
0:05:41	0.168	0.113	0.071	0.07	0.058
0:06:02	0.174	0.117	0.071	0.07	0.058
0:06:23	0.181	0.12	0.072	0.07	0.058
0:06:44	0.188	0.123	0.073	0.071	0.058
0:07:05	0.194	0.127	0.074	0.072	0.059
0:07:26	0.201	0.13	0.074	0.072	0.058
0:07:47	0.207	0.134	0.075	0.072	0.059
0:08:08	0.214	0.137	0.076	0.072	0.058
0:08:29	0.22	0.14	0.076	0.073	0.058
0:08:50	0.227	0.144	0.077	0.074	0.058
0:09:11	0.233	0.147	0.078	0.073	0.059
0:09:32	0.24	0.15	0.079	0.074	0.058
0:09:53	0.246	0.154	0.08	0.075	0.058
0:10:14	0.253	0.158	0.08	0.075	0.06
0:10:35	0.259	0.16	0.081	0.075	0.058
0:10:56	0.265	0.163	0.082	0.075	0.059
0:11:17	0.272	0.166	0.083	0.076	0.059
0:11:38	0.279	0.169	0.083	0.076	0.059
0:11:59	0.284	0.173	0.084	0.077	0.059
0:12:20	0.291	0.176	0.085	0.077	0.059
0:12:41	0.297	0.179	0.086	0.078	0.059
0:13:02	0.304	0.183	0.086	0.078	0.06
0:13:23	0.309	0.186	0.087	0.079	0.059
0:13:44	0.316	0.189	0.088	0.079	0.06
0:14:05	0.322	0.192	0.088	0.079	0.059
0:14:26	0.328	0.195	0.089	0.079	0.059
0:14:47	0.334	0.198	0.09	0.08	0.059
0:15:08	0.34	0.201	0.09	0.081	0.06
0:15:29	0.347	0.204	0.091	0.081	0.06
0:15:50	0.352	0.207	0.091	0.081	0.059
0:16:11	0.359	0.21	0.092	0.082	0.06
0:16:32	0.364	0.213	0.093	0.082	0.06
0:16:53	0.371	0.216	0.093	0.082	0.06
0:17:14	0.377	0.219	0.095	0.082	0.06
0:17:35	0.383	0.222	0.095	0.085	0.06
0:17:56	0.389	0.226	0.096	0.083	0.06
0:18:17	0.395	0.229	0.096	0.083	0.06
0:18:38	0.401	0.232	0.097	0.083	0.06
0:18:59	0.406	0.235	0.098	0.084	0.06
0:19:20	0.412	0.239	0.098	0.084	0.06
0:19:41	0.418	0.24	0.099	0.085	0.06
0:20:02	0.424	0.243	0.099	0.085	0.061
<b>A570/time:</b>	<b>27.11</b>	<b>13.69</b>	<b>3.075</b>	<b>1.793</b>	<b>0.334</b>
<b>known [NAD+] (<math>\mu</math>M):</b>	<b>1</b>	<b>0.5</b>	<b>0.1</b>	<b>0.05</b>	<b>0</b>



← "known\_x's" =SLOPE(known\_y's, known\_x's) =INTERCEPT(known\_y's, known\_x's)  
 ← "known\_y's" slope: 0.0374 intercept: -0.0145

b

	A570	A570
Kinetic read	NADH	NAD+
0:00:05	0.077	0.065
0:00:26	0.082	0.067
0:00:47	0.088	0.068
0:01:08	0.093	0.07
0:01:29	0.098	0.072
0:01:50	0.103	0.074
0:02:11	0.109	0.076
0:02:32	0.114	0.077
0:02:53	0.119	0.079
0:03:14	0.125	0.081
0:03:35	0.13	0.083
0:03:56	0.136	0.084
0:04:17	0.141	0.086
0:04:38	0.145	0.088
0:04:59	0.151	0.09
0:05:20	0.156	0.091
0:05:41	0.161	0.093
0:06:02	0.166	0.094
0:06:23	0.172	0.096
0:06:44	0.177	0.098
0:07:05	0.181	0.099
0:07:26	0.187	0.101
0:07:47	0.192	0.102
0:08:08	0.197	0.104
0:08:29	0.202	0.106
0:08:50	0.207	0.107
0:09:11	0.211	0.109
0:09:32	0.216	0.11
0:09:53	0.222	0.112
0:10:14	0.227	0.114
0:10:35	0.232	0.115
0:10:56	0.236	0.116
0:11:17	0.241	0.118
0:11:38	0.246	0.12
0:11:59	0.251	0.121
0:12:20	0.256	0.123
0:12:41	0.261	0.124
0:13:02	0.265	0.126
0:13:23	0.27	0.127
0:13:44	0.274	0.128
0:14:05	0.279	0.13
0:14:26	0.284	0.131
0:14:47	0.289	0.133
0:15:08	0.293	0.135
0:15:29	0.298	0.136
0:15:50	0.302	0.137
0:16:11	0.307	0.139
0:16:32	0.312	0.14
0:16:53	0.317	0.141
0:17:14	0.322	0.143
0:17:35	0.326	0.144
0:17:56	0.331	0.146
0:18:17	0.336	0.147
0:18:38	0.34	0.148
0:18:59	0.344	0.15
0:19:20	0.349	0.151
0:19:41	0.353	0.153
0:20:02	0.358	0.154
<b>A570/time:</b>	<b>20.77</b>	<b>6.621</b>
<b>Calculated [NAD(H)] (µM):</b>	<b>0.763</b>	<b>0.233</b>
<b>NADH / NAD+:</b>	<b>3.27</b>	



slope: 0.0374      intercept: -0.0145

← calculated [NAD(H)] = (A570/time) \* 0.0374 - 0.0145



## Chapter 6

### Measurement of Phenazines in Bacterial Cultures

Suzanne E Kern and Dianne K Newman

This document is a reproduction of the chapter in press by the same name in a forthcoming book entitled *Pseudomonas Methods*, edited by Allain Filloux and Juan Luis for Humana Press.

Contributions:

I wrote this chapter and generated the data and figures herein.

#### **i. Summary/Abstract**

Certain pseudomonads are capable of producing phenazines—pigmented, reversibly redox-active metabolites that induce a variety of physiological effects on the producing organism, as well as others in their vicinity. Environmental conditions and the specific physiological state of cells can dramatically affect the absolute amounts and relative proportions of the various phenazines produced. The method detailed here—high-performance liquid chromatography (HPLC) coupled to detection by UV-vis absorption—can be used to separate and quantify the amount of phenazines in a *Pseudomonas* culture. Simple spectrophotometric measurements of filtered culture supernatants can be used to quantify certain oxidized phenazines, such as pyocyanin, in cultures. For cases where the conditions

under study are not planktonic cultures, (e.g. soil or biofilms) extracting the phenazines may be a necessary first step.

## ii. Key Words

phenazine, pyocyanin, phenazine-1-carboxylic acid, 1-hydroxyphenazine, PCA, PYO, HPLC, UV-Vis spectroscopy

## iii. Abbreviations

HPLC, high-performance liquid chromatography; PCA, phenazine-1-carboxylic acid; PYO, pyocyanin; 1-OH-PHZ, 1-hydroxyphenazine; NAD(P)H, reduced nicotinamide adenine dinucleotide (phosphate); TFA, trifluoroacetic acid; MOPS, 3-morpholinopropane-1-sulfonic acid

## 1. Introduction

Phenazines are brightly colored small molecules naturally produced by pseudomonads and other microorganisms (**Figure 1**). For example, pyocyanin (PYO) is a well-studied blue phenazine produced by the opportunistic human pathogen *Pseudomonas aeruginosa*. In pseudomonads, biosynthesis of the precursor phenazine molecule phenazine-1-carboxylic acid (PCA) from chorismate is encoded by the *phzABCDEFGG* operon, with additional *phz* genes responsible for adding specific functional groups (Mavrodi *et al*, 2006; 2001). By virtue of their redox activity, phenazines can generate reactive oxygen species upon reducing molecular oxygen (Davis & Thornalley, 1983; Hassan & Fridovich, 1980) and enhance electricity generation in microbial fuel cells (Rabaey *et al*, 2005; Yong *et al*, 2011). In ecological contexts, phenazines are important for the virulence of *P. aeruginosa* (Lau *et al*, 2004) as well as the protection afforded by certain pseudomonads against fungal pathogens of plants (Chin-A-Woeng *et al*, 2003; Mavrodi *et al*, 2006). In addition, they can directly benefit producing cells by making iron more bioavailable (Wang & Newman, 2008; Hernandez *et al*, 2004), enhancing biofilm development (Ramos *et al*, 2010; Wang *et al*, 2011; Dietrich *et al*, 2013), oxidizing the intracellular NAD(P)(H) pool (Price-Whelan *et al*,



2007), enabling anaerobic survival (Wang *et al*, 2010), and acting as inter- and intracellular signals (Dietrich *et al*, 2006).

In recent years, several methods have been developed to probe phenazine levels in specific environments and conditions. These exploit the various properties of phenazines, for instance, i) their redox activity, via cyclic voltammetry studies of biofilms and surrounding medium (Koley *et al*, 2011), ii) their particular fluorescent properties, using multiphoton microscopy for *in situ* detection (Sullivan *et al*, 2011), and iii) their light absorption properties, as measured by ultraviolet and visible spectrum spectroscopy (Reszka *et al*, 2004). Techniques such as thin layer chromatography can be used to separate phenazines (Rane *et al*, 2007), however, for accurate quantification, HPLC-separation coupled to detection by UV-absorption is preferred (Watson *et al*, 1986; Wang & Newman, 2008). Here we describe a common protocol for quantifying phenazines, using as examples pyocyanin, phenazine-1-carboxylic acid, and 1-hydroxyphenazine. This technique is very sensitive (capable of detecting concentrations as low as 2  $\mu\text{M}$  for PYO and PCA, and 20  $\mu\text{M}$  for 1-OH-PHZ), and involves equipment that can be found in many biology and chemistry laboratories. Figure 1 shows examples of phenazines that may be analyzed using reverse-phase chromatography as outlined here. For other phenazines, including 5-methyl-phenazinium-1-carboxylate, alternative separation methods may be necessary (Morales *et al*, 2010). Although this method only describes sample processing for planktonic cultures, HPLC analysis can also be used on other liquid samples, for instance, the soluble phase of sputum from individuals with cystic fibrosis (Hunter *et al*, 2012), and solutions of phenazines extracted from more complex conditions, such as biofilms (*see Note 1*). We also include instructions for determining the concentration of pyocyanin by direct spectroscopy of filtered culture supernatants (*see Note 2*).

## 2. Materials

### 2.1 Reagents

- 1) All solutions, including water, should be HPLC-grade.
- 2) Acidified water solution: 0.1% (vol/vol) trifluoroacetic acid (TFA) in water (*see Note 3*).
- 3) Acidified acetonitrile solution: 0.1% (vol/vol) TFA in acetonitrile (*see Note 3*).

- 4) Growth medium or buffer to serve as blank samples and for background subtraction.
- 5) Mixtures of growth medium or buffer with known concentrations of phenazines.

## 2.2 Equipment and Supplies

- 1) Pipettes and tips.
- 2) Microcentrifuge tubes.
- 3) 0.2  $\mu\text{m}$  pore size filters, either syringe filters or filter tubes (*e.g.* Costar Spin-X HPLC Micro Centrifuge Filter Tubes *see* **Note 4**).
- 4) Microcentrifuge.
- 5) HPLC system with a diode array UV-visible light detector and software for analyzing peak area.
- 6) C<sub>18</sub> reverse-phase column (*e.g.* Waters Symmetry® 5  $\mu\text{m}$  particle size, 4.6 mm by 250 mm).
- 7) Glass sample vials with septum caps, as appropriate for use with an autosampler.

## 3. Methods

Diligently follow all regulations when disposing waste materials.

- 1) Prepare 0.2  $\mu\text{m}$ -filtered solutions of all phenazines of interest at known concentrations (in the same medium as any cultures to be analyzed) for the purpose of generating a standard curve (*see* **Note 5**). In most cases, a standard curve including 5 or more concentrations ranging from 1 to 100  $\mu\text{M}$  will be sufficient for quantifying phenazines in samples.
- 2) Obtain a 0.2  $\mu\text{m}$ -filtered culture supernatant (*see* **Notes 5 and 6**).
- 3) Set up HPLC solvents as follows (*see* **Note 3**):

Solvent A = 0.1% (vol/vol) TFA in water

Solvent B = 0.1% (vol/vol) TFA in acetonitrile

- 4) Follow all procedures for preparing the HPLC instrument for use; prime pumps, turn on detectors and lamps, flush the column for at least 20 minutes and allow the system to stabilize, and ensure that volumes of solvents are adequate for the number of samples to be analyzed.

- 5) Set up the separation profile as follows:
  - Flow rate = 1 mL/minute
  - 0 - 2 minutes: linear gradient from 0 to 15% solvent B
  - 2 - 14 minutes: linear gradient from 15 to 83% solvent B
  - 14 - 16 minutes: linear gradient from 83 to 0% solvent B
  - 16 - 20 minutes: at 0% solvent B
- 6) Inject 100  $\mu$ L of the filtrate onto the HPLC column, either manually or using an autosampler, as appropriate for your HPLC set-up (*see Notes 7 and 8*).
- 7) Use the same separation protocol to analyze solutions of known concentrations of phenazines dissolved in the medium used for culturing. Also run a blank of the medium alone.
- 8) Make a standard curve using the peak areas at 365 nm for each phenazine (*see Note 9 and Figure 2a*).
- 9) Using the standard curves, determine the concentration of phenazine in each sample based on the corresponding peak area (*see Note 9*).

## 4. Notes

- 1) This protocol is intended for measuring phenazines in planktonic cultures. For other sample types (*e.g.* soil, biofilm), phenazines can be extracted and concentrated using chloroform and other solvents, with the particular procedure depending on the phenazine of interest. For more information, see Supplemental Materials in (5). The extract can be dissolved in a small volume of acetonitrile and run according to the HPLC protocol outlined in this Method. In the case of complex solutions or gel-like samples, extensive centrifugation steps may be used to separate the clear liquid containing phenazines from the solid phase of the sample (Hunter *et al*, 2012).
- 2) Solutions containing oxidized pyocyanin can be analyzed very simply in cuvettes using a spectrophotometer. At circumneutral pH, oxidized pyocyanin absorbs maximally at 691 nm, with a molar absorptivity of  $4.31 \text{ mM}^{-1}\text{cm}^{-1}$  (also known as an extinction coefficient,  $\epsilon_{691}$ ) (16). Pellet cells and pass the supernatant through a  $0.2 \mu\text{m}$  filter (such as a filter-column microcentrifuge tube), then vortex the solution for 30 seconds to ensure complete oxidation of any pyocyanin by ambient oxygen. Measure the absorbance at 691 nm ( $A_{691}$ ) of the culture filtrate and the relevant blank solution in 1-cm-pathlength

cuvettes. Subtract  $A_{691}$  of the blank solution from the  $A_{691}$  of the filtered culture supernatant to give the absorbance of PYO ( $A_{PYO}$ ). Calculate the concentration of pyocyanin according to the equation  $[PYO] \text{ (mM)} = A_{PYO} \text{ cm}^{-1} / 4.31 \text{ mM}^{-1}\text{cm}^{-1}$ .

- 3) If a large number of samples will be analyzed by this method, make up solutions of TFA in new bottles of HPLC-grade water and HPLC-grade acetonitrile and label the amended bottles accordingly. For example, to a 4-L bottle of HPLC-grade water, add 4 mL TFA, cap the bottle, and swirl or invert to mix.
- 4) To the best of our knowledge, the type of membrane used for filtration should not affect the retention of phenazines. Still, we advise using one type of membrane for all of the samples that you wish to compare. We commonly use Nylon or cellulose acetate. For further information regarding membrane selection, look for manufacturer product information sheets. The Corning® Filtration Guide is an excellent resource.
- 5) Because the medium used for culturing can cause differences in retention time due to matrix effects it is necessary to run known amounts of phenazines dissolved in the same medium that serves as the background for any biological samples. In addition, a complex medium can interfere with efforts to determine the peak area for specific phenazines (for example, cultures grown in lysogeny broth (LB-Miller) have more background at 365 nm than those in a MOPS (3-morpholinopropane-1-sulfonic acid)-buffered minimal medium, **see Figure 1b**). When possible, use a simple, defined medium as the background for phenazine quantification.
- 6) If the culture of interest has a moderate or high cell density ( $OD_{600} > 0.3$ ), avoid clogging the filter by first pelleting cells and then passing the cleared supernatant through the 0.2  $\mu\text{m}$  pore size filter.
- 7) When using an autosampler, place  $>200 \mu\text{L}$  of filtrate into a clean HPLC sample vial (use an insert for small volumes if sample size is very low).
- 8) To avoid potential carryover of phenazine from one sample to the next, run a water blank between every sample.
- 9) Make standard curves based on the peak area at the retention time determined by running individual standards. Confirm that the standards have maximal light absorbance at the following characteristic wavelengths: pyocyanin 280 nm, phenazine-1-carboxylic acid 250 nm, 1-hydroxyphenazine 262 nm (Fernandez & Pizarro, 1997). (Note that in acidified solution oxidized pyocyanin does not absorb strongly at 691 nm. Whereas the color of pyocyanin is bright blue at neutral pH, it is magenta at low pH.)

Using the traces at 365 nm, set the boundaries for peak area integration where the peak of interest meets the baseline. If the medium is too complex and there are overlapping peaks (that is, the peak of interest does not reach all the way to the baseline), try 1.) repeating the analysis for cells cultured in a less-complex medium, 2.) extending the duration of the relevant segment of the separation protocol (Step 4), or 3.) noting that the calculated areas are only approximate.

## **5. Acknowledgments**

S.E.K. was supported by the National Science Foundation Graduate Research Fellowship Program, and D.K.N. is a Howard Hughes Medical Institute (HHMI) Investigator. We thank the HHMI for supporting our work. R. Hunter, H. Sakhtah, C. Okegbe, and L. Dietrich provided constructive criticism of earlier drafts of this chapter.

## 6. References

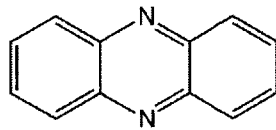
- Chin-A-Woeng T, Bloemberg G & Lugtenberg B (2003) Phenazines and their role in biocontrol by *Pseudomonas* bacteria. *New Phytol* **157**: 503–523.
- Davis G & Thornalley PJ (1983) Free radical production from the aerobic oxidation of reduced pyridine nucleotides catalysed by phenazine derivatives. *Biochim Biophys Acta* **724**: 456–464.
- Dietrich LEP, Okegbe C, Price-Whelan A, Sakhtah H, Hunter RC & Newman DK (2013) Bacterial community morphogenesis is intimately linked to the intracellular redox state. *J Bacteriol.*
- Dietrich LEP, Price-Whelan A, Petersen A, Whiteley M & Newman DK (2006) The phenazine pyocyanin is a terminal signalling factor in the quorum sensing network of *Pseudomonas aeruginosa*. *Mol Microbiol* **61**: 1308–1321.
- Fernandez RO & Pizarro RA (1997) High-performance liquid chromatographic analysis of *Pseudomonas aeruginosa* phenazines. *J Chromatogr A* **771**: 99–104.
- Hassan HM & Fridovich I (1980) Mechanism of the antibiotic action of pyocyanine. *J Bacteriol* **141**: 156–163.
- Hernandez ME, Kappler A & Newman DK (2004) Phenazines and other redox-active antibiotics promote microbial mineral reduction. *Appl Environ Microbiol* **70**: 921–928.
- Hunter RC, Klepac-Ceraj V, Lorenzi MM, Grotzinger H, Martin TR & Newman DK (2012) Phenazine content in the cystic fibrosis respiratory tract negatively correlates with lung function and microbial complexity. *Am J Respir Cell Mol Biol.*
- Koley D, Ramsey MM, Bard AJ & Whiteley M (2011) Discovery of a biofilm electrocline using real-time 3D metabolite analysis. *Proc Natl Acad Sci USA* **108**: 19996–20001.
- Lau GW, Hassett DJ, Ran H & Kong F (2004) The role of pyocyanin in *Pseudomonas aeruginosa* infection. *Trends Mol Med* **10**: 599–606.
- Mavrodi DV, Blankenfeldt W & Thomashow LS (2006) Phenazine compounds in fluorescent *Pseudomonas* spp. biosynthesis and regulation. *Annu Rev Phytopathol* **44**: 417–445.
- Mavrodi DV, Bonsall RF, Delaney SM, Soule MJ, Phillips G & Thomashow LS (2001) Functional analysis of genes for biosynthesis of pyocyanin and phenazine-1-carboxamide from *Pseudomonas aeruginosa* PAO1. *J Bacteriol* **183**: 6454–6465.
- Morales DK, Jacobs NJ, Rajamani S, Krishnamurthy M, Cubillos-Ruiz JR & Hogan DA (2010) Antifungal mechanisms by which a novel *Pseudomonas aeruginosa* phenazine toxin kills *Candida albicans* in biofilms. *Mol Microbiol* **78**: 1379–1392.
- Price-Whelan A, Dietrich LEP & Newman DK (2007) Pyocyanin alters redox homeostasis and carbon flux through central metabolic pathways in *Pseudomonas aeruginosa* PA14. *J*

*Bacteriol* **189**: 6372–6381.

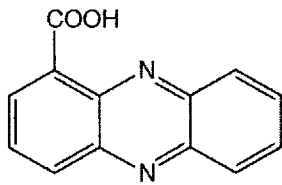
- Rabaey K, Boon N, Hofte M & Verstraete W (2005) Microbial phenazine production enhances electron transfer in biofuel cells. *Environ Sci Technol* **39**: 3401–3408.
- Ramos I, Dietrich LEP, Price-Whelan A & Newman DK (2010) Phenazines affect biofilm formation by *Pseudomonas aeruginosa* in similar ways at various scales. *Res Microbiol* **161**: 187–191.
- Rane MR, Sarode PD & Chaudhari BL (2007) Detection, isolation and identification of phenazine-1-carboxylic acid produced by biocontrol strains of *Pseudomonas aeruginosa*. *J Sci Ind Res* **66**: 627–631.
- Reszka KJ, O'Malley Y, McCormick ML, Denning GM & Britigan BE (2004) Oxidation of pyocyanin, a cytotoxic product from *Pseudomonas aeruginosa*, by microperoxidase 11 and hydrogen peroxide. *Free Radic Biol Med* **36**: 1448–1459.
- Sullivan NL, Tzeranis DS, Wang Y, So PTC & Newman DK (2011) Quantifying the dynamics of bacterial secondary metabolites by spectral multiphoton microscopy. *ACS Chem Biol* **6**: 893–899.
- Wang Y & Newman DK (2008) Redox reactions of phenazine antibiotics with ferric (hydr)oxides and molecular oxygen. *Environ Sci Technol* **42**: 2380–2386
- Wang Y, Kern SE & Newman DK (2010) Endogenous phenazine antibiotics promote anaerobic survival of *Pseudomonas aeruginosa* via extracellular electron transfer. *J Bacteriol* **192**: 365–369.
- Wang Y, Wilks JC, Danhorn T, Ramos I, Croal L & Newman DK (2011) Phenazine-1-carboxylic acid promotes bacterial biofilm development via ferrous iron acquisition. *J Bacteriol* **193**: 3606–3617.
- Watson D, MacDermot J, Wilson R, Cole PJ & Taylor GW (1986) Purification and structural analysis of pyocyanin and 1-hydroxyphenazine. *Eur J Clin Microbiol Infect Dis* **159**: 309–313.
- Yong Y-C, Yu Y-Y, Li C-M, Zhong J-J & Song H (2011) Bioelectricity enhancement via overexpression of quorum sensing system in *Pseudomonas aeruginosa*-inoculated microbial fuel cells. *Biosens Bioelectron* **30**: 87–92.

## 7. Figures

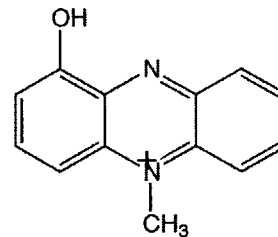
**Figure 1.** Structures of the core phenazine molecule and selected phenazines produced by pseudomonads. Note that the structures indicate the oxidized, protonated forms. Examples of species that may produce each phenazine: **(a)** *P. aeruginosa*, **(b)** *P. aureofaciens*, **(c)** *P. chlororaphis*, **(d)** *P. fluorescens* (Mavrodi *et al*, 2006).



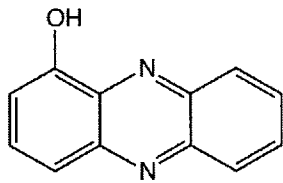
phenazine



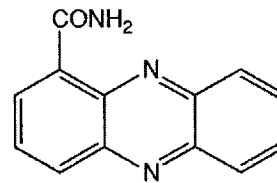
phenazine-1-carboxylic acid (PCA) <sup>a,b,c,d</sup>



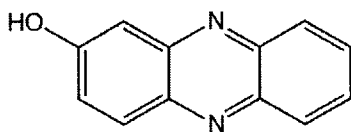
pyocyanin (PYO) <sup>a</sup>



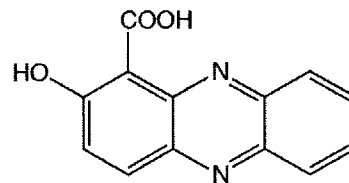
1-hydroxyphenazine <sup>a</sup>



phenazine carboxamide (PCN) <sup>a,c</sup>



2-hydroxyphenazine <sup>b</sup>



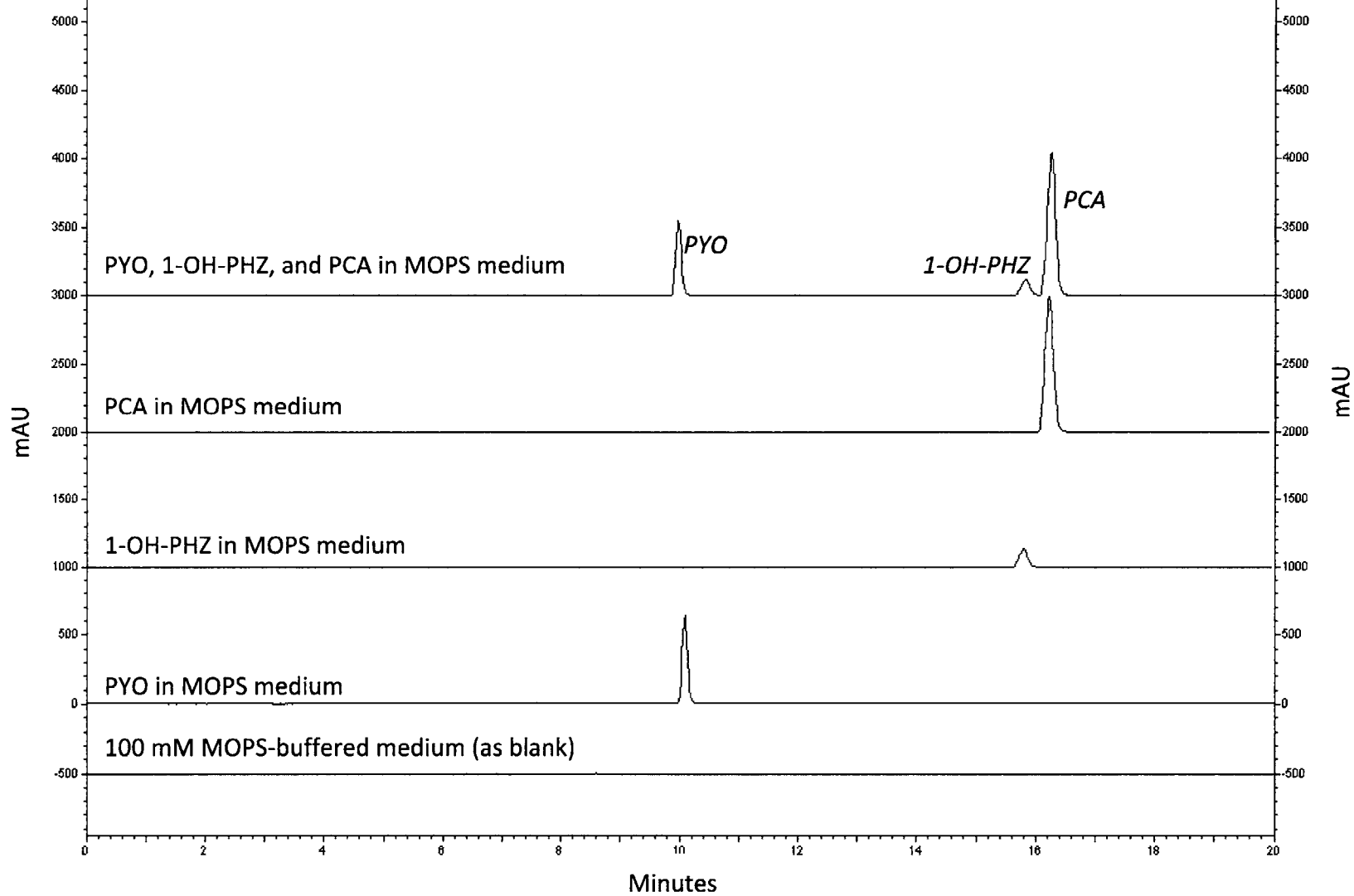
2-hydroxyphenazine-1-carboxylic acid <sup>b</sup>



**Figure 2. a)** HPLC traces at 365 nm (4 nm width) of approximately 100  $\mu$ M PYO, PCA, and 1-OH-PHZ separately and combined in a minimal MOPS-buffered medium. **b)** HPLC traces of wild-type *P. aeruginosa* PA14 cultures grown in LB and MOPS-buffered minimal medium with succinate, and the phenazine-null mutant (PA14  $\Delta$ phzA1-G1  $\Delta$ phzA2-G2 (Dietrich *et al*, 2006)) also grown in MOPS + succinate. Notice the signal interference at 365 nm and the shift in retention times caused by the complex LB medium. A comparison of wild type PA14 grown in a complex versus minimal medium demonstrates that growth conditions affect the production of different types of phenazines. One of the peaks between PYO and PCA in the LB-grown culture supernatant (with a retention time near 15.5 minutes) is likely due to PCN, which is commonly produced by *P. aeruginosa*. MOPS-buffered minimal medium: 100 mM MOPS, 40 mM sodium succinate, 9.3 mM  $\text{NH}_4\text{Cl}$ , 43 mM NaCl, 2.2 mM  $\text{KH}_2\text{PO}_4$ , 1 mM  $\text{MgSO}_4$ , 3.6  $\mu$ M  $\text{FeSO}_4$ . LB medium: 10 g/L NaCl, 10 g/L tryptone, 5 g/L yeast extract. PYO: pyocyanin, PCA: phenazine-1-carboxylic acid, 1-OH-PHZ: 1-hydroxyphenazine.

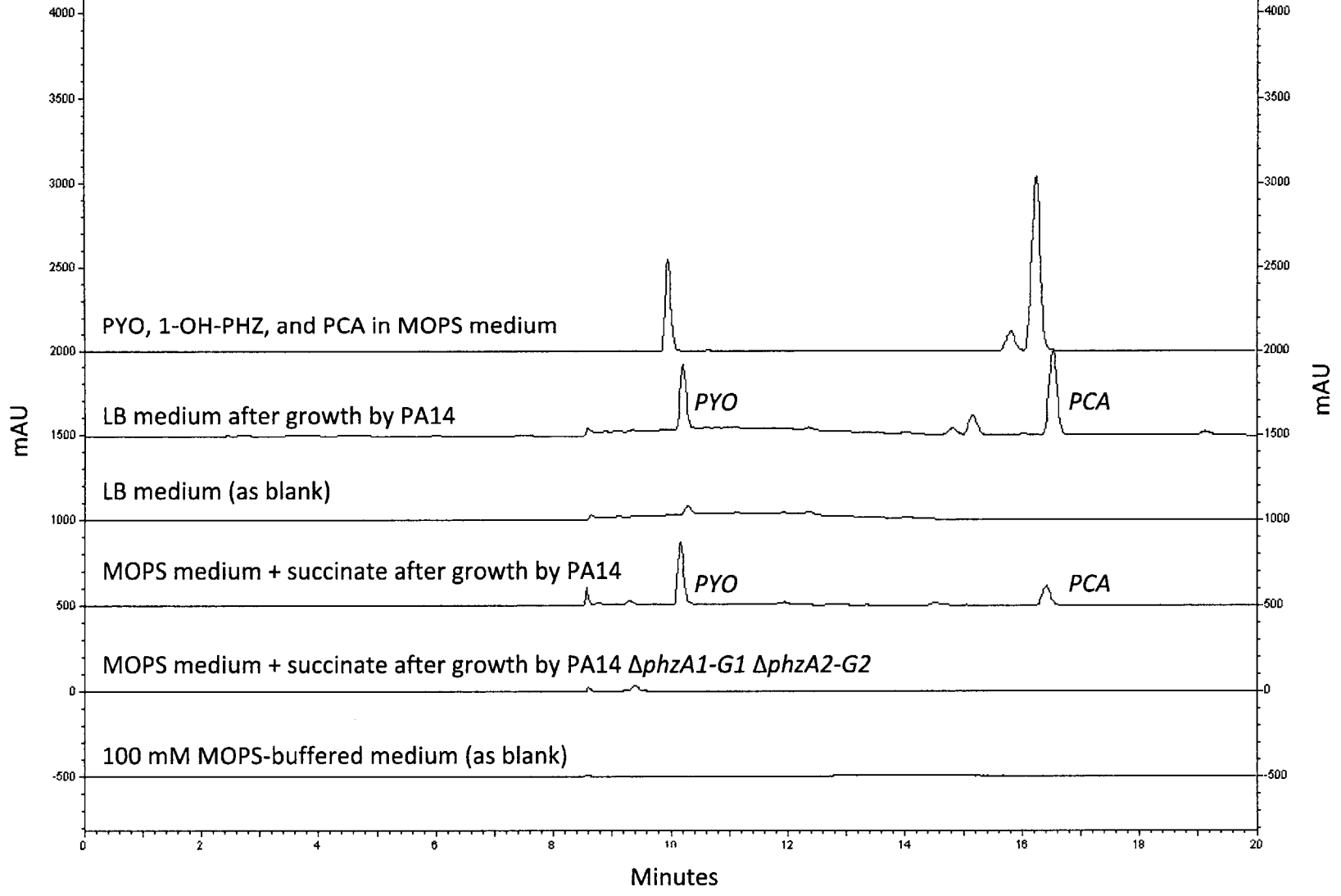
2a

### Purified phenazines



2b

### Phenazines from bacterial cultures





## Chapter 7

### Assay for anaerobic survival by phenazine redox-cycling

#### Contributions:

This document results from my efforts to refine and define the aspects of the experimental setup used in Wang, *et al.* (2010) for future physiological characterizations. I wrote this chapter and made the figures.

## Summary/Abstract

This protocol describes in detail the procedures for performing an anaerobic phenazine redox cycling experiment using *Pseudomonas aeruginosa* PA14, based on published work (Wang Y, Kern SE & Newman DK (2010) Endogenous phenazine antibiotics promote anaerobic survival of *Pseudomonas aeruginosa* via extracellular electron transfer. *Journal of Bacteriology* 192: 365–369). The protocol detailed here has been used before, but described only briefly in the literature (Wang *et al*, 2010).

### 1. Introduction

As soluble, redox-active small molecules, phenazines are capable of accepting electrons from reduced cellular components (*e.g.*, NAD(P)H) and donating electrons to extracellular oxidants, such as ferric iron (Fe<sup>3+</sup>) and molecular oxygen. Soluble redox mediators have been shown to alter the metabolic state of bacteria when an electrode or ferric iron minerals are provided as extracellular oxidants for the mediators (Emde *et al*, 1989; Emde & Schink, 1990; Benz *et al*, 1998). These findings, combined with the understanding that phenazines are produced by *Pseudomonas aeruginosa* at high population density, when oxygen levels approach zero, led us to investigate whether phenazines could sustain growth or survival in the absence of a typical terminal oxidant (*e.g.*, oxygen or nitrate). We found that 10<sup>8</sup> colony forming units of *P. aeruginosa* PA14 per milliliter could survive anaerobically when all of the following were present: glucose, phenazines (at ~75 μM), and a graphite electrode (at +207 mV vs. normal hydrogen electrode). Lacking any one of these components, cells died (Wang *et al*, 2010).

This assay is elegant and simple in its conception, and technically complex in its execution. The difficulty arises from the complicated interplay of numerous variables—biological, chemical, physical, and electrical—all of which must be simultaneously controlled with great precision. The physiology of *P. aeruginosa* is sensitive to a number of slight changes to the procedure outlined here, and because of the well-defined culturing conditions and the ability to vary nearly any aspect of the experimental setup, this assay holds great potential for testing numerous aspects of survival physiology in *P. aeruginosa* and anaerobic physiology of countless other organisms (see Chapter 8).

For an overview of the experimental procedure, **see Figure 1**. The method described in this chapter defines the precise conditions needed to achieve the published results. We have found that slight deviations from what is listed here can result in dramatically different survival outcomes. Advice for troubleshooting is included at the end of this chapter, and further commentary regarding important variables is presented in the appendix.

## 2. Materials

### 2.1 Buffers and solutions

1. MOPS-buffered minimal medium (1 L): 20.92 g MOPS (100 mM), 2.5 g NaCl (42.8 mM), 0.5 g  $\text{KH}_2\text{PO}_4$  (3.7 mM), 5 g  $\text{NH}_4\text{Cl}$  (94 mM), bring to pH 7.2 by adding drops of 6 M NaOH. Add 1 mL of 1 M  $\text{MgSO}_4$  (1 mM). Filter-sterilize the solution using a vacuum filtration system, 0.22  $\mu\text{m}$  pore size, into an autoclaved media bottle. Make a second bottle of medium (500 mL) for washing cells (aerobic). Sparge the first bottle for 15 minutes with  $\text{N}_2$  before moving into the oxygen-free glove box.
2. Solutions (all 0.22  $\mu\text{m}$ -filtered) to add at time of experiment, according to treatment condition:
  - a. 1 mg/mL  $\text{FeSO}_4 \cdot 7\text{H}_2\text{O}$  (100  $\mu\text{L}$  per 100 mL, make fresh),
  - b. 2 M D-glucose (1 mL per 100 mL = 20 mM),
  - c. approximately 2 mM phenazine solution in MOPS minimal medium. (**see Note 1**).
3. 1x phosphate buffered saline (PBS, 1 L): 8 g NaCl (137 mM), 0.2 g KCl (2.7 mM) 1.44 g  $\text{Na}_2\text{HPO}_4$ , 0.24 g  $\text{KH}_2\text{PO}_4$  (10 mM total  $\text{PO}_4$ ). Adjust pH to 7.2 using HCl. Autoclave to sterilize.
4. LB-agar plates: 25 g/L LB-Miller mixture, 15 g/L Bacto agar, ~20 mL per petri plate for thin plates (**see Note 2**).
5. Liquid LB-Miller media for culturing: 250 mL per 1 L flask at 25 g/L (**see Note 3**).

### 2.2 Consumables and other supplies

6. In oxygen-free glove box: sterile 96-well microtiter plates, pipettes and tips, fully charged electric pipetter for large volumes, serological pipettes (50 mL, 5 mL), container for waste/tips, Ag/AgCl reference electrodes (Basi RE-5B, #MF 2079, **see**

- Note 4)** stored in 15 mL 3M KCl in a 50 mL conical tube, (optional: 1-cm-thick Styrofoam panel with same dimensions as the top of the stir plate or an individual glass vessel).
7. At bench for experiment setup: 250 mL sterile LB in 1 L flasks, 30-mL glass culture tubes, graphite rod electrodes (Alfa Aesar #14738), platinum mesh electrodes (homemade, **see Note 5**), sterile 25 mL glass pipettes, electric pipetter, autoclaved 450-mL centrifuge bottle(s) (**see Note 6**), sterile disposable 50-mL conical tubes.
  8. At bench for daily sampling: sterile reagent reservoirs, LB-agar plates, 200  $\mu$ L multichannel pipette, 50  $\mu$ L multichannel pipette, pipette tips, fine-point permanent marker (*e.g.*, Sharpie).

### 2.3 Equipment

9. Specialized equipment: oxygen-free glove box with temperature control (MBraun® Unilab glove box with N<sub>2</sub>-only atmosphere, connected to a vacuum pump and water chiller), potentiostat leads (Gamry®, including Universal Dummy Cell for calibrations), 4- or 9-position magnetic stir plate.
10. Common laboratory equipment: static incubator (at 37°C for growing bacterial colonies on agar plates), shaking incubator (at 37°C for growing liquid bacterial cultures), centrifuge, vortex mixer, light box for counting CFU on petri plates.

### 2.4 Software

11. Spreadsheet and graphing program, such as Excel, for plotting bacterial population growth and death curves.

## 3. Methods

### 3.1 Set-up

#### A. Two or more days ahead of start:

1. Prepare buffers and solutions, excluding FeSO<sub>4</sub> solution, which oxidizes and precipitates quickly.



2. Move supplies into glove box: vortex mixer, MOPS buffer, 2 M glucose, serological pipettes, fully-charged mechanical pipetter, pipettes and tips, 96-well microtiter plates, container for waste/tips.
3. Ensure that glass reactors are bleached, washed, and autoclaved, ready to go.
4. Make and pour LB-agar plates.
5. From the  $-80^{\circ}\text{C}$  frozen stock, streak out a fresh plate of each bacterial strain to be studied (*i.e.*, *P. aeruginosa* PA14  $\Delta\text{phz1/2}$ ).
6. Ensure that the glove box and Gamry potentiostats are in good working order, and ready for use (**see Notes 7 and 8**).

**B. One day ahead of start ( $t_{-1}$ ):**

7. Adjust glove box water chiller to  $32^{\circ}\text{C}$ .
8. Prepare  $\sim 2$  mM phenazine (wrapped in foil to protect from light) and move into glove box.
9. Assemble glass reactors and transfer them to the oxygen-free glove box. (*see Preparing anaerobic reaction vessels*, Steps 21 through 28, below)
10. 12 hours before flask inoculation ( $\sim 17.5$  hours before intended time of harvesting cells): Inoculate 7 mL LB in yellow-cap tube from patch of colonies on plate with freshly grown strain of interest.
11. Verify that electrodes are fully functional (**see Notes 4 and 5**).

**C. Day of starting experiment ( $t_0$ ):**

*i. Preparing bacterial cultures*

12. Measure  $\text{OD}_{500}$  of each 12-hour overnight culture and inoculate 250 mL LB medium in 1 L flasks with 4 to 5 mL of the overnight cultures for a starting  $\text{OD}_{500} \sim 0.06$ .
13. Monitor  $\text{OD}_{500}$  periodically during incubation with shaking ( $37^{\circ}\text{C}$ , 250 rpm, **see Note 9**).
14. At  $\text{OD}_{500}$  between 2.75 and 2.85 (after about 5.5 hours of growth), pipette 50 mL culture into 50 mL conical tube, one tube for each reactor. If many reactors will have cells from the same flask, pour the entire 250 mL culture into a sterile 450 mL centrifuge bottle (**see Note 6**).
15. Pellet cells (10 minutes at 6,000 rcf,  $22^{\circ}\text{C}$ ) and pour off supernatant.

16. Resuspend cells in 25 mL MOPS minimal medium by pipetting. If using a large centrifuge bottle, transfer to a 50 mL conical tube.
17. Pellet cells (8 minutes at 5,500 rcf, 22°C) and pour off supernatant. Repeat for a total of 2 washes.
18. Resuspend cells in MOPS to an OD<sub>500</sub> around 75 (**see Note 10**).
19. In upright, tightly-capped tubes, transfer cells as well as fresh 1 mg/mL FeSO<sub>4</sub>•7H<sub>2</sub>O solution to oxygen-free glove box (**see Note 11**).
20. Continue at step 30, below.

*ii. Preparing anaerobic reaction vessels*

21. At the bench, set up reactors with carbon working electrode, platinum mesh counter electrode, and stoppers, as appropriate (**see Note 12 and Figure 2**).
22. Transfer glass reactors along with any other large equipment into the MBraun through the large airlock (**see Note 13**).
23. Set up vessels inside the glove box. Pipette into the large chamber by opening a stoppered port: buffered minimal medium (to a final volume of 100 mL with all other components), and, as relevant to the test condition, 1 mL sterile 2 M D-glucose, around 3 mL of sterile phenazine dissolved in MOPS medium to final concentration around 75 μM in reactor. In the smaller counter electrode chamber: ~6.5 mL buffered minimal medium (**see Note 14**).
24. Mount the Ag/AgCl electrodes into each vessel with electrodes (**see Notes 4 and 15**).
25. Position the vessels over the stirring positions on the stir plate. Verify that vessels are stably balanced and that the stir bar will not bump into either electrode.
26. Attach potentiostat leads: red and orange on Pt counter electrode, white on Ag/AgCl reference electrode, blue and green on carbon working electrode, black unattached (**see Note 16 and Figure 3**). Record which electrodes and potentiostats are associated with each vessel. Turn on the stir plate to achieve a visible vortex of the solution (to just below level 4).
27. Turn on the potentiostats for each vessel, in order, as appropriate. Before adding cells, perform a test run with high sampling frequency to ensure that the circuit is sound (**see Note 17**).

28. On the day of starting the experiment: add 100  $\mu\text{L}$  sterile  $\text{FeSO}_4$  solution to each vessel, and briefly vortex to mix and pipette cells ( $\sim 1$  mL) into glass vessels to achieve an approximate final  $\text{OD}_{500}$  of 0.70.
29. Start long-term potentiostat settings (**see Note 17**).
30. Record start time, when cells were added to vessels.
31. Between 1 and 5 hours after starting magnetic stirring, check the temperature of each culture with a thermometer and adjust conditions as appropriate so that the temperature difference across all vessels is within  $1^\circ\text{C}$  (**see Note 18**).

### 3.2 Time point sampling ( $t_0$ , $t_1$ , etc.)

1. Note the time of sampling and record information from the Gamry Framework experiment windows: time (ks), most recent current reading for each potentiostat ( $\mu\text{A}$ ). Record  $\text{O}_2$  reading (ppm) from the MBraun display.
2. Ensure that the small airlock is anaerobic.
3. Pipette 20  $\mu\text{L}$  of each culture into a separate well in the first row or column of a sterile 96-well microtiter plate.
4. Remove the microtiter plate from the glove box through the airlock, and perform a 10x dilution series ending at  $10^{-5}$  (20  $\mu\text{L}$  into 180  $\mu\text{L}$  PBS, mix by pipetting, change tips, and repeat for a total of five rows, **see Note 19**).
5. Using the multichannel pipette, spot 10  $\mu\text{L}$  of each dilution of interest, up to 8 spots, then tip the plate vertically and let the spots run into long drips. Draw lines between drips to facilitate later CFU counting (**see Note 20**). Also include a buffer blank.
6. Incubate drip plates at  $37^\circ\text{C}$  overnight, then count colonies (**see Note 21**). Record dilution level and CFU counts after 20-24 hours of incubation. Leave room in your record sheet for including a second round of counts at  $\sim 42$  hours.

### 3.3 Data workup

1. Transfer CFU counts and dilution level data to a spreadsheet. From this, calculate the number of viable cells, as well as the average and standard deviation or standard error of the mean (SEM) for each vessel (**see Note 22**).
2. Plot the averages  $\pm$  standard deviation or SEM of each sample over time. Subtract the start date and time from the date and time of sampling to plot days since the start of anaerobic incubation. Change the y-axis to  $\log_{10}$  scale.

### 3.4 Cleanup ( $t_n$ )

1. Turn off potential applied to each vessel by pressing “Skip” three times in each potentiostat window within the Gamry Framework.
2. Disconnect potentiostat leads from each vessel’s electrodes and try to keep the leads from getting tangled. Turn off the stir plate. Remove the Ag/AgCl electrodes from each vessel and replace them in the storage solution after wiping clean with a paper towel. Seal the cap of the storage tube tightly, making sure not to catch the electrode lead between the tube and cap.
3. Evacuate and refill the large airlock and transfer vessels out of the glove box. Remove all fittings and fixtures. Store stoppers, O-rings, and screw caps in a 95% ethanol solution. Discard graphite rods in biohazardous waste. Return Pt electrodes to their storage tube in a drawer for safe keeping.
4. To reset vessels for the next time:
  - a. Pour out and sterilize cultures with bleach.
  - b. Squirt bleach onto the glass frits and soak empty vessels in a 10% bleach solution (deionized water) for >1 hour, then rinse and wash with Alconox and scrub with a brush. Rinse thoroughly in deionized water.
  - c. Reassemble vessels with red O-ring between main chamber and lid, small magnetic stir bar, and ground-glass adapters, as appropriate (**see Figure 4**).
  - d. Wrap each vessel in aluminum foil and sterilize by autoclaving.
  - e. Store in a safe place (*e.g.*, drawer) in case of earthquakes.

### 4. Notes

1. Preparing a solution of pyocyanin from powder form is tricky because its dissolution is incomplete. Solubility is aided by warming up the liquid to as high as 55°C for at least 10 minutes, with occasional vortexing. Since PYO does not dissolve fully (up to about 1.7 mM in MOPS-buffered medium), filter the solution and use the molar absorptivity ( $\epsilon_{691} = 4.31 \text{ mM}^{-1} \text{ cm}^{-1}$ ) to calculate the actual concentration. PCA will dissolve fully to at least 2.5 mM in MOPS-buffered water, and its concentration can therefore be determined by weight/vol if a microbalance is available for weighing out powdered PCA (8.41 mg in 15 mL).

2. Moderately dry LB-agar plates work best for getting easy-to-count colonies. If colonies look broad and fluffy, there is too much moisture. For best counts, pour thin plates, about 20 mL per dish, and leave them to dry in stacks on the bench for 2 to 4 days. For longer-term storage, package into a plastic sleeve and move to the cold room (4°C) for up to 3 months. If plates must be used the same day they are poured, dry them for at least 30 minutes in a sterile laminar flow hood with the lids off.
3. For uniformity, when preparing to culture more than one strain at a time, mix up a single batch of LB medium in a beaker with magnetic stirring. Once fully mixed, decant 250 mL into each 1-L flask, cover the mouth of each flask with foil, and autoclave for 20 minutes.
4. For proper functioning of Ag/AgCl electrodes, be very careful to follow all guidelines laid out by the manufacturer. If using brand new electrodes follow instructions for removing the yellow silicone coating, then hold the electrode upright and flick it gently to remove any bubbles that may be trapped near the frit, at the bottom. These electrodes should always be in contact with an aqueous solution; for storage, keep electrodes in a 50 mL conical tube with 10-15 mL of a 3 M KCl solution. Cover the tube in foil to protect the electrodes from light, and store upright. During experiments the electrodes must be submerged in the culture medium, but not so far as to possibly touch the magnetic stir bar. Always keep one Ag/AgCl electrode in pristine condition--never use it for an experiment. Use this electrode to measure the relative potential of the other Ag/AgCl electrodes before each experiment:
  - 1) Transfer all electrodes to a tube with buffered salt water (*i.e.*, sterile MOPS medium).
  - 2) Use a multimeter set to read in millivolts. Touch one lead to the never-used electrode, and the other end to each Ag/AgCl electrode to be used in the experiment.
  - 3) Make note of the difference in potential of each electrode from the never-used electrode. As long as the electrodes for the experiment are all within 5 mV of each other, they are fine to use. The voltage difference between these and the never-used electrode should remain under 20 mV, at which point, a full set of new reference electrodes should be purchased.
5. The platinum electrodes are homemade and extremely delicate. A platinum mesh is connected by platinum wire to a copper wire housed inside a glass tube. To keep the

copper from reacting with salts, etc., the glass housing is sealed with waterproof epoxy resin. Check that the electrodes are functional by touching the multimeter's leads to the top (Cu wire) and bottom (platinum mesh) of each. Resistance should be close to 0 Ohm, and potential should be 0 mV. If either is high, there is a break somewhere in the wires. For assistance in fixing these electrodes, go to Nate Lewis's electrochemistry lab (2<sup>nd</sup> floor of Noyes Laboratory at Caltech) and ask anyone there for assistance with electrode repair. *Do NOT throw away a broken electrode.* The components can be reattached, and the platinum mesh and wire are very expensive.

6. Use the 450 mL centrifuge bottles for pelleting cells when 2 or more vessels will have the same strain. After the first round of pelleting, resuspend cells and transfer the concentrated culture to a 50 mL conical for subsequent wash steps. For experiments with only 1 vessel per strain, it is simpler to pellet 50 mL of culture in a 50 mL plastic, sterile conical tube at the outset.
7. See the lab's MBraun User Guide for information on regular maintenance and upkeep. Briefly,
  - Check that all electrical connections (*e.g.*, multi-outlet surge protector) inside the glove box are working. This is especially important for running the stir plate and vortex and charging the Drummond Pipet-Aid.
  - As a rule of thumb, keep circulation running at all times, but if there is a large pulse of oxygen in the chamber, or solvents that should not contact the catalyst, turn off circulation to take the catalyst off-line. Follow directions to purge the box for at least 10 minutes before turning on circulation again.
  - Oxygen level readings run higher when moisture is present in the glove box due to interference with the oxygen detector. The detector may drift by as much as 10 ppm per year in its detection capabilities and can be calibrated by MBraun for \$1200 (this takes 6 weeks). Keep airlocks under slight vacuum when not in use to prevent slow diffusion of oxygen into the glove box atmosphere. Be sure to vacuum and refill the antechambers before opening to the box atmosphere, as oxygen may enter the antechambers while they are under vacuum.
  - The MBraun catalyst should be regenerated at least every 3 months, and anytime the catalyst seems to remove oxygen more slowly than usual.

- The hatches on either end of each airlock should remain closed unless materials are in the process of being moved into or out of the antechamber.
  - Vacuum pump oil should be changed after every regeneration, however, if the leaky Edwards pump is still attached, no explicit oil changes are necessary--just keep mopping up leaking oil with paper towels in the drip pan every week or so, and top off with oil as needed, about every two to three weeks.
  - Make sure that the water chiller is in working order and can hold a given temperature.
8. The Gamry potentiostats should be calibrated at least yearly using the Gamry Universal Dummy Cell and the Calibration program in the Gamry Framework. For each potentiostat, one-at-a-time, connect leads to the calibration side of the dummy cell as follows: red--counter, orange--counter sense, green--working, blue--working sense, white--reference. We do not have a Faraday cage to block out interfering electromagnetic waves, but you can achieve good calibration results by ensuring that the dummy cell is on an insulating surface (*i.e.*, plastic), and that you don't move your arms in and out of the glove box during the execution of the calibration program. The vacuum pump and valves turning on and off might affect readings, although this isn't likely. Select Experiments→A: Utilities→1: Calibration. Follow the prompts. Each calibration takes approximately 5 minutes to complete. Repeat until all 4 potentiostats have been successfully calibrated.
  9. To obtain accurate OD readings at higher cell densities dilute cultures 1:10 in sterile medium (for example, 50  $\mu$ L sample + 450  $\mu$ L LB yields a volume sufficient to detect in a semi-micro cuvette). The Beckman spectrophotometer stops reading linearly at optical densities above 0.7.
  10. Start by adding buffer to achieve a final volume of about 1.5 mL (for a pellet from 50 mL of culture, or 6 mL if starting from 250 mL of culture), then check the OD<sub>500</sub> of a 1:100 dilution in MOPS-buffered medium and add more medium to adjust the total volume as needed to achieve an OD of 75 (calculate using  $\text{conc}_1 \cdot \text{vol}_1 = \text{conc}_2 \cdot \text{vol}_2$ ).
  11. Whenever possible, transfer supplies in and out of the glove box through the small airlock. Compared to using the larger airlock, this saves time and N<sub>2</sub> gas. Leave the airlocks under slight vacuum (-15 in. Hg) when not in use to minimize diffusion of oxygen into the glove box.

12. Turn on Bunsen burner flame to work in a sterile environment. All glass vessels should have a stir bar, and a large red O-ring between the main chamber and the lid. For vessels that will have electrodes, there should also be two ground-glass fittings in place and all of these components should be assembled, wrapped in aluminum foil, and autoclave-sterilized. For glass vessels that will not have electrodes attached, unwrap aluminum foil and add stoppers (size 00 and size 0) to each port/opening. For vessels that have electrodes, set up as follows:

- a. Start by unwrapping and adding stoppers to the short, integrated screw-top adapter (size 00, green) and the port next to it, going counter-clockwise (size 0, black).
- b. Place an O-ring onto a new graphite rod, about 2 inches from the top, and spray the bottom half of the rod with 70-90% ethanol.
- c. Insert the graphite rod into the third port of the large chamber, where there should be a ground-glass joint adapter with a threaded screw-top fitting.
- d. Adjust the position of the O-ring until the rod rests at 2-3 mm above the bottom of the chamber. Secure with an open-centered black screw top.
- e. Handling the platinum counter electrode very carefully, take the adapter from the counter electrode chamber and slide it over the top (wire and glass housing) of the electrode.
- f. Still holding the electrode and adapter, slide an O-ring onto the wire at the top, and position it about 5 inches from the bottom of the electrode.
- g. Rest the electrode in the adapter and then insert into the counter electrode chamber, making sure that the platinum mesh does not contact the bottom (this could bend and break the platinum wire).
- h. Position the O-ring so that the platinum mesh is 4-7 mm from the bottom of the counter electrode chamber. Secure with an open-centered black screw cap.
- i. Be sure to bring 1 black screw cap for each vessel with electrodes to secure the Ag/AgCl electrode once inside the glove box.

13. When using the large antechamber (airlock):

- a. Place materials inside, close the exterior hatch and tighten firmly.
- b. Ensure that the vacuum pump is set to the lowest strength using the dial on the side of the pump. The pump still pulls a strong vacuum, but will do so



more slowly. A rapid decrease in pressure can damage equipment inside the airlock.

- c. Turn the black knob from perpendicular to parallel to the vacuum pump line (vertical, end pointing downwards) to evacuate the antechamber for 10 minutes.
  - d. Close the vacuum pump valve (black handle) and slowly open the refill valve (yellow handle horizontal, parallel to the pipe that connects to the glove box atmosphere) to refill the antechamber halfway, to -15 in. Hg, and leave in this position for at least 10 minutes.
  - e. Repeat steps (b) and (c) for a total of 3 evacuations of the antechamber and, finally, refill the antechamber completely to equilibrate the pressure between the box atmosphere and airlock before attempting to open the interior antechamber hatch.
  - f. Slide the tray into the glove box to make reaching the materials easier and unload. Slide tray all the way back into the antechamber and close the hatch.
  - g. Apply slight vacuum (-15 in. Hg) to the big airlock to minimize oxygen diffusion into the glove box.
14. Use a sterile plastic 50 mL serological pipette to add the medium to each chamber (compared to using a 25 mL pipette it makes remembering how much you have added easier and reduces awkward movements in the glove box). Be aware that as you move your arms around in the hard-sided box the pressure changes and may cause the pipette to drip. You can minimize pressure changes by moving one arm back as the other moves forward, attempting to keep the volume of displaced air uniform. When pipetting into the counter electrode chamber in particular, add the medium very slowly, being careful not to introduce any bubbles at the frit adjoining the two chambers of the glass vessel. A large bubble can break the electric circuit and can result in a high voltage being applied, which kills the cells.
15. To properly attach the reference electrode:
- a. Plunge the Ag/AgCl electrode into ~20 mL fresh MOPS buffer in a 50 mL conical tube to rinse off the 3 M KCl storage solution. Check to make sure that there are no bubbles at the bottom of the electrode, near the frit.

- b. Verify that there is an O-ring near the top of the glass portion of the electrode, and place the electrode into the integrated screw-top port of the main chamber's lid.
  - c. Adjust the position of the O-ring so that the bottom edge of the electrode is submerged in the medium, but above the height of the stir bar. (An accidental encounter with the stir bar could easily break the electrode, and also ruin that experimental condition.)
  - d. Secure with an open-center black screw cap (**see Figure 3b**).
16. Spend time arranging the potentiostat leads so that they do not yank on any of the electrodes and/or tip the vessel or its lid. If a lid tips up on one edge, it is a good idea to secure the lid to the main chamber using a piece of tape.
17. To start a controlled-voltage run:
- a. Gamry Framework → Experiment → D: Physical Electrochemistry → 4: Controlled Potential Coulometry.
  - b. Select a potentiostat (0, 1, 2, or 3, matching the numbers written on orange tape on the electrode leads) and label files with easy-to-interpret names. Include identifying information in the Notes section, if desired.
  - c. Set parameters:
    - i. Electrode area = 1 to 6 cm<sup>2</sup>, according to your estimate of submerged surface area
    - ii. Pre-step Voltage (V) = 0 vs E<sub>ref</sub>, Pre-step Delay Time (s) = 0
    - iii. Step 1 Voltage (V) = 0 vs E<sub>ref</sub>, Step 1 Time (s) = 3.2E+006 sec
    - iv. Step 2 Voltage (V) doesn't matter, first step lasts 2,000 days.
    - v. Sample Period (s) = 5 (for test run only, to ensure quick readout of possible errors)
    - vi. I/E Range Mode = Fixed
    - vii. Max Current (mA) = 100
    - viii. IRComp = None
    - ix. PF Corr. (ohm) = 50
    - x. Leave these boxes unchecked: Decimate, Init. Delay, Conditioning, Advanced Pstat Setup.
    - xi. Electrode Setup = On
    - xii. Press OK

- xiii. Electrode Type = Solid
  - xiv. Leave Purge/Stir Cell “off” unchecked
  - xv. Press OK to start.
- d. Important: If any adjustments are necessary (because of electronic errors) press “Pause” to stop the applied voltage before readjusting any electrodes. Press the button again to resume readings.
  - e. If everything is functioning properly, press “Skip” three times to exit that file, then start a new one with all of the same parameters, except set Sample Period (s) = 300 seconds.
18. Temperature variability between culturing conditions must be minimized (less than 1°C difference across all treatments) to keep from introducing an unintended variable to the experiment. Higher temperatures lead to faster rates of death in non-survival treatment conditions. The ideal temperature for *P. aeruginosa* in this assay seems to be between 31 and 34°C. Cultures that are too warm can be elevated and insulated from the stir plate by placing the reactor vessels on a thin piece of Styrofoam (~1 cm thick), which reduces the culture temperature by 2 – 3°C. The water chiller can also be used to hold the ambient temperature at least as high as 33°C. Electrical heat “tape” could be used to push individual treatment temperatures higher, if desired.
19. For a quick and easy dilution series:
- a. Pipette 180 µL PBS to all remaining wells for the dilution series (*e.g.*, if samples are in row A, pipette PBS into rows B through E for a dilutions up to 10<sup>-5</sup>. For calculation purposes, plating 10 µL results in a 10<sup>-7</sup> final dilution factor) and to some unused wells. This makes it easy to include a 10 µL drip of buffer on a plate as a blank to ensure the buffer’s sterility.
  - b. Add 180 µL to the first row/column containing the 20 µL sample of culture. Pipette up and down 3 or 4 times to mix.
  - c. Using a 50 µL multichannel pipette, transfer 20 µL from first row/column to the next, pipette up and down 10-12 times to mix, change tips.
  - d. Repeat until the end of the dilution series
20. Up to 8 drips can fit onto a single plate, but 4 to 6 is preferable because the drips are longer and separate cells from one another better than the short drips achievable with 8 per plate. At the beginning of the experiment, with initial OD<sub>500</sub> ~0.75, plate

10  $\mu\text{L}$  of  $10^{-5}$  and  $10^{-6}$  dilutions. Make sure that plates are labeled with sample IDs and dilution level. Avoid letting drips reach the edge of the plate and/or run into each other. After plating, draw lines between drips for easier discrimination between samples when counting CFUs. Also include one or two drips of PBS alone from the dilution plate to verify that sample counts are accurate and not the result of contaminated dilution buffer. A good dilution yielding reliable counts results in between 20 and 90 colonies. Up to 100 is still okay.

21. Later in the experiment, as cells die, a second round of counting may be necessary, at 42 to 48 hours of incubation at  $37^{\circ}\text{C}$ , to account for slow-growing or small colonies.
22. To determine CFU/mL for each sample, divide the number of CFU counted by the dilution factor and volume (in mL) plated. For example, 50 CFU in 10  $\mu\text{L}$  of a  $10^{-5}$  dilution =  $5 \times 10^8$  CFU/mL ( $50 \text{ CFU} / (10^{-2} \text{ mL} \times 10^{-5})$ ). Set up a spreadsheet that you can use over and over as a template, and leave space to include/add second-day counts, in case it will be informative to plot how many cells grew slowly.

## 5. Troubleshooting

*If positive controls do not survive:*

1. Check growth phase. One side-by-side comparison of cells at different growth phases demonstrated that exponential phase cells do not survive as well as stationary phase cells, and demonstrate a rapid decline in survival. Late-stationary phase cells do not survive as well in the long term, with CFU counts that gradually decline over several days, and differences between treatments are not very pronounced. Late-stationary phase cells also exhibit greater variability from experiment to experiment than “younger” cultures.
2. Check electrochemical set-up. Look out for orange/red data points in the Gamry plots--these indicate an error that should be addressed immediately, or the experiment should be restarted. If wires or electrode leads touch one another then the potentiostat is unable to apply the correct voltage and the bacterial cells will likely die. (Note: working and working sense (green and blue) may touch each other, as well as counter and counter sense (red and orange)). Also watch out for bubbles at the frit in the vessel and at the frit in the reference electrode. The error “CA OVLD”

(control amplifier overload) indicates that the control amplifier of the potentiostat cannot apply the designated voltage, often due to a break in the electrical circuit (e.g., air bubble).

3. Check for contamination. While it was never found to be the main problem, it is possible that certain compounds in solution could be toxic to anaerobic survival. For this reason, it may be useful to periodically bake the bottoms of the reactor vessels at high temperature to burn off any organics, and to check the purity of all reagents.

*If negative controls do not die:*

4. Check for oxygen contamination in the MBraun glove box. Oxygen levels in a well-maintained MBraun box should reach as low as below the detection limit of 0.1 ppm. Readings are made artificially higher by the presence of moisture in the atmosphere, which is unavoidable when bottles, tubes, and especially the glass reactor vessels contain liquid. The MBraun catalyst and oxygen detector need special care to remain in working order (see MBraun maintenance and upkeep documents). On a regular basis, the catalyst should be regenerated by initiating the automatic regeneration program. Lower the chance of oxygen contamination by keeping the pressure in the box at a minimum of 2 mbar (gloves should stick out straight), leaving the antechambers under slight vacuum, and replacing gloves and HEPA air filters in a preventative manner. The oxygen detector may lose accuracy by as much as 10 ppm per year, and should be serviced annually (we did not send it for calibration for its first five years). This process is costly in terms of both money (\$1200) and time (6 weeks), so plan accordingly.
5. Check growth phase. Overnight cultures of *P. aeruginosa* seem to gradually decline in viability regardless of treatment (+/- phenazine redox cycling, +/- glucose). One possible explanation: cells may adapt to low oxygen conditions present during early stationary phase, but may run out of necessary nutrients or energy stores by late stationary phase and survive in a pseudo-dormant state, possibly initiated by nutrient (not including O<sub>2</sub>) starvation.

## 6. References

- Benz M, Schink B & Brune A (1998) Humic acid reduction by *Propionibacterium freudenreichii* and other fermenting bacteria. *Appl Environ Microbiol* **64**: 4507–4512.
- Emde R & Schink B (1990) Oxidation of glycerol, lactate, and propionate by *Propionibacterium freudenreichii* in a poised-potential amperometric culture system. *Arch Microbiol* **153**: 506–512.
- Emde R, Swain A & Schink B (1989) Anaerobic oxidation of glycerol by *Escherichia coli* in an amperometric poised-potential culture system. *Appl Microbiol Biot* **32**: 170–175.
- Wang Y, Kern SE & Newman DK (2010) Endogenous phenazine antibiotics promote anaerobic survival of *Pseudomonas aeruginosa* via extracellular electron transfer. *J Bacteriol* **192**: 365–369.

## 7. Figures

**Figure 1.** Overview of experimental procedure.

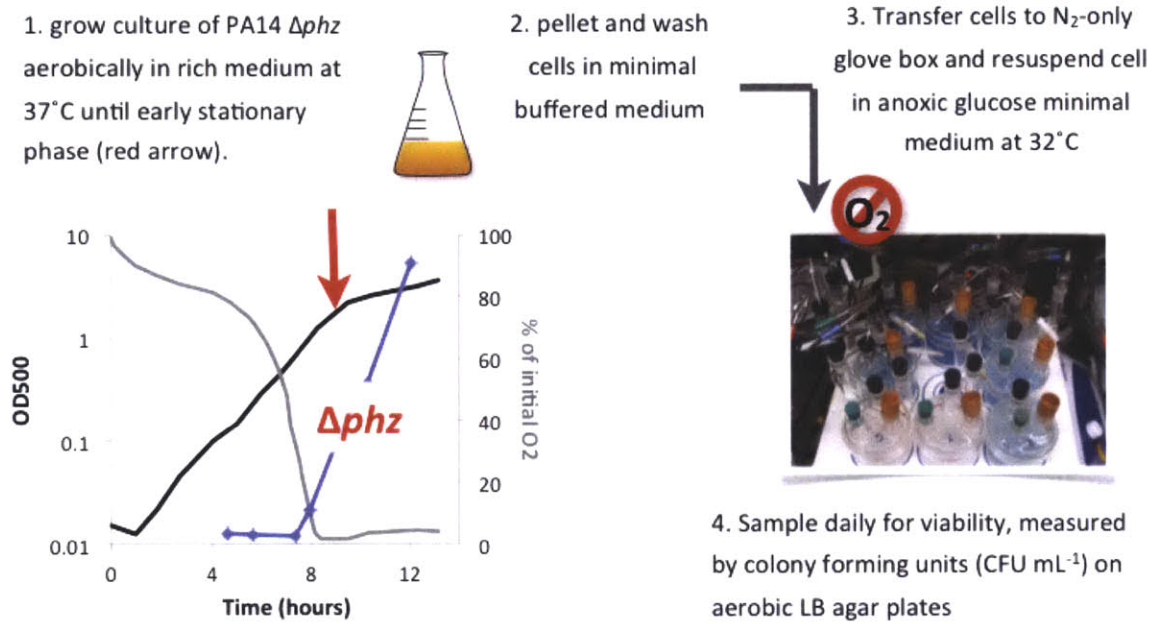


**Figure 2.** Sequence for preparing reactor vessels. Shown here are the steps completed prior to transferring vessels into the anoxic glove box. **a)** The supplies needed for vessels with electrodes: autoclaved glass vessel with large o-ring, magnetic stir bar, and 2 ground glass/screw top adapters, homemade platinum ( $\text{Pt}^0$ ) mesh electrode, new graphite rod (working electrode), 2 small o-rings, ethanol-sterilized stoppers (size 00 and 0), and 2 black open-top screw caps. **b)** Add stoppers to ports without glass adapters, and slide o-ring 2-3 inches from the top of the graphite rod. **c)**

**a**



**d)** Thread the  $\text{Pt}^0$ -electrode wire through a ground-glass adapter, then slide on an o-ring about 4 inches from the bottom of the  $\text{Pt}^0$  mesh. **d)** Add both electrodes and secure with open-top screw caps. Ensure that neither electrode touches the bottom. Once inside the glove box, the Ag/AgCl electrode will replace the green (size 00) stopper in the short screw-top port. **e)** For reactors without electrodes, remove glass adapters and seal all ports with stoppers (size 00 and 0).

**b**



**c**



**d**



**e**





**Figure 3.** Schematic and photos of assembled reactors. **a, b)** Three electrodes are needed in order to poise the phenazine-oxidizing potential: working electrode (graphite), counter electrode (platinum), and reference electrode (silver/silver chloride). *P. aeruginosa* cells in the main chamber reduce the oxidized phenazines. **c)** Image of experimental setup with eight reactors, four with phenazine-oxidizing potentials applied and four without.

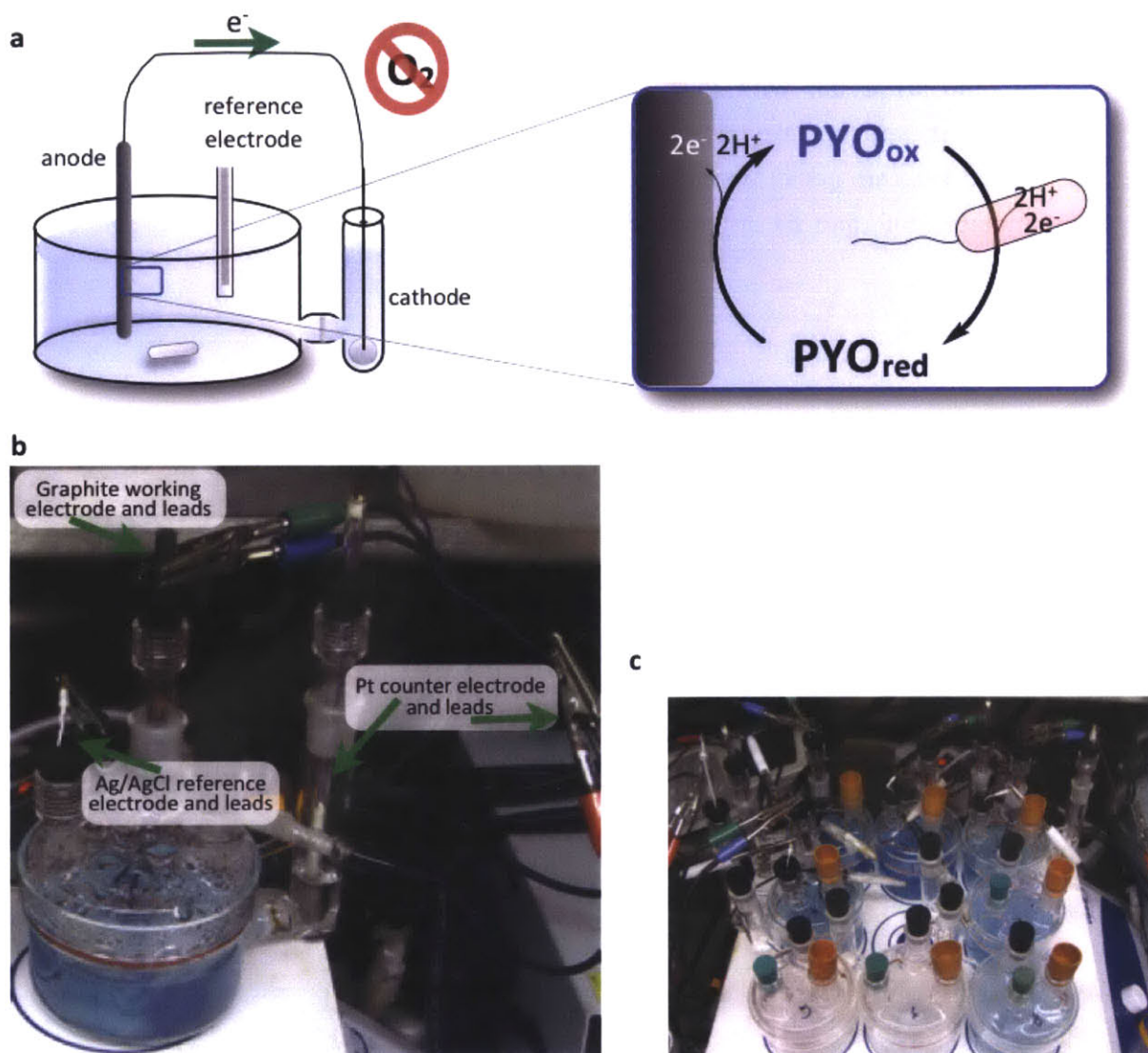
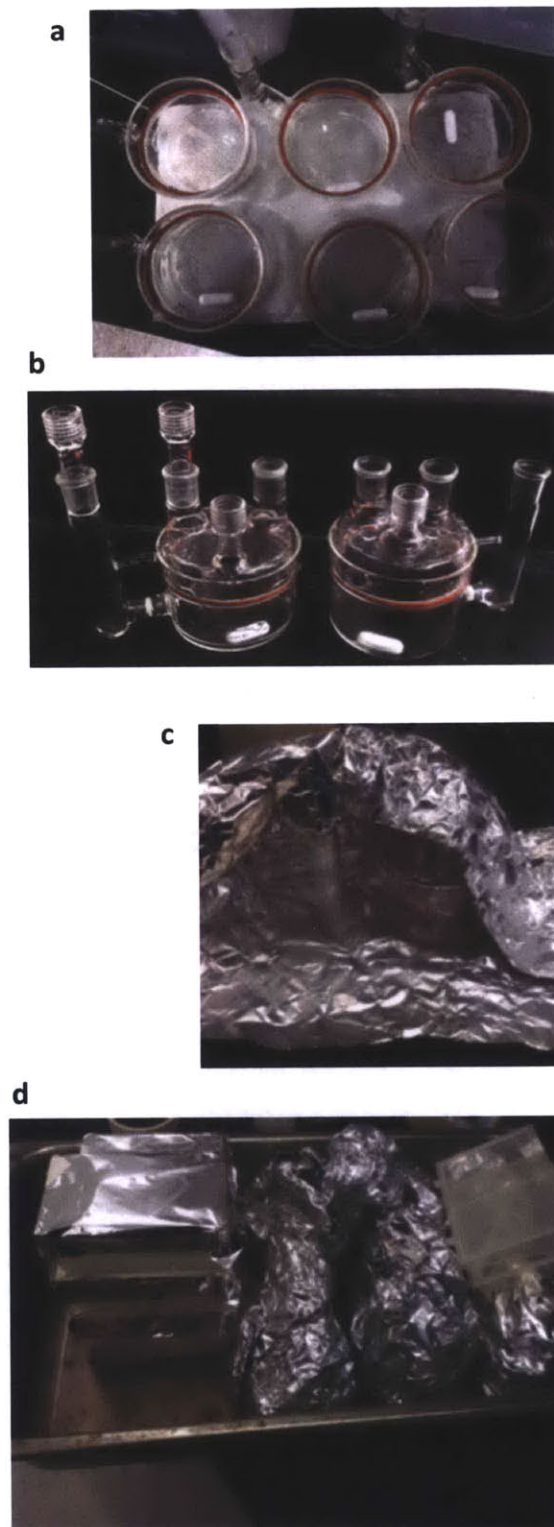


**Figure 4.** Photos of reactors being assembled in preparation for sterilization and storage after being treated with bleach, washed with soap, and rinsed with deionized water. Each reactor gets **a)** a magnetic stir bar and rubber gasket, and **b)** a lid, with glass adapters, if appropriate. Then, assembled reactors get **c)** wrapped in aluminum foil, and **d)** autoclave-sterilized.



## **Chapter 8**

### **Conclusions and Future Directions**

## Summary

This body of work represents a step forward in our understanding of the possible roles of phenazines in the physiology of *P. aeruginosa*, using the model strain PA14 (and genetic mutants derived therefrom). Phenazine molecules are produced by a variety of environmental and clinical bacterial isolates, typically when bacterial populations reach high cell densities, upon activation of their quorum-sensing systems. Phenazines are well known for their antibiotic activity against other organisms; however, the direct physiological consequences to the organisms that produce them have been a focus of study over only the past decade or so (Chapter 2).

The work in Chapter 3 established that oxidized phenazines can maintain the viability of anaerobic *P. aeruginosa* PA14, provided that glucose is also present in the medium as an energy source. In Chapter 4, several physiological characterizations of non-growing anaerobic cells pointed to the core requirements of survival, and revealed how phenazine redox cycling contributes to anaerobic viability through metabolic interactions. The method for the phenazine redox cycling assay is straightforward but requires a high level of precision and attention to detail. Along with Chapter 7, Appendix 1 articulates the many variables that impact the outcome of viability and death in this experimental set-up. These variables point to interesting features of *P. aeruginosa* physiology that merit further study.

## Anaerobic survival physiology

With new insights regarding the underpinnings of anaerobic survival by *P. aeruginosa* PA14, several follow-up studies could expand the relevance and utility of recent findings. Metabolic reconstruction and flux models exist for *P. aeruginosa* (Oberhardt *et al*, 2008; 2010), however micro-aerobic and anaerobic pathways could be expanded to include the effects of oxygen deprivation on NAD<sup>+</sup>-requiring pathways, and interactions with redox-active phenazines. Details such as these could be added to metabolic flux models and subsequently put to use in several contexts of interest, including human infections and agricultural biocontrol.

The anaerobic phenazine redox cycling set-up provides a unique and powerful experimental condition for testing numerous aspects of anaerobic survival. Due to biological and technical complications that I encountered over the course of this work, only the very first

level of characterizations is complete. We now suspect that glucose, but not succinate, can support survival because a sufficient amount of ATP can be produced via substrate level phosphorylation. ATP hydrolysis bolsters the membrane potential by the proton-translocating function of the  $F_1F_0$  ATPase. Pyruvate fermentation appears to be central to cell survival in the presence of glucose, and phenazines facilitate the recycling of NADH to  $NAD^+$ , which is required to balance the NADH produced in the conversion of glucose to pyruvate and acetate. Mutants in the pyruvate fermentation pathways support this conclusion, and it appears that the original decision to incubate the anaerobic cells with glucose was fortuitous.

Using this experimental set-up, there are many follow-up studies that could further elucidate the physiology of PA14 and other organisms. In particular, the following questions could be addressed using this assay.

- I. *Is glucose the only substrate capable of sustaining anaerobic survival with phenazine redox cycling?* To determine the metabolic pathways available for anaerobic survival, it will be important to test whether other carbon sources (aside from glucose and succinate) permit survival.
- II. *What physiological states permit survival under ensuing anaerobic conditions?* Growth phase is important, but the substrate for growth might also be relevant to the ability of cells to withstand future anaerobiosis. To test this notion, it would be worthwhile to alter the physiological state of cells (*i.e.*, their growth conditions) used in the anaerobic survival assay.
- III. *How do *P. aeruginosa* cells respond to anaerobiosis, and what are the differences in responses between surviving and dying cell populations?* An experiment designed to interrogate the regulation of gene expression of cells during anaerobic survival, as compared to anaerobic population decline using RNASeq, would likely be the best approach. This data set could be complemented by comprehensive metabolite analyses, however standard proteomics approaches are less likely to reveal information about the states of cells during survival, as the signal of newly synthesized proteins is very low and largely masked by the overwhelming presence of preexisting proteins.
- IV. *Are other organisms capable of deriving a fitness benefit from phenazine redox-cycling?* The same experimental setup could be used to investigate the survival and growth phenotypes of other organisms, alone and in combination with *P. aeruginosa*.

Potentially interesting microorganisms include *Staphylococcus aureus* and other co-inhabitants of *P. aeruginosa* infection sites, as well as soil-borne microorganisms that might coexist in rhizosphere ecosystems.

V. *Under what other contexts does phenazine redox cycling affect P. aeruginosa fitness?*

This question could be answered by measuring the survival of *P. aeruginosa* when competed against other organisms in mixed-species incubation experiments; for instance, with other soil dwellers and/or microbes common to cystic fibrosis lung infections.

VI. *What cellular components are involved in phenazine redox cycling?* This anaerobic survival assay utilizing phenazine redox-cycling could be employed as a secondary screen to test the viability of putative “phenazine reductase” mutants, or the influence of specific drugs on phenazine-cycling cells.

## **Phenazine reduction by *P. aeruginosa***

The means by which phenazine reduction takes place in *P. aeruginosa* has been a topic of intense interest in our lab for several years. Despite various attempts at determining whether, and how, this process is mediated, we still do not have a concrete answer. Figure 1 presents models for ways in which phenazines might undergo cell-mediated reduction. Preliminary experimental evidence in PA14 (Price-Whelan, 2009) and known interactions of phenazines with the electron transport chain of other organisms (Armstrong *et al*, 1971; Baron & Rowe, 1981) point toward the likelihood of the model depicted in Figure 1a, however, the relevant electron-transport chain component is not yet known. Knowledge of how phenazines interact with the cells that produce them would allow a more rational design of experiments with *P. aeruginosa*, and offer a starting point for understanding phenazine reduction across a wide variety of organisms, including other producers (such as biocontrol strains of *P. fluorescens* and *P. chlororaphis*) and the organisms with which these producers coexist, including commensal organisms, infection site hosts, or competitors.

Whether all of the phenazines produced by *P. aeruginosa*, or any other organisms for that matter, undergo reduction in the same manner is entirely unknown. Because the different phenazines have varying rates of reactivity with oxidants such as oxygen and ferric iron (Wang & Newman, 2008) due to their precise reduction potential, which is a reflection of the chemical structure and environmental parameters, it is possible that these rates of

reactivity with reductants may vary in the cell as well. For instance, cells in stationary phase reduce phenazines more quickly than exponential phase cells (Price-Whelan *et al*, 2007); however, at any given time, there is no delay in cells reaching their maximal phenazine-reduction rate. This observation suggests that any cellular machinery involved in this process is already present, possibly serving another (constitutive) purpose, and therefore does not require induction.

Preliminary evidence from the anaerobic phenazine redox-cycling survival assay suggests that *P. aeruginosa* PA14 cells may utilize a different kind of metabolism when provided with PCA compared to PYO (see Appendix 1). Thus, any “reductases” predicted using one phenazine should be tested with other phenazines as well to see whether there is any variation in reduction rates, or whether another “reductase” might be functional for a separate subset of the phenazines. Further, it would be very interesting to look for homology of cellular components that serve as phenazine reductases across other phenazine producers as compared to non-producing organisms.

The assay for pyocyanin reduction rate could be a helpful tool for the discovery or verification of mutants or conditions resulting in altered pyocyanin reduction physiology. New efforts focusing on PCA reduction are underway in the lab, and it is likely that the interactions of phenazines within *P. aeruginosa* will be more precisely understood in the near future. This effort remains a worthwhile pursuit, as understanding the process of cellular phenazine reduction at a molecular level could inform rational drug design against problematic organisms that produce and derive fitness benefits from the presence of phenazines. It will be important to also understand what compounds *in situ* might serve as oxidants; oxygen, nitrate, and various minerals are known to oxidize phenazines, and melanin or other oxidized organic molecules might also facilitate phenazine redox-cycling, and could offer other avenues for disabling this process.

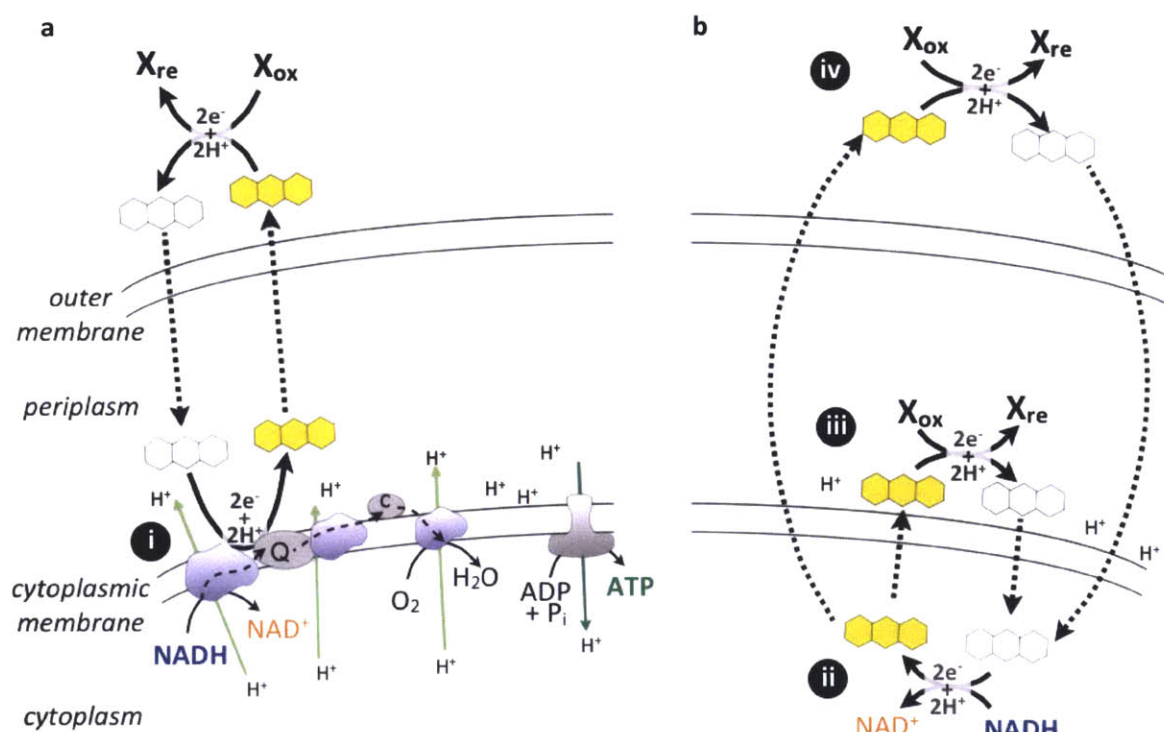
## References

- Armstrong AV, Stewart-Tull DE & Roberts JS (1971) Characterisation of the *Pseudomonas aeruginosa* factor that inhibits mouse-liver mitochondrial respiration. *J Med Microbiol* **4**: 249–262
- Baron SS & Rowe JJ (1981) Antibiotic action of pyocyanin. *Antimicrob Agents Chemother* **20**: 814–820
- Oberhardt MA, Goldberg JB, Hogardt M & Papin JA (2010) Metabolic Network Analysis of *Pseudomonas aeruginosa* during Chronic Cystic Fibrosis Lung Infection. *J Bacteriol*
- Oberhardt MA, Puchałka J, Fryer KE, Martins dos Santos VAP & Papin JA (2008) Genome-scale metabolic network analysis of the opportunistic pathogen *Pseudomonas aeruginosa* PAO1. *J Bacteriol* **190**: 2790–2803
- Price-Whelan A (2009) Physiology and mechanisms of pyocyanin reduction in *Pseudomonas aeruginosa* Ph.D. Thesis. California Institute of Technology, USA
- Price-Whelan A, Dietrich LEP & Newman DK (2007) Pyocyanin alters redox homeostasis and carbon flux through central metabolic pathways in *Pseudomonas aeruginosa* PA14. *J Bacteriol* **189**: 6372–6381
- Wang Y & Newman DK (2008) Redox reactions of phenazine antibiotics with ferric (hydr)oxides and molecular oxygen. *Environ Sci Technol* **42**: 2380–2386



## Figures

**Figure 1.** Schematics of possible redox interactions of phenazines. Reduced phenazines (carrying the additional 2 e<sup>-</sup> and 2 H<sup>+</sup>) are colored gray, while oxidized phenazines are white. **a)** Oxidized phenazines might acquire electrons through interactions with a component of the respiratory chain (i), located in the cytoplasmic membrane. **b)** Alternatively, phenazines might undergo reduction in the cytoplasm (ii). Oxidation might occur in the periplasm (iii) or beyond the boundary of the cell (iv).





## **Appendix A**

**Effects of varying experimental conditions on *P. aeruginosa***

**PA14 anaerobic survival with phenazine redox cycling**

**Contributions:**

I carried out and documented the work described in this chapter.

## Introduction

In the course of pursuing physiological characterizations of *P. aeruginosa* PA14 cells surviving anaerobically in the presence of redox-cycling phenazines, it became clear that numerous factors are involved in determining the precise survival outcome of any individual experiment. In an effort to contribute to the overall understanding of the physiology of cells in this context, this appendix chapter documents the variables that I found to be important to control during anaerobic phenazine redox-cycling experiments (described in detail in Chapter 7).

## Materials and Methods

The protocols used to generate the data presented here were identical to those listed in Chapter 6, with changes as noted in Results and Discussion.

## Results and Discussion

### Growth phase effects on survival

Early-stationary phase cultures of *P. aeruginosa* PA14 grown in rich LB medium have so far demonstrated the most reproducible survival and death outcomes for positive and negative controls, accordingly. An  $OD_{500}$  of about 2.8 has worked well. (For a key to growth phase terminology and an example growth curve for PA14 grown in liquid LB medium, see Figure 1.)

Numerous attempts at using cells grown to late-stationary phase (approximately 19 hours) in LB medium yielded results unlike those published in the original, complete data set (Wang *et al*, 2010). Instead of clear differences between survival and death conditions as published (often 1000-fold by day 6), in these experiments using late-stationary phase cultures, all conditions showed a gradual die-off (for an example data set, see Figure 2). There were no perfect survival outcomes and the difference between “survival” and “death” conditions was often under 20-fold.

In an experiment aimed at explicitly comparing survival outcomes for cells grown to different optical densities, results were inconsistent with prior findings: the late-stationary

phase cells survived perfectly. Exponential phase cells, which had not been tested before, were found to die very quickly regardless of the presence of phenazines and an oxidizing potential (see Figure 3a). These results were recapitulated with the same initial cultures in sealed anaerobic Balch tubes and measured daily for CFU (Figure 3b). For this experiment it was very challenging to set up the growth conditions such that each flask was ready for harvesting at the same time; consequently, this did not serve as an ideal test of the relevance of growth phase. Exponential phase cells were harvested at OD<sub>500</sub> 1.07, while the late-exponential phase cells grew only to OD<sub>500</sub> 1.70. Neither set of cells survived well. Later, the most reliable condition for robust survival was determined to be in early-stationary phase, at OD<sub>500</sub> near 2.8, so it may be consistent that both conditions were unable to survive. The cells grown overnight were inoculated from a liquid culture and grown for 19 hours. Optical density measurements showed that by the time of harvest, the culture had passed through its peak (OD<sub>500</sub> measured as high as 3.39 at one hour before harvest, and harvested at 3.22).

This experiment deserves repeating, but in combination with prior results, suggests that exponential phase cells are not capable of surviving with phenazine redox cycling and that late-stationary phase cells vary in their ability to survive anaerobically. This variability could be due to mutations and adaptations that occur within populations in stationary phase, such as the phenomenon termed growth advantage in stationary phase (GASP, (Finkel, 2006).

Growth phase of the cultures may also impact the redox state of cells during anaerobic incubation. Early measurements of anaerobic levels of NADH/NAD<sup>+</sup> revealed very high ratios (over 10) for cells without phenazines and potential, and were obtained with cells that had been grown to late-stationary phase. More recent characterizations failed to find such dramatic differences between treatment conditions (highest ratios were below 3), which may be due to using early-stationary phase cells, rather than much older cultures.

## **Ammonium**

A high level of ammonium chloride in the anaerobic culturing medium is necessary for the pattern of survival and death as previously published (Wang 2010).

This experimental setup initially employed an anaerobic buffered minimal medium containing 93 mM ammonium chloride, as previously published (Palmer *et al*, 2007). As this

level of  $\text{NH}_4\text{Cl}$  was substantially higher than the amount of glucose provided for the anaerobically surviving cells (20 mM), I switched to a recipe with 10-fold less ammonium chloride, 9.3 mM. Three separate attempts at using only 9.3 mM  $\text{NH}_4\text{Cl}$  revealed no strong difference in survival between conditions, with nearly 100% of cells surviving, although oxygen contamination may have contributed to the outcomes of two of these. A follow-up control experiment showed that in sealed, anaerobic culture tubes, cells with 93 mM  $\text{NH}_4\text{Cl}$  died rapidly at 37°C, while those with 9.3 mM remained viable longer (see Figure 4). This phenomenon may be specific to ammonium, or it may be a general stress response to high salt conditions.

### **Minimum levels of phenazine to support anaerobic survival via redox cycling**

PA14 might be able to survive via phenazine redox cycling with phenazine levels as low as 10  $\mu\text{M}$ .

The concentration of phenazines used throughout most of the redox-cycling experiments was always in the range of 70 to 90  $\mu\text{M}$ . We speculated that it might be possible to achieve anaerobic survival with far lower levels, since phenazines can undergo repeated cycles of reduction and oxidation. One experiment aimed to address this question by comparing survival outcomes of cells incubated with 8.5, 25, or 85  $\mu\text{M}$  pyocyanin. Although survival was incomplete, all three treatments that included pyocyanin survived better than the condition without any pyocyanin at all, by at least 1000-fold (see Figure 5). (Unfortunately, late-stationary-phase cultures were employed for this particular experiment, before it was clear that early-stationary phase cells were best to use.) Since the presence of only 8.5  $\mu\text{M}$  enhanced anaerobic survival in comparison to no phenazines at all, it may be that phenazine levels in the very low micromolar range can mediate electron transfer to a sufficient degree to enable anaerobic survival of PA14.

### **Pyocyanin sensitizes cells to lysis during aerobic CFU plating**

Aerobic dilutions, plating, and incubation yield CFU counts that underestimate the number of viable cells in anaerobic cultures, but only when pyocyanin is present and the population of cells has started to die.

Starting by the fourth day of a typical anaerobic survival experiment, dying cultures incubated with pyocyanin (+PYO –potential) grow fewer colonies when diluted, plated, and incubated aerobically than anaerobically. In one experiment testing these plating conditions

side-by-side, anaerobic CFU counts for +PYO –potential matched those of the other negative controls (–PYO –potential, and –PYO +potential), whereas aerobic CFU counts were about 3-fold lower (see Figure 6).

This difference in plating efficiency is likely due to the generation of toxic levels of superoxide, which develop when reduced pyocyanin reacts with oxygen. This may harm cells that have adjusted to anaerobic conditions upon sudden exposure to oxygen.

### **Temperature effects and recommendations**

Within the range of 30° to 37°C, higher temperatures lead to a faster decline in viability under anaerobic conditions.

In one experiment designed to directly test temperature effects on anaerobic survival in sealed Balch tubes, cells at 37°C rapidly lost viability starting at day 1, whereas those at 30°C lost viability more slowly until day 4 of anaerobic incubation (see Figure 7a). At 5 days, 7% of the cells incubated at the lower temperature were still viable, as compared to only 0.0007% for cells at 37°C.

Temperatures have ranged as widely as 3 degrees Celsius in a single experiment, anywhere between 28 and 34°C across all experiments, and may have affected the survival outcomes for the different conditions.

### **Pyocyanin may induce lysis of anaerobic PA14 cultures**

Anaerobic cultures with pyocyanin appear to lyse earlier but maintain viability longer than anaerobic cultures without pyocyanin.

When investigating the cause of more rapid population decline in negative control cultures containing pyocyanin, (resolved by plating anaerobically as described above), a separate experiment involving sealed tubes of cultures with and without PYO yielded new insights about a possible role of PYO under anaerobic conditions. Interestingly, regular measurements of optical density and colony forming units revealed that cultures with PYO became optically clear much sooner, while maintaining higher CFU counts than cells without PYO (Figure 7 a and b, see especially days 6 through 9 for cultures at 30°C, and day 3 for cultures at 37°C).

This is a very preliminary dataset and the interpretation involves substantial speculation. More replicates and controls would need to be performed to verify that the cultures in this

experiment were completely free of oxygen, which can transiently reach low part-per-million levels in the Coy glove bag, where daily sampling took place. Trace levels of oxygen could react with PYO and the effects seen here might not be attributable to reduced PYO, but instead, to ROS. Microscopy of the cultures would be useful for interpreting the early decrease in optical density for those with PYO compared to those without it. Oxygen exposure during sample preparation and observation might introduce artifacts.

A potentially interesting conclusion following from this observation is that PYO may cause inviable cells to lyse, liberating fermentable substrates that enable anaerobic survival (*e.g.*, arginine and pyruvate), and leading to sustained population viability. Cells without PYO may not have a mechanism for fully lysing and liberating useable substrates, leaving the culture still cloudy, yet with substantially lower counts of viable cells. Even if trace levels of oxygen are responsible for the finding here, pyocyanin might yield similar effects for *P. aeruginosa* in the environment and in infections, where oxygen levels are sometimes undetectable by our measurement tools, but may nonetheless be sufficient to impact microbial metabolism, or to generate ROS.

### **PYO vs. PCA for current output**

Potentiostat data show a distinctly different pattern of phenazine oxidation (and vessels show different pattern of phenazine reduction) in experiments with PCA vs. PYO. Regardless of the phenazine present, the overall survival outcome appears to be the same (Wang *et al*, 2010 and unpublished). Cells begin reducing PYO right away, building up to a “steady-state” that lasts for the duration of the experiment. The color of the cultures remains a pale blue—indicating a mix of oxidized (blue) and reduced (colorless) PYO—over the majority of the experiment. Usually in the last day or two of the experiment, the cultures turn brighter blue, and the current decreases, which indicates slower PYO reduction by the cells. This could be due to electrode fouling by biofilms, lower metabolic activity, or a decrease in viable cell number.

In contrast, with experiments involving PCA, there was a repeatable pattern of reduction rate oscillation over the course of a week of anaerobic incubation. As with PYO, cells with PCA reduced phenazine most quickly within the first day, but then by the third day dropped off to a very low level of current. Reduction rates would increase once more for 4 to 12 hours and then decrease. This pattern was evident by the current measured at the electrode, and also by the color of the cultures (very pale yellow when oxidized, bright yellow when



reduced). The oscillations in current happened at different times for the different cultures in the same experiment, which probably rules out a technical problem (*e.g.* oxygen contamination).

It should be noted that many of the experiments utilizing PYO were performed with late-stationary phase cells, whereas those with PCA were performed more recently and used early-stationary phase cells, at OD<sub>500</sub> 2.8. This apparent difference between PYO and PCA deserves more systematic comparison, but is suggestive of possibly different metabolic modes for anaerobic survival in this context. It may prove interesting to consider differences in the roles that PYO and PCA play in the overall metabolism of *P. aeruginosa*, as suggested earlier (Hernandez & Newman, 2001; Price-Whelan *et al*, 2006; Wang & Newman, 2008).

## Conclusions

The results presented here were obtained through careful monitoring of experimental setup, but were rarely repeated. With further study, many of the parameters mentioned in this appendix chapter could yield interesting insights about anaerobic survival physiology, and physiological impacts of phenazines.

## References

- Finkel SE (2006) Long-term survival during stationary phase: evolution and the GASP phenotype. *Nature Rev Microbiol* **4**: 113–120
- Hernandez ME & Newman DK (2001) Extracellular electron transfer. *Cell Mol Life Sci* **58**: 1562–1571
- Palmer KL, Aye LM & Whiteley M (2007) Nutritional cues control *Pseudomonas aeruginosa* multicellular behavior in cystic fibrosis sputum. *J Bacteriol* **189**: 8079–8087
- Price-Whelan A, Dietrich LEP & Newman DK (2006) Rethinking 'secondary' metabolism: physiological roles for phenazine antibiotics. *Nature Chem Biol* **2**: 71–78
- Wang Y & Newman DK (2008) Redox reactions of phenazine antibiotics with ferric (hydr)oxides and molecular oxygen. *Environ Sci Technol* **42**: 2380–2386
- Wang Y, Kern SE & Newman DK (2010) Endogenous phenazine antibiotics promote anaerobic survival of *Pseudomonas aeruginosa* via extracellular electron transfer. *J Bacteriol* **192**: 365–369

## Figures

**Figure 1.** Example growth curve (log scale). A late-stationary phase liquid culture of PA14  $\Delta phz1/2$  was diluted 1:500 into 250 mL fresh LB in a 1-L flask. The culture was aerated by shaking at 250 rpm and incubated at 37°C. The arrow indicates the point at which cells are harvested (pelleted and washed with minimal medium) for use in the anaerobic phenazine redox-cycling survival assay. Different growth phases are indicated on the chart for reference.

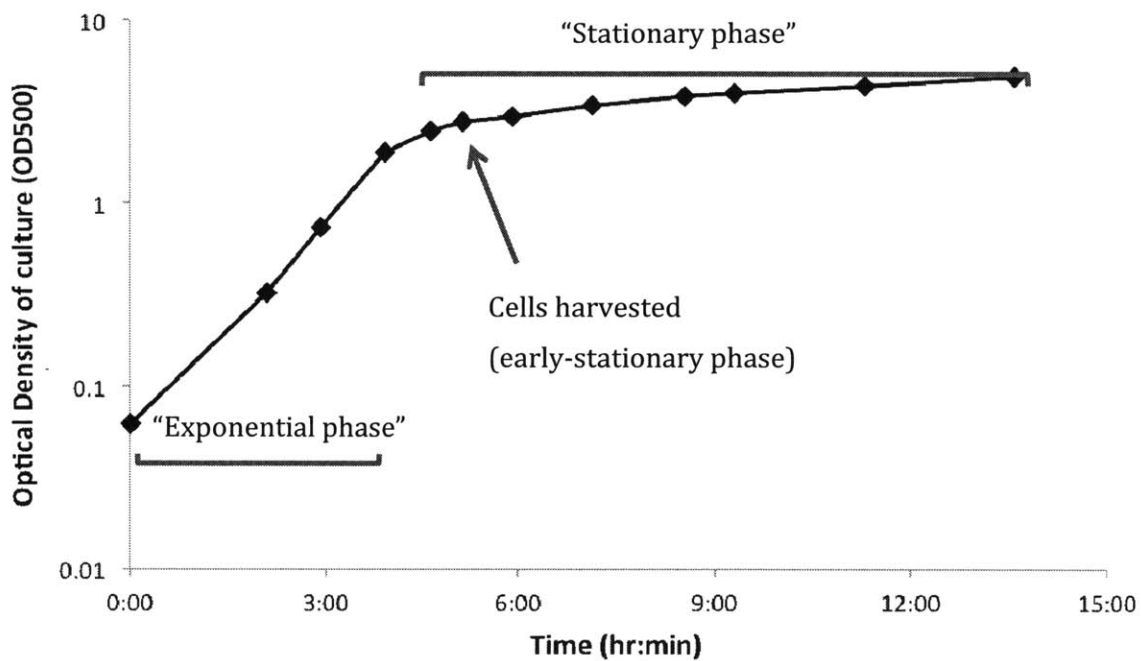


**Figure 2.** Late-stationary phase cultures do not follow the same survival and death patterns as previously published (Wang *et al*, 2010). A single culture of PA14  $\Delta phz1/2$  was grown from a single colony inoculum for 19 hours in 600 mL LB medium (2 L flask) at 37°C with shaking. Cells were pelleted and resuspended three times to wash the cells before adding them to anaerobic cultures at a final OD500 of around 1.0. Pyocyanin and an oxidizing potential were present as indicated.

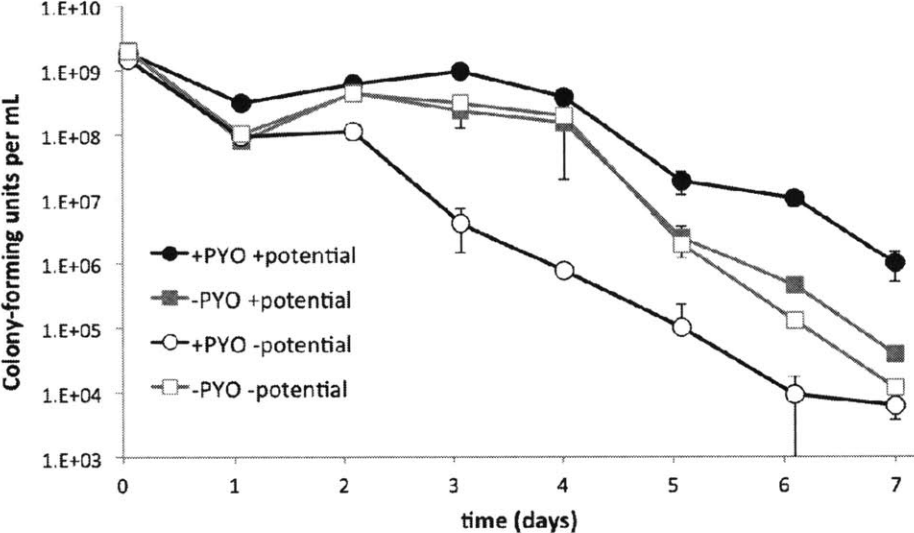
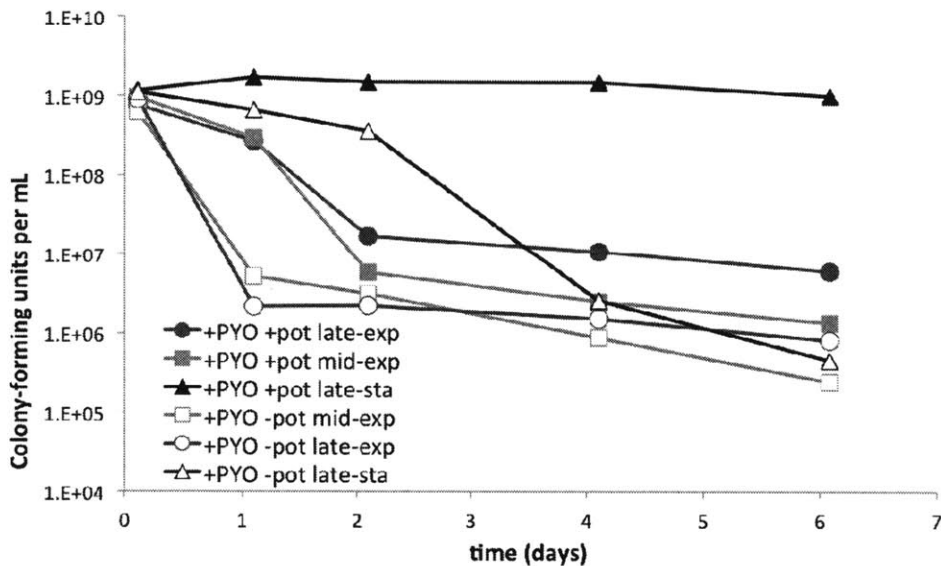


**Figure 3.** The growth phase of cells alters the duration of anaerobic survival. PA14  $\Delta phz1/2$  cells were grown aerobically in LB medium for 19 hours (late-stationary phase), or 6 hours (mid- and late-exponential) to OD500 3.2 (late-stationary), 1.7 (late-exponential), or 1.07 (mid-exponential). Cells were washed and incubated **a)** aerobically with pyocyanin and an oxidizing potential as indicated, or **b)** sealed in stoppered Balch tubes.

**a**



**b**

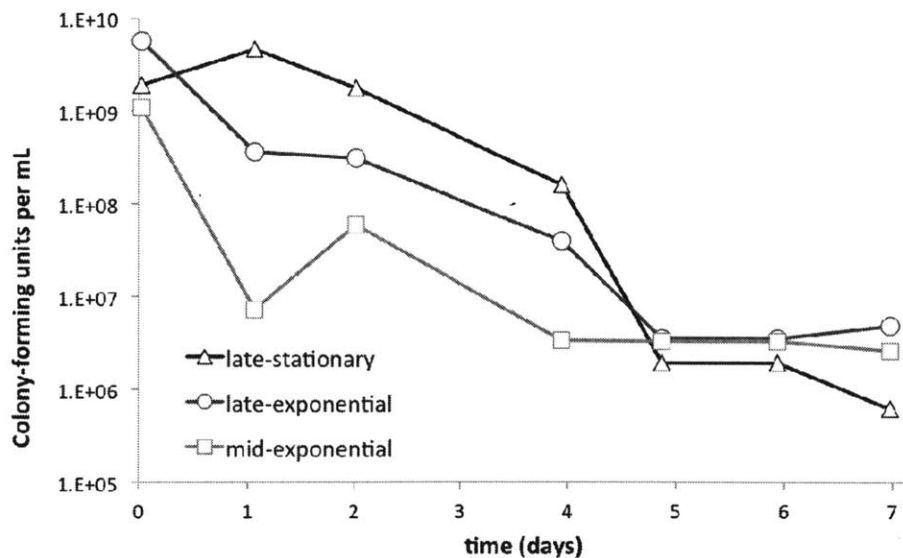


**Figure 4.** Differential viability of PA14  $\Delta phz1/2$  cells after 2 days of anaerobic incubation with varying concentrations of ammonium. Cells were grown to OD500 2.8 in LB and washed as outlined in the Method of Chapter 6. Cells were incubated anaerobically in sealed Balch tubes with the level of ammonium indicated (9.3 or 93 mM) in the defined MOPS minimal medium.

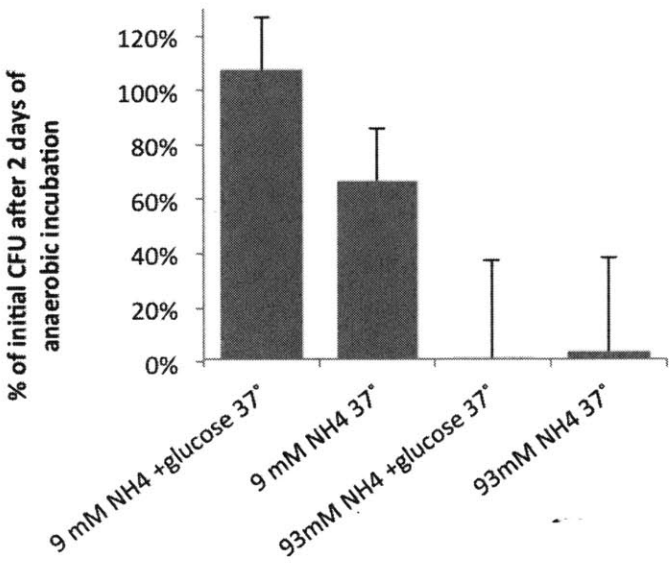


**Figure 5.** Anaerobic survival via phenazine redox cycling with varying levels of pyocyanin in the liquid culture. Cells were grown overnight in LB and incubated anaerobically with different amounts of pyocyanin in the defined MOPS-buffered minimal medium with glucose.

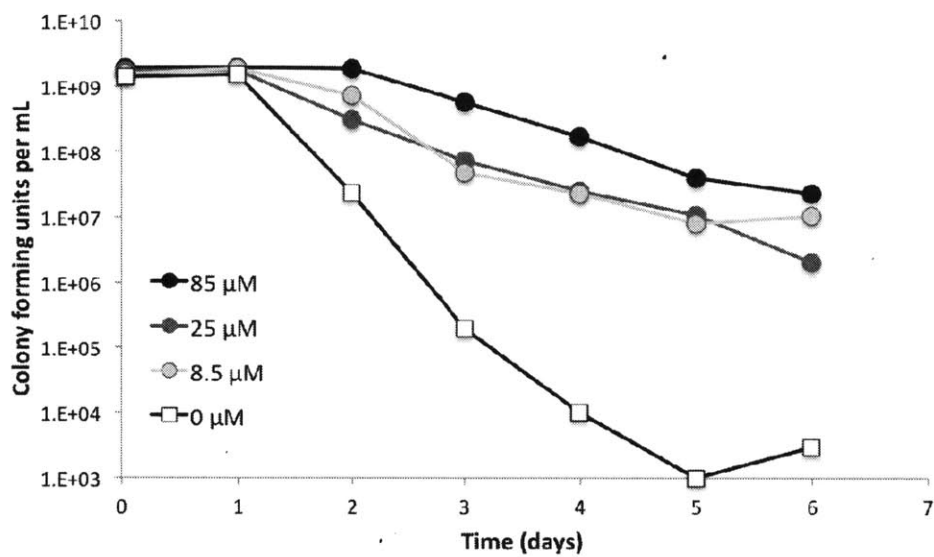
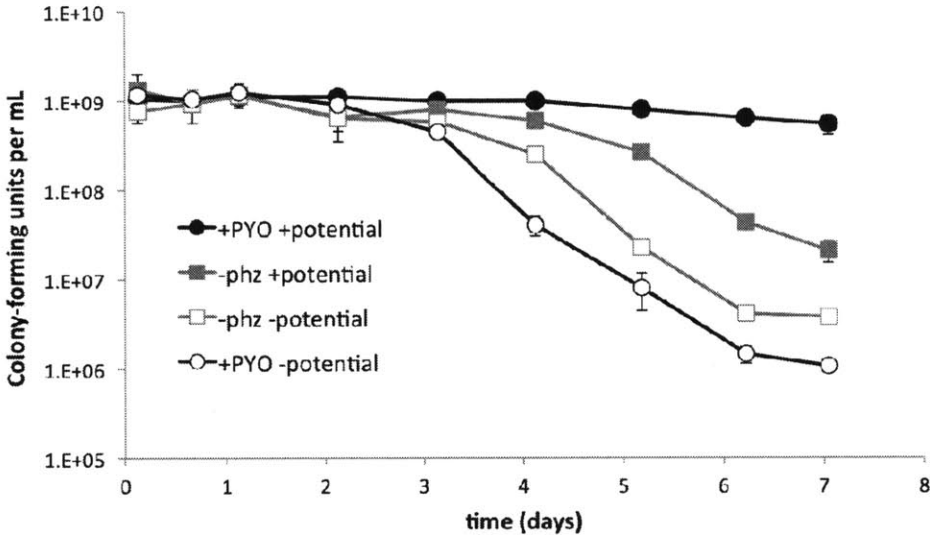


**Figure 6.** Viability as measured by colony forming units on LB agar plates prepared and incubated **a)** aerobically and **b)** anaerobically. Note that all conditions, except cells with pyocyanin but without an oxidizing potential (open black circles), show the same count whether plated aerobically or anaerobically. Aerobic plating of cells with pyocyanin but without potential results in counts that are nearly 5-fold lower than when cells were plated in the absence of oxygen.

**a**



**b**

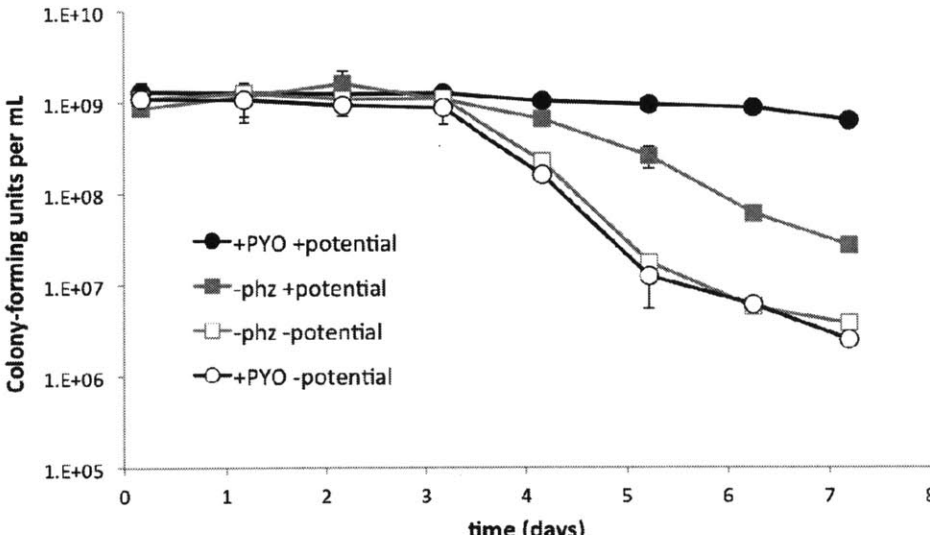
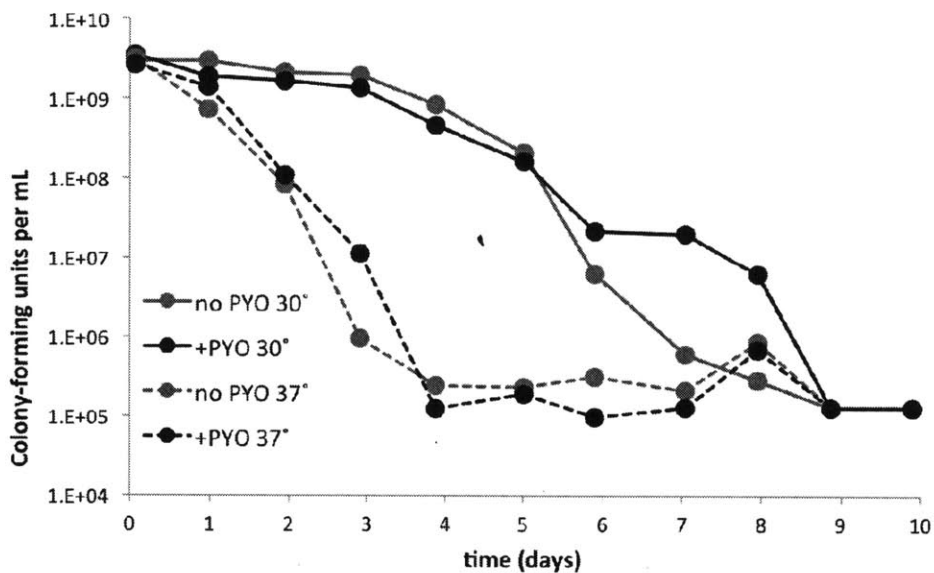


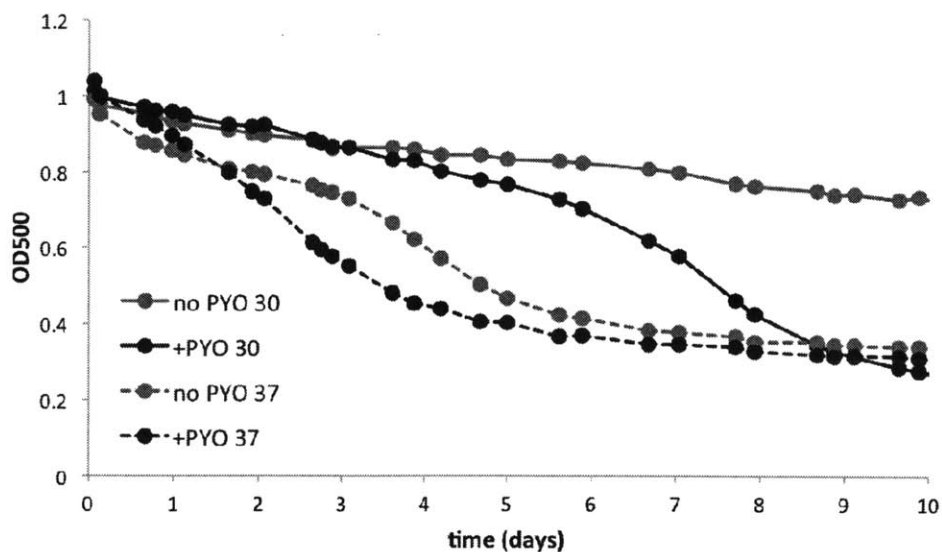


**Figure 7.** Cell viability and culture optical density during anaerobic incubation. PA14  $\Delta phz1/2$  cells were grown aerobically in 250 mL LB (in 1 L flask), washed with MOPS-buffered medium, and then mixed with 85  $\mu\text{M}$  pyocyanin as indicated. Sealed Balch tubes were incubated at either 30° or 37°C and sampled for **a)** CFU and **b)** optical density over ten days.

**a**



**b**





## **Appendix B**

### **Applications of an assay to measure pyocyanin reduction rates by mutants of *Pseudomonas aeruginosa***

**Contributions:**

I carried out and documented the work presented in this chapter.

## Introduction

The ability to produce and redox cycle phenazines confers fitness benefits to *Pseudomonas aeruginosa* under particular environmental conditions. For example, when respiratory electron acceptors are in very low supply, oxidized phenazines can balance the redox state of the NAD(H) pool (Price-Whelan *et al*, 2007) and permit anaerobic survival (Wang *et al*, 2010). Additionally, reduced phenazines can react with insoluble, and chelator-bound Fe(III) to yield soluble, bioavailable Fe(II) (Wang & Newman, 2008; Wang *et al*, 2011). Phenazines are also important for the normal development of biofilms in various pseudomonads (Maddula *et al*, 2006; 2008; Ramos *et al*, 2010; Wang *et al*, 2011). A central aspect of all of these interactions is the ability of cells to add electrons to available oxidized phenazines. Yet, the mechanism of cellular phenazine reduction remains unknown.

Previous efforts to determine whether cellular components are involved in the process of phenazine reduction used a genetic screen of mutants in a non-redundant transposon mutant library of *P. aeruginosa* PA14 (Liberati *et al*, 2006), and approximated the rate of pyocyanin reduction spectrophotometrically (Price-Whelan, 2009). The methods used in that study identified two transposon-insertion mutants with slow reduction rates: *gpsA*, which encodes glycerol-3-phosphate dehydrogenase, and *fbcC*, which encodes a subunit of the cytochrome  $bc_1$  complex (complex III). Reduction rate results were very low, and therefore promising, for the *fbcC* mutant, but ultimately somewhat unreliable because this mutant demonstrated a growth defect. Because of this, slower reduction rates may have been confounded by other factors. In addition, its reduction rates might have been measured at an earlier phase of growth as compared to wild type and the other mutants, which would introduce a known variable for pyocyanin reduction—cells in the exponential phase of growth reduce pyocyanin more slowly than cells in stationary phase (Price-Whelan *et al*, 2007). The *gpsA* mutant had very low levels of NADH, a substrate that seems to be required for phenazine reduction, and also exhibited growth defects (Price-Whelan, 2009).

The previous method was useful in picking up strong pyocyanin reduction phenotypes; a more sensitive and higher-throughput method became possible upon the addition of new equipment to the laboratory. A substantial limitation to the original method was the variability in the initial amount of pyocyanin present in each culture tested, and since the reaction kinetics of pyocyanin reduction depend on the initial concentration of pyocyanin (shown in Figure 1), the new approach, reported here, involved adding extra pyocyanin to

freshly diluted cultures. With a 96-well-plate colorimetric assay performed in an oxygen-free atmosphere, not only could we repeat the screen for mutants with reduction phenotypes, but we could also use the assay as a measurement of cellular physiology under several test conditions at the same time.

Pyocyanin has been the focus of phenazine-reduction assays because of its spectrophotometric properties, which are amenable to measurement in a wide variety of conditions, including cultures growing in rich LB medium. Oxidized pyocyanin absorbs maximally at 691 nm, the reason for its characteristic blue color, while reduced pyocyanin is colorless but fluorescent, with excitation at 330 nm and emission at 490 nm. Within an oxygen-free atmosphere, the rate of pyocyanin reduction can be monitored by the decrease in absorbance at 691 and concomitant increase in fluorescence.

In this chapter, I discuss several applications of the pyocyanin reduction assay that I developed, including a test of respiratory chain mutants, an attempt to determine whether levels of cellular NADH correlate with the rate of pyocyanin reduction, and a test of the effects of methylene blue on the rate of pyocyanin reduction by PA14.

## **Materials and Methods**

### **Bacterial strains and culture conditions**

Strains used in this study are listed in Table 1.

Cultures of *P. aeruginosa* PA14 were grown in liquid LB medium overnight with an initial inoculum from a patch of colonies grown overnight at 37°C on an LB agar plate. For experiments involving other growth substrates, cultures of *P. aeruginosa* PA14  $\Delta phz1/2$  were grown from exponential phase LB culture inocula in the given media, shaking at 250 rpm at 37°C for 18 hours (OD<sub>500</sub> between 3 and 4) unless otherwise indicated. Cultures were moved from the aerobic incubator to the anaerobic chamber. 80  $\mu$ L of cell cultures were added to the wells of a microtiter plate containing fresh medium (100  $\mu$ L each well) and the reduction rate assay was performed as described. Where indicated, NAD(H) was extracted from cultures as quickly as possible upon transition to the anaerobic glove bag, as described below.

## Construction of *P. aeruginosa* mutants

PA14 and PA14  $\Delta phz1/2$  mutants with unmarked, in-frame deletions in *pqsA*, *cyoABCD*, and *cioAB* were constructed using the primers listed in Table 2. Approximately 1kb of DNA on either side of the target gene was amplified using primers listed in Table 1, identified as [*gene name*]<sub>1</sub>, 2, 3, and 4. The PCR fragments were combined in *Saccharomyces cerevisiae* InvSc1 (DKN569) with linearized pMQ30 (purified from DH5 $\alpha$ , strain DKN303), a plasmid encoding a gentamicin resistance cassette and the *sacB* gene for counter-selection with sucrose. Rather than overlap extension PCR, this approach utilizes the DNA repair mechanisms of yeast to ligate PCR fragments with plasmid DNA. The ligated plasmid was extracted and transformed into *E. coli* BW29427 (DKN164), a conjugation strain and DAP (diaminopimelic acid) auxotroph. The plasmid containing the gene deletion sequence was transferred into *P. aeruginosa* through biparental conjugation on LB agar plates containing DAP. *P. aeruginosa* conjugants were selected by plating on LB agar plates with 100  $\mu\text{g}/\text{mL}$  gentamicin sulfate. Following overnight growth in liquid culture, counter-selection on LB plates with sucrose (100 g/L) yielded *P. aeruginosa* strains that no longer carried the plasmid. From these, colony PCR using primers [*gene name*]<sub>c1</sub>, c2, c3, and c4 was used to find the colonies lacking the gene of interest. Sequences of the PCR products confirmed the identity and accuracy of the deletion mutants.

## Pyocyanin reduction assay

All steps were performed in an oxygen-free glove bag (Coy) with an atmosphere of 95% N<sub>2</sub> and 5% H<sub>2</sub>. The absorbance at 500 and 691 nm and fluorescence (excitation at 330 nm, emission at 490 nm) of the sample wells was measured and recorded using a BioTek Synergy 4 plate reader held at an internal temperature of 37°C. In each sample well of a clear plastic 96-well microtiter plate, 80  $\mu\text{L}$  of cell culture plus 100  $\mu\text{L}$  of fresh LB were mixed gently by pipetting. Following an initial reading of A<sub>500</sub>, A<sub>691</sub>, and fluorescence, the plate was removed from the plate reader so that 20  $\mu\text{L}$  of a MOPS-buffered solution of 0.8 mM pyocyanin at pH 7.2 could be added to each well by multichannel pipette (for 80  $\mu\text{M}$  final pyocyanin concentration). The plate was returned to the plate reader, and A<sub>500</sub>, A<sub>691</sub> and fluorescence data were recorded at least once per minute for at least 20 minutes. Rates of change in spectral properties (A<sub>691</sub> or fluorescence) over time were determined with a linear regression through the first 5 minutes of data collection. These rates were then

divided by the optical density of the cells, to normalize for cell count. This calculation was made as follows:

$$\frac{\frac{\Delta fls}{time}}{OD500cells - OD500blank}$$

## **NAD(H) measurements**

The method for measuring NAD<sup>+</sup> and NADH was based on established protocols (San *et al*, 2002; Price-Whelan *et al*, 2007). For each condition, two 1.6-mL samples in 1.7 ml plastic tubes were centrifuged for 1 min at maximum speed (16,000×g). The supernatant was removed and 200 μL of either 0.2 M HCl (for NAD<sup>+</sup> extraction) or 0.2 M NaOH (for NADH extraction) was added and mixed by vortexing. After 10 minutes at 55°C the samples were cooled on ice before 200 μL of 0.1 M NaOH (for NAD<sup>+</sup>) or 0.1 M HCl (for NADH) was added drop-wise while vortexing. After pelleting cell debris (5 minutes at maximum speed), 150 μL of the supernatant was transferred to a fresh tube for storage.

To assay the amount of NAD<sup>+</sup> or NADH in each sample, 15 μL of extracted sample or a standard of known NAD<sup>+</sup> concentration was added to 80 μL of the colorimetric assay reagent mix in a 96-well microtiter plate. The reagent mix contained 250 mM bicine buffer, pH 8.0, 5 mM EDTA, 12.5% ethanol (v/v), 0.525 mM thiazolyl blue, 4.2 mM phenazine ethosulfate. The 96-well plate was then moved out of the anoxic environment and heated to 30°C inside a BioTek Synergy 4 plate reader. To initiate the colorimetric assay, 5 μL of a 1 mg mL<sup>-1</sup> solution of alcohol dehydrogenase II (Sigma A3263) in 100 mM bicine, pH 8.0, was added to each well. With intermittent shaking, the plate reader then recorded the appearance of reduced thiazolyl blue (with an absorbance peak at 570 nm) every minute for 30 minutes. Concentrations of NADH and NAD<sup>+</sup> were calculated using the slope and intercept derived from A<sub>570</sub>/time of the standard curve.

## **Results**

### **Development of the pyocyanin reduction assay**

The goal of establishing a new protocol for determining the rate of cellular pyocyanin reduction was to make available an easy and high-throughput method for investigating the physiology pertaining to pyocyanin reduction.

Results here show that increasing the concentration of pyocyanin leads to quicker reduction rates (Figure 1) for a given growth substrate for any given growth phase, however reduction rates can vary greatly by substrate. Both the absorbance at 691 nm ( $A_{691}$ ), indicating oxidized pyocyanin, and fluorescence measurements (excitation at 340 nm and emission at 490 nm), which correlate with concentration of reduced pyocyanin, are reliable metrics for following the rate of pyocyanin reduction. Particularly at lower rates of reduction, fluorescence may yield more reliable results due to the higher signal-to-noise ratio for fluorescence compared to  $A_{691}$  readings, which are impacted somewhat by the presence of cells. A non-linear regression (such as a Lineweaver-Burk plot) of pyocyanin spectral changes over time would likely give more accurate reduction rates than the linear approximations of the initial rate used here.

### **Pyocyanin reduction by respiratory cytochrome mutants**

Phenazines have been shown to drain electrons from respiratory chain components of mitochondria, including succinate dehydrogenase and quinols (Harman & MacBrinn, 1963; Armstrong *et al*, 1971). With the long-term goal of identifying the site of pyocyanin reduction in *P. aeruginosa* through combinations of mutants and respiration-inhibiting drugs, I began by constructing mutants in two quinol oxidases and tested their pyocyanin reduction rates in comparison to wild type (PA14  $\Delta phz1/2$ ) and  $\Delta fbcC \Delta phz1/2$ . The mutants were deleted in the cytochrome bo3 complex ( $\Delta cyoABCD$ ) and the cyanide insensitive oxidase complex ( $\Delta cioAB$ ), singly and in combination in a PA14  $\Delta phz1/2$  background. When grown in succinate, there appeared to be a slightly lower reduction rate for  $\Delta cioAB$ , than wild type ( $\Delta phz1/2$ ) or the  $\Delta cyoAB$  mutant, but nothing nearly as severe as the reduction rates for  $\Delta fbcC$  (Figure 2a).

We thought that growth in succinate might increase the levels of succinate dehydrogenase, which has been shown in mitochondria to transfer electrons to pyocyanin (Harman & MacBrinn, 1963). If true for *P. aeruginosa*, this could mask the effects of deficiencies in other components of the respiratory chain that might contribute to pyocyanin reduction. I then chose to test cells grown in glutamate, a substrate that would not feed directly into the TCA cycle. With glutamate, there was no difference in pyocyanin reduction rates between the control ( $\Delta phz1/2$ ) and any of the mutants, except for  $\Delta fbcC$  again (Figure 2b), which has previously been shown to have a slow pyocyanin reduction phenotype (Price-Whelan, 2009). The growth phase of the cells for the glutamate experiment was not ideal; whereas



the pyocyanin reduction rate for the succinate-grown cells was measured in early stationary phase, for glutamate grown cells the reduction rate assay was performed on exponential and late-stationary phase cells (because growth in this condition took much longer than expected, and early stationary phase occurred overnight).

### **Pyocyanin reduction in the presence of nitrate**

Nitrate can serve as a terminal oxidant of the *P. aeruginosa* respiratory chain, allowing for anaerobic growth. Nitrate cannot oxidize reduced pyocyanin on its own, however, pyocyanin becomes oxidized in the presence of *P. aeruginosa* cells and nitrate. I incubated PA14  $\Delta phz1/2$  cells in sealed glass tubes with 20 mM succinate and 10 mM nitrate and found no evidence of pyocyanin reduction until long after cells appeared to cease growing (as measured by the optical density at 500 nm of the cultures, Figure 3). Although nitrate levels were not measured, the onset of observable pyocyanin reduction likely occurred when nitrate was fully consumed.

### **Shifting redox state via alternate substrate metabolism**

With the hypothesis that higher levels of NADH would correspond to faster rates of pyocyanin reduction, I set out to alter cells' ratio of NADH/NAD<sup>+</sup> and determine the impact on pyocyanin reduction rate. In order to shift the redox state of the NAD(H) pool, I incubated *P. aeruginosa*  $\Delta phz1/2$  with various substrates. As shown in Figure 4, the reduction rates and concentration of NADH varied slightly between conditions, however there was not a clear trend between increasing [NADH] and the rate of pyocyanin reduction.

### **Methylene blue and pyocyanin reduction**

Methylene blue is a redox-active small molecule with structural similarity to phenazines. It is also approved as a pharmaceutical drug for the treatment of some human diseases, including malaria (Färber *et al*, 1998). Given prior findings that demonstrated an anaerobic survival phenotype for PA14 with oxidized phenazines but not methylene blue, despite the eventual reduction of this compound (Wang *et al*, 2010), we wondered whether methylene blue could impede the rate of pyocyanin reduction in cell-suspension assays. If this were possible, methylene blue could be considered for use as a drug to compete with phenazine utilization by *P. aeruginosa*.

A single experiment was performed using *P. aeruginosa* PA14  $\Delta phz1/2$  mixed with different amounts of methylene blue and pyocyanin, alone and in combination. As a further control, solutions of each compound separately and in combination were also analyzed over time in the absence of cells. Reduction rates did not differ for a given concentration of pyocyanin, regardless of the presence of methylene blue across a wide range of concentrations (2 to 200  $\mu$ M, Figure 5).

## Discussion

### Pyocyanin reduction by respiratory cytochrome mutants

In order to perform targeted studies of potential pathways of phenazine reduction, we partnered with the laboratory of Eric Rosenfeld of Université de La Rochelle in La Rochelle France. The Rosenfeld lab performs high-precision measurements of oxygen consumption by planktonic bacteria using both standard oxymetry and high-resolution respirometry (HRR). In *P. aeruginosa*, the presence of PYO causes an increase in the apparent respiratory rate ( $O_2$  consumption rate) when cells have no source of energy (*e.g.* glucose, succinate) (Friedheim, 1931). We planned to look for cellular components that are possibly involved in the process of pyocyanin reduction by combining mutants deficient in some components of the highly branched *P. aeruginosa* respiratory pathway (Figure 6) with various drugs targeting other components of the pathway. In principle, this would allow us to stop electron flow at various points in the respiratory chain in different experiments and then, by using HRR, figure out where PYO picks up electrons. If we could stop electrons “upstream” of where PYO gets its electrons, then the increase in  $O_2$  consumption (caused by reaction with reduced PYO) would not occur. However, if the block were “downstream” of where PYO picks up electrons, then the  $O_2$  consumption rate should increase as usual. *P. aeruginosa* is notoriously resistant to the effects of drugs (Wright, 2007) and this turned out to be a substantial impediment to the progress of this work. In addition, HRR requires that cells reach a steady state of oxygen consumption before the agent of interest (phenazine) is added, but a steady state was rarely achieved.

I constructed mutants in both quinol: oxygen oxidoreductases involved in *P. aeruginosa* respiration: cytochrome bo3, encoded by *cyoABCD*, and CIO, the cyanide insensitive oxidase, encoded by *cioAB* (Figure 6). The removal of both quinol oxidases ( $\Delta cyoABCD \Delta cioAB$ ) is

expected to force all electrons through the cytochrome bc1 complex (complex III), cytochrome c, and one of three terminal oxidases (two *cbb3*-type and one *aa3*). Preliminary results show that the mutant with the strongest effect on PYO reduction rate is the mutant lacking a subunit of complex III ( $\Delta fbcC$ ). Neither of the quinol oxidase mutants showed a strong PYO reduction phenotype, however we do not know to what degree these enzyme complexes were expressed in wild type cells under the conditions used in this experiment.

### **Pyocyanin reduction in the presence of nitrate**

When nitrate is present in the medium, pyocyanin reduction appears to cease. This could either be due to a complete lack of pyocyanin reduction, or due to rapid reoxidation of reduced pyocyanin through cell-mediated interactions with nitrate. We have only observed nitrate oxidation of reduced pyocyanin when PA14 cells were present in the medium. This result has been shown by combining nitrate with the filtered supernatant from an aerobically grown culture of PA14, after cells have completely reduced the pyocyanin (as evidenced by the disappearance of blue from the medium). To avoid the introduction of oxygen, the culture of cells must be pelleted anaerobically. The addition of nitrate or nitrite to the filtered supernatant alone has no effect on the redox state of the reduced pyocyanin. However, upon adding cells to nitrate and the anoxic supernatant, pyocyanin rapidly turns blue once again. (Nitrite was not tested in this way). Thus, we know that cells can oxidize pyocyanin in the presence of nitrate.

Nitrate serves as an alternate terminal electron acceptor for *P. aeruginosa* when oxygen levels are very low, so it is possible that all available electrons flow only to nitrate even when pyocyanin is present. We do not know whether nitrate directly competes against phenazines for electrons at a given enzyme complex. What seems most likely is that phenazines undergo both reduction and oxidation when nitrate is around, just as we assume happens when oxygen is present, although we have not measured pyocyanin reduction in a well-aerated culture. Whereas a typical aerobic culture still has regions with very little dissolved oxygen, nitrate would be present at equivalent amounts throughout the medium. Results presented here suggest that the benefits of phenazine redox cycling would likely not apply when nitrate is present.

## Shifting redox state via alternate substrate metabolism

NAD(H) is a critical cofactor of central metabolic pathways, and therefore a simple change in the ratio of the oxidized and reduced forms could cause profound changes to *P. aeruginosa* metabolism. The overall aim of this set of experiments was to look for a correlation between [NADH] and the rate of pyocyanin reduction. Because shifting the ratio of NADH/NAD<sup>+</sup> was achieved by providing cells with different substrates, a number of other effects could have ensued, and impacted the measured reduction rates. Because phenazine reduction is not yet well understood, it might be that the metabolic changes exert other effects on the rate of pyocyanin reduction independent of the NADH/NAD<sup>+</sup> ratio.

While different substrates resulted in differences in the NAD(H) pool and the PYO reduction rate, they also surely affected many other aspects of cellular physiology. For example, cells provided with nitrate or pyruvate had an alternate electron sink, which may have permitted greater flux through pathways that yield reduced cofactors (e.g. FADH<sub>2</sub>, NAD(P)H), but could have resulted in any number of other unrecognized consequences. The phase of growth from which cells were harvested for this experiment likely had a very strong impact on the possible pyocyanin reduction rate. Previous work from our lab has shown that reduction rates (normalized by optical density of the culture) increase from exponential phase into stationary phase (Price-Whelan *et al*, 2007). Another problem inherent to the reduction assay as articulated here is the length of time needed to bring cells into the anaerobic chamber through the purge and refill cycles of the air-lock, during which time the culture metabolism could start to shift and the temperature might decrease to as low as room temperature, ~22°C. Time delay and changes in temperature are likely to be important variables any time this assay is performed, but when trying to catch cells in particular physiological states, the three-minute delay might leave enough time for important metabolic shifts to occur. After passing through the airlock, more time is needed to pipette cells into the microtiter plate, and to take measurements (although the reduction rates appear to stay consistent over time, following a predictable concentration-dependent trajectory).

## Methylene blue and pyocyanin reduction

The inclusion of methylene blue in liquid cultures of *P. aeruginosa* PA14 does not appear to alter the rate of pyocyanin reduction. This suggests that methylene blue would likely not

interfere with the physiological benefits derived from phenazine redox cycling. Under other environmental conditions or with other phenazines, the results could be different, however this preliminary data set suggests that methylene blue is not a useful choice for disarming *P. aeruginosa* in the presence of pyocyanin.

The development of a high-throughput physiological assay that measures the rate of pyocyanin reduction allows systematic analyses of various environmental, genetic, and physiological effects on the rate of pyocyanin reduction. This pyocyanin reduction assay could be used as a complement to other analytical techniques in looking for and characterizing mutants in phenazine reduction, which is an area of current investigation within the lab.

## References

- Armstrong AV, Stewart-Tull DE & Roberts JS (1971) Characterisation of the *Pseudomonas aeruginosa* factor that inhibits mouse-liver mitochondrial respiration. *J Med Microbiol* **4**: 249–262.
- Dietrich LEP, Price-Whelan A, Petersen A, Whiteley M & Newman DK (2006) The phenazine pyocyanin is a terminal signalling factor in the quorum sensing network of *Pseudomonas aeruginosa*. *Mol Microbiol* **61**: 1308–1321.
- Färber PM, Arscott LD, Williams CH, Becker K & Schirmer RH (1998) Recombinant *Plasmodium falciparum* glutathione reductase is inhibited by the antimalarial dye methylene blue. *FEBS Lett* **422**: 311–314.
- Friedheim EA (1931) Pyocyanine, an accessory respiratory enzyme. *J Exp Med* **54**: 207–221.
- Grant SG, Jessee J, Bloom FR & Hanahan D (1990) Differential plasmid rescue from transgenic mouse DNAs into *Escherichia coli* methylation-restriction mutants. *Proc Natl Acad Sci USA* **87**: 4645–4649.
- Harman JW & MacBrinn MC (1963) The effect of phenazine methosulphate, pyocyanine and EDTA on mitochondrial succinic dehydrogenase. *Biochem Pharmacol* **12**: 1265–1278.
- Liberati NT, Urbach JM, Miyata S, Lee DG, Drenkard E, Wu G, Villanueva J, Wei T & Ausubel FM (2006) An ordered, nonredundant library of *Pseudomonas aeruginosa* strain PA14 transposon insertion mutants. *Proc Natl Acad Sci USA* **103**: 2833–2838.
- Maddula VSRK, Pierson EA & Pierson LS (2008) Altering the ratio of phenazines in *Pseudomonas chlororaphis* (*aureofaciens*) strain 30-84: effects on biofilm formation and pathogen inhibition. *J Bacteriol* **190**: 2759–2766.
- Maddula VSRK, Zhang Z, Pierson EA & Pierson LS (2006) Quorum sensing and phenazines are involved in biofilm formation by *Pseudomonas chlororaphis* (*aureofaciens*) strain 30-84. *Microb Ecol* **52**: 289–301.
- Price-Whelan A (2009) Physiology and mechanisms of pyocyanin reduction in *Pseudomonas aeruginosa* Ph.D. Thesis. California Institute of Technology, USA.
- Price-Whelan A, Dietrich LEP & Newman DK (2007) Pyocyanin alters redox homeostasis and carbon flux through central metabolic pathways in *Pseudomonas aeruginosa* PA14. *J Bacteriol* **189**: 6372–6381.
- Rahme LG, Stevens EJ, Wolfort SF, Shao J, Tompkins RG & Ausubel FM (1995) Common virulence factors for bacterial pathogenicity in plants and animals. *Science* **268**: 1899–1902.
- Ramos I, Dietrich LEP, Price-Whelan A & Newman DK (2010) Phenazines affect biofilm formation by *Pseudomonas aeruginosa* in similar ways at various scales. *Res Microbiol* **161**: 187–191.

- San K-Y, Bennett GN, Berríos-Rivera SJ, Vadali RV, Yang Y-T, Horton E, Rudolph FB, Sariyar B & Blackwood K (2002) Metabolic engineering through cofactor manipulation and its effects on metabolic flux redistribution in *Escherichia coli*. *Metab Eng* **4**: 182–192.
- Shanks RMQ, Caiazza NC, Hinsa SM, Toutain CM & O'Toole GA (2006) *Saccharomyces cerevisiae*-based molecular tool kit for manipulation of genes from gram-negative bacteria. *Appl Environ Microbiol* **72**: 5027–5036.
- Wang Y & Newman DK (2008) Redox reactions of phenazine antibiotics with ferric (hydr)oxides and molecular oxygen. *Environ Sci Technol* **42**: 2380–2386.
- Wang Y, Kern SE & Newman DK (2010) Endogenous phenazine antibiotics promote anaerobic survival of *Pseudomonas aeruginosa* via extracellular electron transfer. *J Bacteriol* **192**: 365–369.
- Wang Y, Wilks JC, Danhorn T, Ramos I, Croal L & Newman DK (2011) Phenazine-1-carboxylic acid promotes bacterial biofilm development via ferrous iron acquisition. *J Bacteriol* **193**: 3606–3617.
- Wright GD (2007) The antibiotic resistome: the nexus of chemical and genetic diversity. *Nature Rev Microbiol* **5**: 175–186.

## Tables

**Table 1. Strains used in these studies**

Strain	Description	Reference
<i>P. aeruginosa</i>		
PA14	Clinical isolate UCBPP-PA14, wild type	Rahme <i>et al</i> , 1995
PA14 $\Delta phz1/2$	PA14 with clean deletions of the phenazine biosynthesis operons <i>phzA1-G1</i> and <i>phzA2-G2</i>	Dietrich <i>et al</i> , 2006
PA14 $\Delta phz1/2$ $\Delta cioAB$	Phenazine-null PA14 with clean deletion of the cyanide insensitive oxidase, <i>cioAB</i>	This study (DKN1306)
PA14 $\Delta phz1/2$ $\Delta cyoABCD$	Phenazine-null PA14 with clean deletion of the cytochrome bo3 complex, <i>cyoABCD</i>	This study (DKN1305)
PA14 $\Delta phz1/2$ $\Delta cyoABCD \Delta cioAB$	Phenazine-null PA14 with clean deletions of <i>cyoABCD</i> and <i>cioAB</i>	This study (DKN1307)
PA14 $\Delta phz1/2 \Delta fbcC$	Phenazine-null PA14 with clean deletion of c subunit of cytochrome bc1 complex, <i>fbcC</i>	Price-Whelan, 2009
<i>E. coli</i>		
DH5 $\alpha$	Host for cloning	Grant <i>et al</i> , 1990
BW29427	Host for cloning, DAP auxotroph	KA Datsenko, B Wanner (unpublished)
<i>S. cerevisiae</i>		
INVSc1	Fast growing strain for homologous recombination; <i>MATa his3<math>\Delta</math>1 leu2 trp1-289 ura3-52</i>	Invitrogen
Plasmids		
pMQ30	Conjugal suicide vector for creating clean gene deletions	Shanks <i>et al</i> , 2006
p $\Delta cioAB$	2 kb fragment containing $\Delta cioAB$ cloned into pMQ30 (in DH5 $\alpha$ )	This study (DKN1301)
p $\Delta cyoABCD$	2 kb fragment containing $\Delta cyoABCD$ cloned into pMQ30 (in DH5 $\alpha$ )	This study (DKN1300)



**Table 2. Primers used in the construction of PA14 mutants**

Sequence Name	Sequence
cyoABCD_1	TAC TGC CGC CAG GCA AAT TCT GTT TTA TCA GAC CGC TTC TGA TAA CCA ACG GCA GAG TCC
cyoABCD_2	CCT TCC ATC GAT TAA GGC CGG AAG GGG CCA TGA CGT GAA GCT GA
cyoABCD_3	TCA GCT TCA CGT CAT GGC CCC TTC CGG CCT TAA TCG ATG GAA GG
cyoABCD_4	GGA ATT GTG AGC GGA TAA CAA TTT CAC ACA GGA AAC AGC TAC CAT GAA TAC CCT GCG CCA
cyoABCD_c1	CTC GTT GCG ACG ATC CAT GAA GTA
cyoABCD_c2	CGC TGT TCA TCA AGG AAC GAC TCA
cyoABCD_c3	GCG ATC AGG TTG CCG AAG ATG ATT
cyoABCD_c4	TAT CCC TGG GTC GGC CTG TT
cioAB_1	CTG CCG CCA GGC AAA TTC TGT TTT ATC AGA CCG CTT CTG GCC GAT TCG AGT TCC TTG AAC
cioAB_2	GGA CCA TAT GCG GCG CCT CCG GCA ACT CCT CTT CAG GTT C
cioAB_3	GAA CCT GAA GAG GAG TTG CCG GAG GCG CCG CAT ATG GTC C
cioAB_4	GGA ATT GTG AGC GGA TAA CAA TTT CAC ACA GGA AAC AGC TGG GTG GAG CAC GAG ATA TTC
cioAB_c1	TGG TGT TGA TAA GGT CCA GGT CGA
cioAB_c2	TGG TTT GGC CGC GTT ATC TCG TT
cioAB_c3	GCG GTC GCT TTC CAA TGA CAA GAA
cioAB_c4	TCA TCG AAA CGG ACA TGC TGA TCG
pMQ30_1	TTT GAT GCC TGG CAG TTC CCT ACT
pMQ30_2	AGT TAG CTC ACT CAT TAG GCA CCC
	Primer sets used to generate $\Delta pqsA$ , (not used in this study)
pqsA_1	GGA ATT GTG AGC GGA TAA CAA TTT CAC ACA GGA AAC AGC TAG GAA GCC GAA CAG ATC AGC
pqsA_2	TCG CTG AAG AGG GAA CGT TCT GTC ATG TTG ATT CAG GCT GTG GG
pqsA_3	CCC ACA GCC TGA ATC AAC ATG ACA GAA CGT TCC CTC TTC AGC GA
pqsA_4	CTG CCG CCA GGC AAA TTC TGT TTT ATC AGA CCG CTT CTG GCA AGG TGC AAC AAT GGA CAG
pqsA_c1	TGA AGT CGA GCA GGT TGG AGA TGT
pqsA_c2	TTT CCC GTT CCT GAC AAA GCA AGC
pqsA_c3	ATG ATG TCG CGG TTC TCG ATC AGA TG
pqsA_c4	TTT CCA AAC GCA GCA ACC ACT GCT

## Figures

**Figure 1.** Effect of increasing pyocyanin concentration on the rate of pyocyanin reduction by PA14  $\Delta phz1/2$ . Cells were grown aerobically in minimal medium with 20 mM succinate up to the optical densities ( $OD_{500}$ ) specified in the legend, harvested between 3 and 24 hours of growth. PYO reduction rates were determined by the change in  $A_{691}$ /time, then normalized to the number of cells by dividing the reduction rate by the  $OD_{500}$  of the sample (before the addition of PYO).

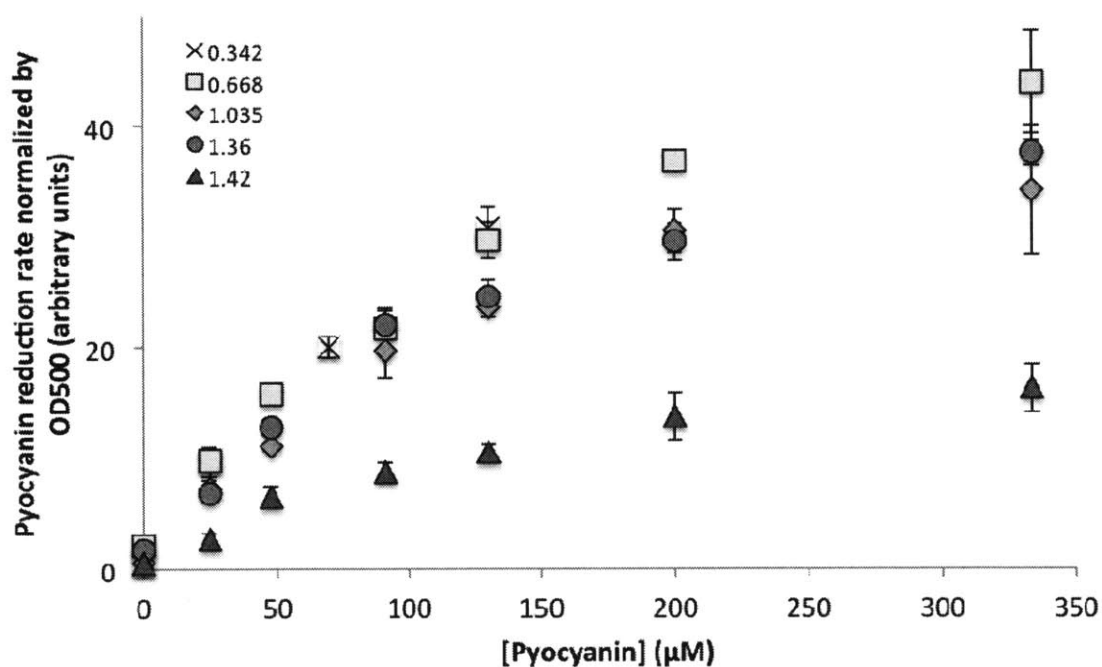
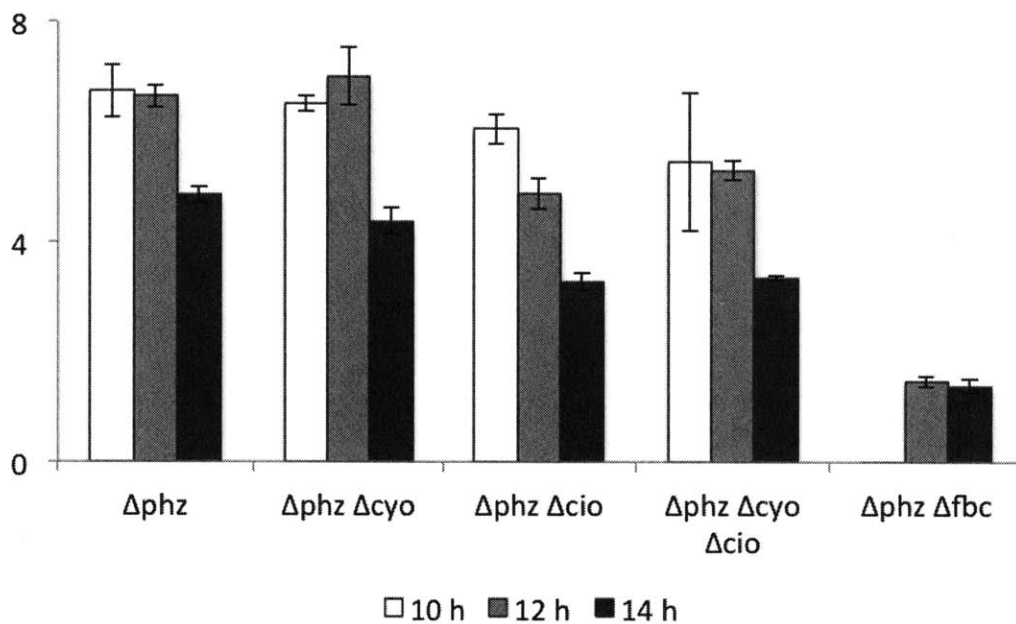


**Figure 2.** Pyocyanin reduction rates at different points in growth for cytochrome mutants grown on **a)** succinate and **b)** glutamate. Error bars represent the standard deviation of technical triplicates.

**a**



**b**

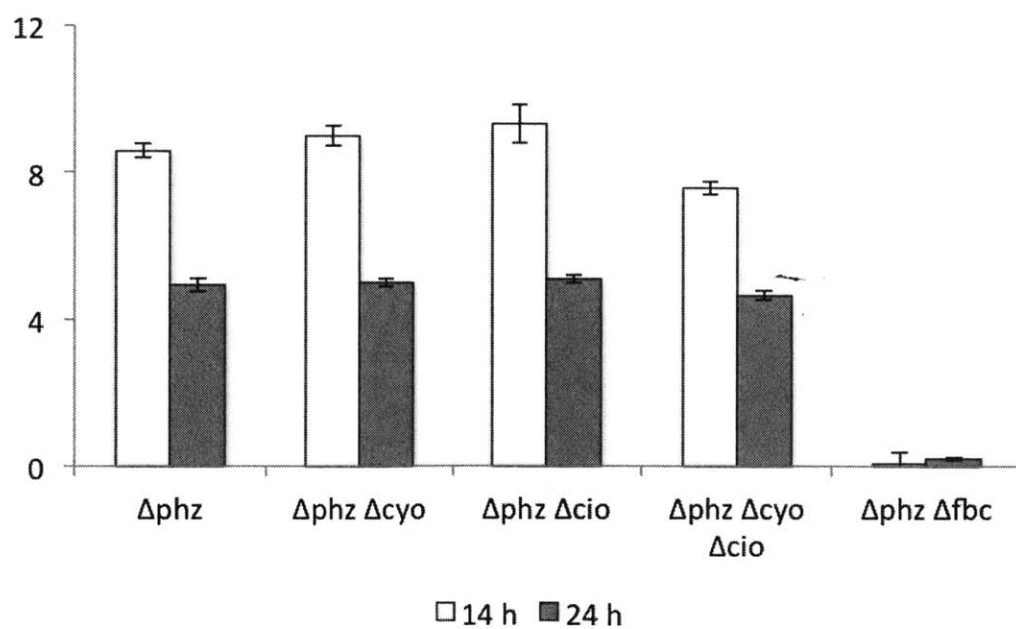


**Figure 3.** Pyocyanin reduction by anaerobic PA14  $\Delta phz1/2$  cells incubated with 20 mM succinate and 10 mM nitrate in buffered medium. Single data sets are shown and are representative of triplicates. Filled circles indicate  $OD_{500}$ , used to measure cell growth. Open symbols connected by dashed lines indicate  $A_{691}$ , which decreases when oxidized pyocyanin undergoes reduction and changes from blue to colorless. Pyocyanin added during cell growth did not undergo reduction until more than 20 hours later, likely when nitrate was fully depleted.

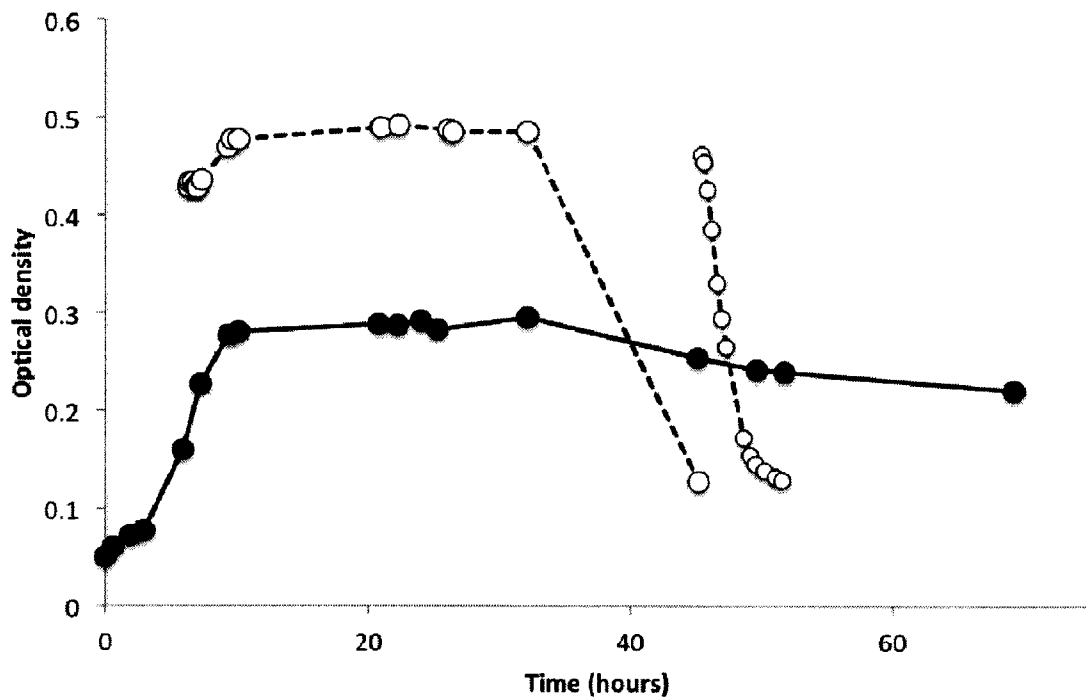


**Figure 4.** Correlation between pyocyanin reduction rate and the concentration of NADH (normalized to number of cells). PA14  $\Delta phz1/2$  cells were grown aerobically with the substrates indicated. A similar pattern of [NADH] vs. PYO reduction rate exists when comparing %NADH of the total NAD(H) pool (not shown). Error bars indicate the standard deviation of biological triplicates.

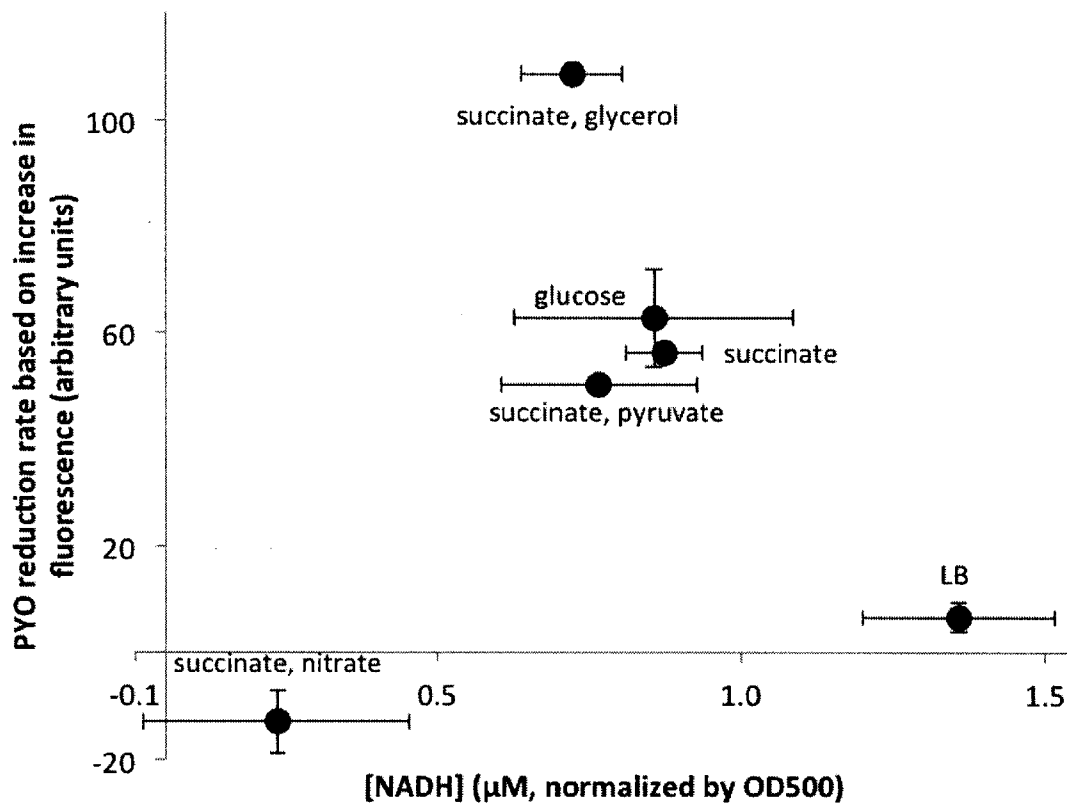


**Figure 5.** Impact of the presence of methylene blue (MB) on the rate of pyocyanin reduction by PA14  $\Delta phz1/2$  across a wide range of concentrations. High levels of pyocyanin were paired with low levels of methylene blue, and low levels of pyocyanin were paired with high levels of methylene blue in order to test not only different concentrations, but different ratios of the two potential substrates.

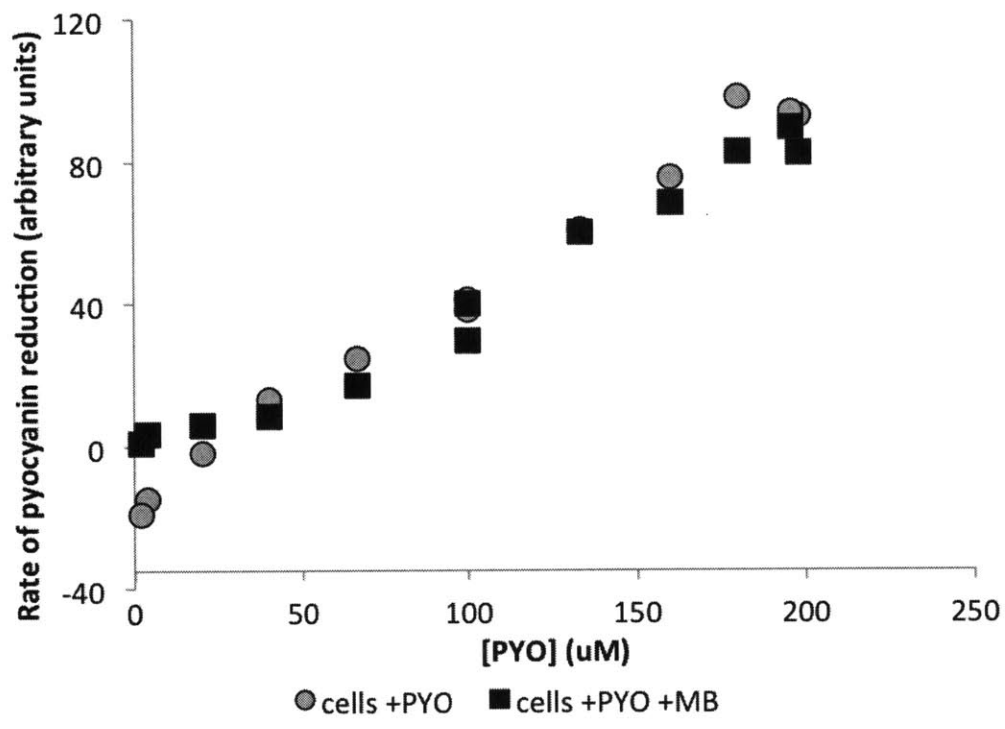


**Figure 6.** Schematic representation of the *P. aeruginosa* respiratory chain. Arrows represent the flow of electrons (blue) or protons (brown). Mutants in the quinol oxidases (bo3 and CIO) were constructed and tested for their ability to reduce pyocyanin.

